ESTABLISHING *IN VITRO* MODELS OF NEUROINFLAMMATION TO INVESTIGATE NEUROIMMUNE RESPONSES IN NEUROCYSTICERCOSIS

by

Amalia Naita Awala

AWLAMA001

Department of Human Biology

SUBMITTED TO THE UNIVERSITY OF CAPE TOWN

In fulfilment of the requirements for the degree

Doctor of Philosophy in *Neuroscience*

Supervisor:

Dr Joseph Valentino Raimondo

Co-supervisor:

Dr Rachael Dangarembizi

Department of Human Biology
University of Cape Town

October 2023

The Future Leaders- African Independent Research (FLAIR), Wellcome Trust and the

The University of Cape Town are acknowledged for financial support.

Declaration

I, **Amalia Naita Awala**, hereby declare that the work described in this dissertation is my own (except where acknowledgements indicate otherwise) and that neither the whole work nor any part of it has been, is being, or will be submitted for another degree at this or any other educational institute.

I empower the university to reproduce, for the purpose of research, the whole work or any part thereof.

Signature: Signed by candidate

Date: 14 October 2023

Abstract

Neurocysticercosis (NCC), a parasitic infection of the central nervous system (CNS) caused by the larvae of the cestode *Taenia solium,* is the leading cause of adult-acquired epilepsy in the world. A surprising clinical manifestation of NCC is that viable larvae can exist in the brain for extended periods with no symptomatology, but when they die, clinical symptoms develop. Clinical evidence suggests that the hallmark of symptomatic NCC is neuroinflammation; however, the neuroinflammatory mechanisms underlying this disease remain grossly understudied, and how innate immune cells respond to this infection is still debated. One of the reasons for this is that there is a lack of reliable experimental models of inflammation at the level of the brain that allow for cell-type specific tracking of inflammation in innate immune cells. Thus, this thesis's first aim was to establish the rodent-derived organotypic brain slice culture (OBSC) system as an *in vitro* model for investigating neuroinflammatory signalling and activation of microglia and astrocytes in the brain. To validate this model of neuroinflammation, OBSCs from neonatal mice were treated with the pro-inflammatory stimulant lipopolysaccharide (LPS) for 24 hours and compared to untreated control slices. Inflammatory activation of microglia and astrocytes was measured by tracking the activation of the inflammatory transcription factor nuclear factor for interleukin 6 (NF-IL6), a robust biomarker for tracking neuroinflammation in glial cells. Inflammation was confirmed by measuring the concentrations of pro-inflammatory cytokines IL-6 and TNF-α released by OBSCs in the culture medium. Lastly, we used single-nucleus RNA sequencing to investigate these inflammatory changes at a transcriptomic level. My results show that LPS significantly increased NF-IL6 activation in microglia and astrocytes and increased the release of both IL-6 and TNF-α. At the transcriptomic level, I observed an upregulation of major inflammatory genes such as *CCL5* and *Timp1* in both microglia and astrocytes in response to LPS treatment, further confirming inflammation. Having demonstrated that OBSCs present a robust platform for investigating neuroinflammatory mechanisms in brain infections, the second aim of this thesis sought to use this established model to investigate how viable *Taenia* larvae modulate neuroinflammation in NCC. The potential immunomodulatory effects of the *Taenia* larvae on glial activation and inflammation was assessed by concurrently treating OBSCs with both LPS and *Taenia* larvae homogenate. I found that the co-application of LPS and *Taenia* larvae homogenate suppressed the LPS-induced microglial and astrocytic activation, pro-inflammatory cytokine release, and prevented the upregulation of key inflammatory genes. Together, this observed anti-inflammatory effect could explain how *Taenia* larvae can exist in the human brain without eliciting symptomatology from the host. This thesis's final aim was to set up a comparable translational *in vitro* human model of neuroinflammation using human

acute and organotypic brain slice cultures (hOBSCs). Using the inflammatory transcription factor NF-IL6 as a marker for glial activation, I found that at baseline, hOBSCs displayed higher levels of microglial and astrocytic activation than human acute slices. Additionally, untreated control and LPS-treated hOBSCs both displayed high levels of NF-IL6 activation. However, cytokine data revealed low concentrations of pro-inflammatory cytokines IL-6 and TNF-α in culture medium in untreated control hOBSCs that increased when slices were exposed to LPS, highlighting an inflammatory reaction. Taken together, these findings provide novel insights into understanding the neuroinflammatory mechanisms underlying NCC and highlight the utility of organotypic brain slice cultures in studying neuroimmune responses in diseases of an inflammatory nature such as NCC.

Acknowledgements

Firstly, the most important thank you goes to my excellent supervisor Joe; thank you for taking a chance on a wild Namibian girl who only had a dream. I have learned so much from you on how to be a great leader and scientist. Thank you for believing in me and reassuring me that I belong. You have fostered an amazing and supportive lab where I could always learn, be challenged, and grow both as a researcher and a person.

Secondly, I would like to extend my utmost appreciation to my mentor and co-supervisor, Rachael. It has been such a privilege to work and learn from you; you inspire me to be a better scientist each day. Thank you for being a trailblazer, a beacon, and a reference point for young female African neuroscientists such as myself.

This thesis, in its entirety, is dedicated to my mother, the first person to ever believe that I could achieve this, even when I did not. Mama, thank you for pushing me, for believing in me, and for speaking for me when I was still finding my voice. Our dream is finally being realized, and I wish you could be here to celebrate with me. I hope wherever you are, the sunshine is the brightest, and they have endless fields of sunflowers. I miss and love you wholeheartedly.

To my sisters, Alina and Wilhelmina, thank you for holding down the fort when I could not; your support and laughs through this journey have kept me going. Thank you to my father, Daniel, who, even when he did not agree with or understand my choices to pursue this degree, has remained my biggest champion and supporter.

I would also like to extend my gratitude to Sasha, Hayley, and Anja, who got me settled into the lab and have been brilliant colleagues and scientists to work with. I cannot forget the colleagues and friends from the various 'Teams', Team Human, Maahir and Emily from Team Crypto, who have become dear friends and have always supported me with experiments, chit-chats, and bubble tea. The second generation of Team Tapeworm, thank you, Tess, for taking on that challenge with me! I also cannot forget team snRNA-seq; what a team and what an honour!

Thank you to all the members and brilliant minds of the Raimondo and Dangarembizi Labs; this journey would have been dull without you all.

A special shout out to my best friend and soulmate, Tariro; I believe God put you in my life when I needed you the most. It has been a privilege navigating life and science with you. To my loves, Mahle, Nathan, Selly, Azi, Mbo (and baby Drip), Juju, Josh, Fanidh, Zinzi, and the ladies of Elyenge, you have shown me what true friendship means, I can never thank you enough for that.

In a professional capacity, I would also like to extend immense gratitude to Dr Jeremy Woodward, who helped us immensely with our size exclusion chromatography experiments, the members of the UCT confocal microscope unit, especially Mrs Suzanne Cooper, who taught me how to use the confocal microscope and was patient with me in the beginning when I was out of my depth. Lastly, the members of the UCT-RAF (animal facility), Mr Rodney Lukas who gently taught me how to handle animals and Mr Abdul Samuels (AK) for always taking care and looking after our rodent friends.

Table of Contents

List of Figures

Chapter 1

Chapter 2

Chapter 3

Chapter 4

Chapter 5

List of Tables

List of Abbreviations

Symbol	Description
aCSF	Artificial cerebrospinal fluid
AED(s)	Antiepileptic drug(s)
ANOVA	Analysis of variance
AS	Ammonium Sulphate
BBB	Blood-brain barrier
CA	Cornu ammonis
CNS	Central nervous system
COX-2	Cyclooxygenase-2
CR	Chemokine receptors
CT	Computed tomography
DALY	Disability-adjusted life year
DAMPs	Damage-associated molecular patterns
GABA	Gamma-aminobutyric acid
GFAP	Glial fibrillary acidic protein
GFP	green fluorescent protein
hOBSCs	Human organotypic brain slice cultures
IFN-γ	Interferon-gamma
IBA1	Ionized calcium-binding adaptor molecule 1
IL-1β	Interleukin- 1 beta
IL-2/6/10/18	Interleukin -2/6/10/18
ILAE	International League Against Epilepsy
IQR	Interquartile range
JAK/STAT	Janus kinase/signal transducer and activator of transcription
K^+	Potassium
KA	Kainic acid
LPS	Lipopolysaccharide
M. corti	*Mesocestoides corti*
MMP	Matrix metalloproteinase
MAPK	Mitogen-activated protein kinase
MCH I/II	Major histocompatibility complex I/II
MFI	Mean fluorescent intensity
MRI	Magnetic resonance imaging
MyD88	Myeloid differentiation primary response 88
NCC	Neurocysticercosis
NF-IL6	Nuclear factor for interleukin 6
NF-κB	Nuclear Factor Kappa-light-chain-enhancer of activated B cells

OBSCs	Organotypic brain slice cultures
PAMPs	Pathogen-associated molecular patterns
PBS	Phosphate buffered saline
PFA	Paraformaldehyde
PRR	Pattern recognition receptor
SD	Standard deviation
SEM	Standard error of the mean
snRNA-sequencing	Single nucleus RNA-sequencing
SP	Substance P
STAT-3	Signal transducer and activator of transcription 3
T. crassiceps	*Taenia crassiceps*
Th1/2	T-helper 1/2
TLR	Toll-like receptor
TLR4	Toll-like receptor 4
TNF-α	Tumour necrosis factor-alpha
UMAP	Uniform Manifold Approximation and Projection
WHO	World Health Organization

CHAPTER 1

INTRODUCTION

1.1 NEUROCYSTICERCOSIS: ITS PREVALENCE AND BURDEN

Neurocysticercosis (NCC) is the most common parasitic infection of the central nervous system (CNS), and it is caused by the larval form of the pig tapeworm *Taenia solium (T. solium)* (García et al., 2003; Prasad et al., 2008). Even though global prevalence rates of NCC remain unknown, the disease is primarily endemic to developing regions such as Sub-Saharan Africa, Latin America, and South Asia **(**see **Fig 1.1)** (Butala et al., 2021). The World Health Organization (WHO) estimates that 2.56 - 8.30 million people suffer from NCC worldwide, with a disability-adjusted life year (DALY) burden of 2.3 million, a measure that accounts for both early pre-mature death due to an illness, as well as years lost from an individual's life where they were not in complete health (Butala et al., 2021). However, as with other neglected tropical illnesses, these figures are likely underreported and underestimated, and the burden of NCC is likely to be much more significant than reported.

Contrary to the typically held idea that NCC is a disease of the developing world, increasing travel and migration to and from endemic regions have made NCC a global disease with incidence reported even in developed regions (Burneo & Cavazos, 2014). The USA, for example, reports more cases of imported NCC than any other developed country in the world, with estimates ranging from 0.2 to 0.6 cases per 100,000 of the general population, with higher estimates reported amongst Hispanic populations (Serpa & White, 2012).

Epileptic seizures are the most common presenting symptom in NCC, occurring in about 70% to 90% of all symptomatic cases (Carpio & Romo, 2014). As a result, NCC is the leading cause of adult-acquired epilepsy in the world. In endemic regions, it is estimated that about 30% of all epilepsy cases are comorbid with an NCC diagnosis (Bern et al., 1999; Gripper & Welburn, 2017; Ndimubanzi et al., 2010). This is accompanied by a significant burden of morbidity and mortality, with reports estimating 50,000 NCC-related deaths annually (Preux & Druet-Cabanac, 2005; Roman et al., 2000; World Health Organization, 2016). Regrettably, in some parts of the world,

patients with epilepsy are highly stigmatised, with many communities regarding it as a disease of spiritual aetiology (Abdel Ghaffar et al., 2021; Mao et al., 2022), which can have negative implications on the physical and mental well-being of patients.

Symptom manifestations in NCC are frequently nonspecific; as a result, diagnosing the disease still proves challenging. The most reliable form of diagnosis is neuroimaging techniques, specifically computed tomography (CT) and magnetic resonance imaging (MRI) scans, which are expensive and not readily available in rural areas where the disease is most prominent (Mafojane et al., 2003; Ndimubanzi et al., 2010). More recently, serological tests have also been developed to measure antibodies to *T. solium* in infected patients. However, these tests frequently lack sensitivity in patients with light (viable) NCC infections (Nash & Garcia, 2011); thus, neuroimaging remains the best way to diagnose the disease.

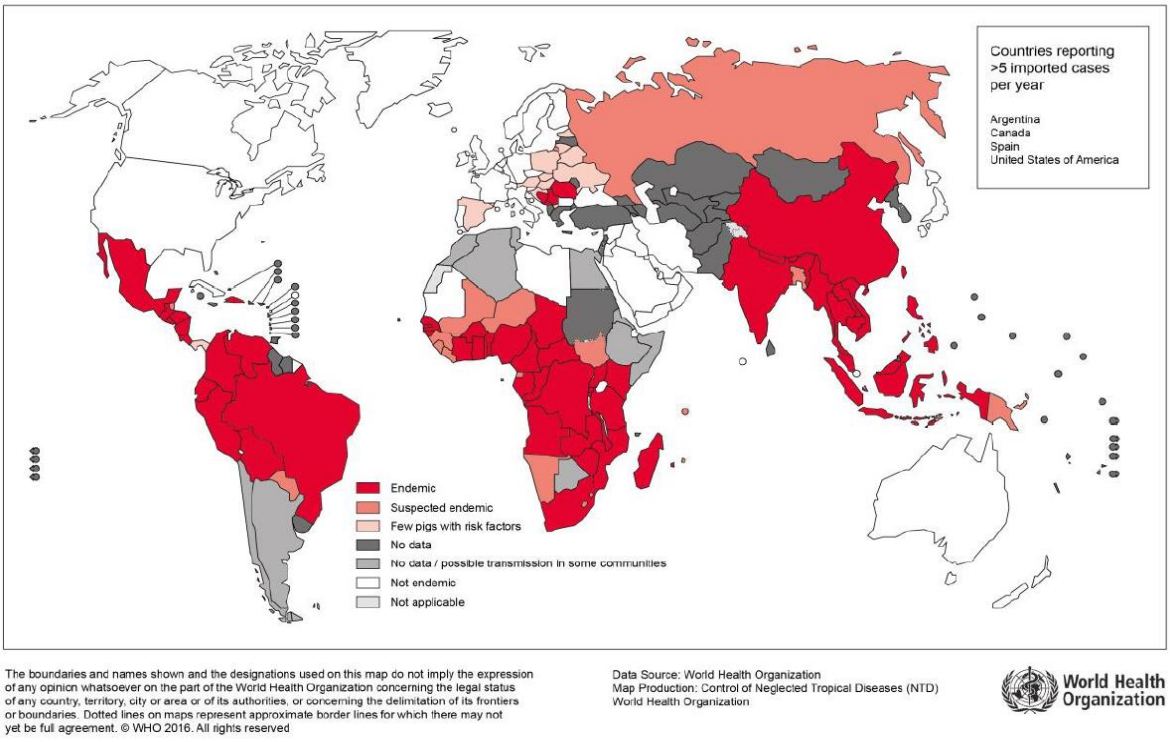

Figure 1.1 The global prevalence of neurocysticercosis. Regions with high endemicity include sub-Saharan Africa, Latin America, and South Asia. Taken from WHO fact sheet (Endemicity of *Taenia solium*" 2015, accessed May 2023).

Generally, treatment for NCC involves the administration of cysticidal drugs such as albendazole, usually administered simultaneously with corticosteroids to reduce the ensuing inflammation (García et al., 2002). In addition, antiepileptic drugs (AEDs) are

also administered if late-onset seizures manifest in NCC. Unfortunately, the administration of AEDs is usually chronic, with reports highlighting that up to 33% of patients with seizures remain refractory to AED treatment (Patsalos & Perucca, 2003). As a result, treatment of epilepsy secondary to NCC may present a significant long-term financial burden for patients, especially in the frequently affected low- and middle-income communities.

While treatment for NCC may prove costly for patients, the financial burden of the disease extends beyond the cost of treatment. The WHO estimates that in some endemic regions, NCC symptoms cause up to two-thirds of wage earners to lose their jobs, and a significant fraction of those are unable to return to the workforce (WHO, 2016). In 2002, annual losses due to NCC were estimated to be as high as US$25 million in 10 endemic countries in West and Central Africa (WHO, 2016). In regions such as the Eastern Cape of South Africa, where NCC prevalence rates may be as high as 20% (Ndimubanzi et al., 2010), US$5 million in losses were incurred because of NCC in 2004 (Carabin et al., 2006; WHO, 2016). This highlights that the financial burden of NCC is not limited to the patients alone but can also have broader adverse economic implications on communities and entire nations.

NCC is a preventable disease and a preventable cause of acquired epilepsy; however, because the burden of the disease falls largely on developing countries, few resources, both monetary and time, have been invested into understanding the molecular and cellular processes of the disease. It is thus up to African researchers like myself to invest our time and resources into understanding and elucidating the pathophysiological processes underlying this debilitating disease to help prevent, manage, and treat this infection.

1.2 NEUROCYSTICERCOSIS: AETIOLOGY AND DISEASE PRESENTATION

1.2.1 The *Taenia solium* parasite life cycle

Humans are the only definitive hosts of *T. solium* and can become infected by the larval form of the parasite by ingesting raw or undercooked pork meat infected with the *T. solium* cysticerci (De Lange et al., 2018; White, 2000). Upon ingestion, the larvae mature into adult tapeworms in the human small intestine, developing into segmented proglottids with a scolex (White, 1997, 2000). Each proglottid contains infectious oncospheres (eggs), which are excreted via human faeces (De Lange et al., 2018; White, 1997). Many patients with adult tapeworms remain asymptomatic, mainly because oncospheres cannot enter the bloodstream at this stage, hypothesised to be because of an absence of gastric and intestinal fluids needed to activate them (De Lange et al., 2018; Steyn et al., 2022; White, 1997, 2000).

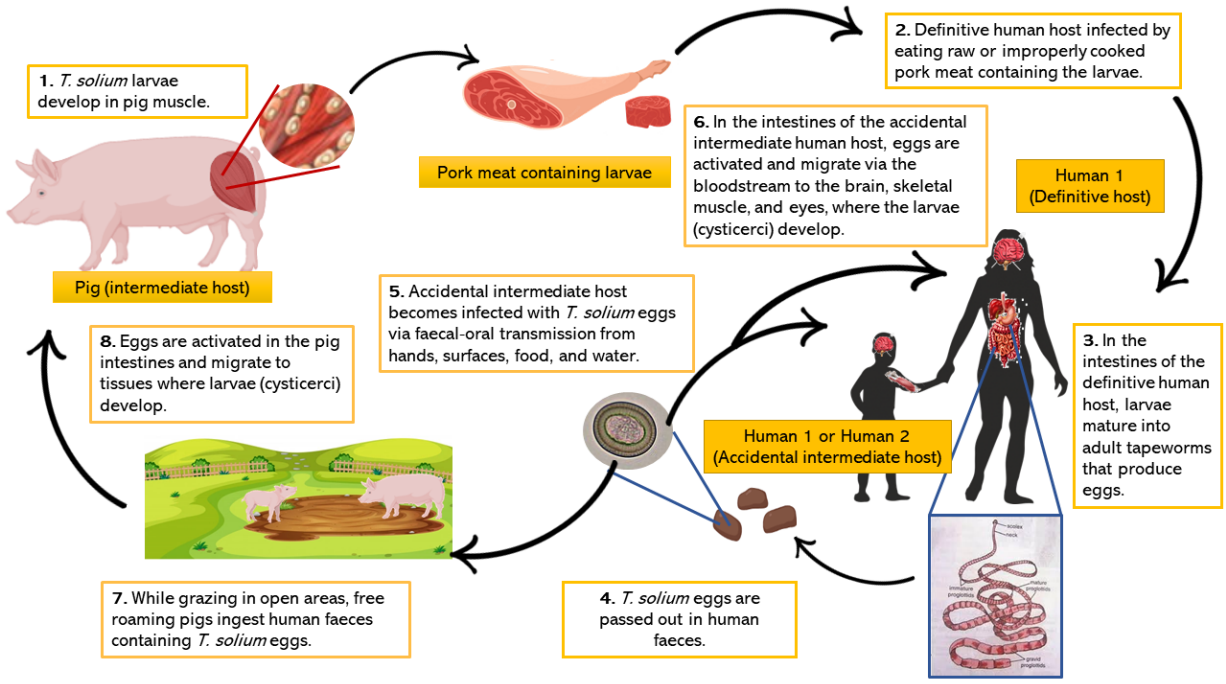

Figure 1.2 The life cycle of *Taenia solium* (Taken from Steyn, Awala et al. 2022, where I am a co-author).

Pigs, the intermediate hosts of *T. solium*, are infected via ingestion of human faeces containing the *T. solium* oncospheres (White, 1997). It is for this reason that *Taenia* infection is exceptionally high in regions where free-range pig rearing is practised. Once ingested, the oncospheres hatch and are activated by gastric and intestinal fluids in the pigs' digestive system (White, 1997). Activated oncospheres force themselves through intestinal walls, entering the bloodstream and lodging into the pigs' muscle,

nervous and subcutaneous tissue, where they develop into cysticerci (De Lange et al., 2018; White, 1997, 2000).

NCC comes about when humans also accidentally ingest *T. solium* oncospheres from human faecal matter (White, 1997). This transmission usually occurs through the consumption of contaminated food and water or inadvertently by ingesting minute amounts of faeces from someone in the household who is a tapeworm carrier. (De Lange et al., 2018). As in pigs, oncospheres are activated in the human gut by gastric and intestinal fluids, penetrating the intestinal walls and entering the bloodstream. They then lodge into various tissues, particularly muscle but also tissue of the central nervous system where they develop into cysticerci, i.e., NCC **(**see **Fig 1.2)** (De Lange et al., 2018; Steyn et al., 2022; White, 1997, 2000).

1.2.2 Symptoms of neurocysticercosis

There are two types of NCC: (1) parenchymal NCC, where cysts lodge into the brain parenchyma and the most common symptom is seizure development, and (2) extra-parenchymal NCC, where cysts lodge in subarachnoid and ventricular spaces and the most prominent symptom is intracranial hypertension (Prodjinotho et al., 2020), this work focuses on parenchymal NCC.

Symptom manifestation in parenchymal NCC is incredibly diverse, and their presentation and disease severity are primarily dependent on cyst numbers and size, their developmental stage, the location of infection and most importantly, host immune responses (Garcia et al., 2014). A systematic review of the most prominent symptoms in symptomatic NCC reported seizures in 78% of patients (Carabin et al., 2011). Other reported clinical symptoms include headaches, increased intracranial pressure that can lead to migraines and dizziness, focal deficits, hydrocephalus, and meningitis (Carabin et al., 2011; Garcia et al., 2014; Nash & Garcia, 2011).

1.2.3 *Taenia solium* cyst progression

A puzzling clinical manifestation of NCC is that the disease progresses in stages, each of which elicits different immune responses in the host and is thus accompanied by different clinical symptoms. These symptoms range from entirely asymptotic to more severe symptomatology, i.e., seizures (White, 2000). The development of cysticerci (cysts) in the human brain is divided into four stages as characterised by neuroimaging

techniques (CT scans and MRI scans): the vesicular or viable stage, the colloidal stage, the granular-nodular stage, and the calcified stage **(**see **Fig 1.3)** (Fleury et al., 2016; White, 2000).

Vesicular/ viable stage

In parenchymal NCC, there is a period of months or even years following the initial infection and establishment of cysts in the brain, where patients remain asymptomatic; this is known as the vesicular/ viable cyst stage (De Lange et al., 2018; White, 1997, 2000). This asymptomatic phase of the disease is hypothesised to arise due to the ability of the viable cysts to employ immune modulatory mechanisms and use host-derived molecules to 'mask' their surface structures and evade detection by the hosts' immune system (De Lange et al., 2018; Stringer et al., 2003; White, 1997). Viable cysts are described as translucent fluid sacs that elicit minimal host inflammatory response; however, what little they do elicit is mainly composed of T and B lymphocytes, plasma cells, and eosinophils surrounding the cysts (Fleury et al., 2016; White, 2000). Experimental systems have shown that viable larvae can modulate the host immune responses and inflammatory responses by maintaining an anti-inflammatory environment characterised by a T-helper 2 (Th2) response (Steyn et al., 2022; White, 2000). It has also been demonstrated that asymptomatic NCC patients display higher serum levels of anti-inflammatory cytokines, e.g., interleukin 10 (IL-10), whereas symptomatic patients display higher serum levels of pro-inflammatory cytokines, e.g., interleukin 6 (IL-6) (Prasad et al., 2009; Verma et al., 2011). With that, viable cysts have also been shown to secrete a serine proteinase inhibitor that prevents complement activation for pathogen recognition, thereby preventing detection from the host's innate immune cells (Merle et al., 2015; White et al., 1997). Furthermore, this proteinase inhibitor also inhibits lymphocyte activation and cytokine production (White et al., 1997), allowing for the maintenance of an anti-inflammatory milieu that is favourable for cyst survival.

Transitional cysts (colloidal and granular-nodular stages)

When cysts start to degenerate, through natural attrition or after administration of anti-helminthic treatment, they lose their ability to modulate host immune responses. Degenerating cysts are often referred to as transitional cysts and comprise the colloidal and granular-nodular cyst stages. Here, the cyst walls begin to lose their

integrity and become flooded by host immune cells in the colloidal stage of infection (White, 2000; White et al., 1997). As the inflammatory response continues, the cyst walls eventually collapse, and the cyst becomes encompassed by fibrosis and granuloma in the granular-nodular stage (White, 2000). The transitional cyst stage is characterised by a predominant T-helper 1 (Th1) response with increased release of pro-inflammatory cytokines such as tumour necrosis factor-alpha (TNF-α), interleukin-1 beta (IL-1β), and interferon-gamma (IFN-γ) (Lama et al., 2015; Prodjinotho et al., 2020). With that, transitional cysts are highly correlated with seizure occurrence, which is thought to be a consequence of the host inflammatory processes in response to degrading cysts (Clinton White, 2019; White et al., 1997). As a result, most epileptiform activity recorded in this disease is observed at this stage of infection. Transitional cysts are also accompanied by astrocytic proliferation, which results in astrogliosis, an increase in the expression of adhesion molecules such as intercellular adhesion molecule 1 (ICAM-1), as well as disruptions to the blood-brain barrier (BBB) facilitating the infiltration of peripheral immune cells to cyst sites (Prodjinotho et al., 2020; White, 2000). As resident and peripheral immune cells combine with parasitic cyst material, they form granulomas around the cysts, which are easily identifiable on CT and MRI scans (Prodjinotho et al., 2020)

Calcified cysts

Over time, these granulomas fully calcify in what has sometimes been referred to as inactive or silent NCC (White, 2000). Calcified cysts have, however, been highly associated with seizure occurrence in some symptomatic patients where a Th1 response dominates (Nash et al., 2004). One study, for example, found a high prevalence (83%) of calcified cysts among seizure patients in a small rural village in Mexico (Fleury et al., 2003; Nash et al., 2004). In addition, neuroimaging studies have shown that calcified lesions may also present with perilesional oedema, which has also been correlated with seizures (Nash et al., 2004; White, 2000).

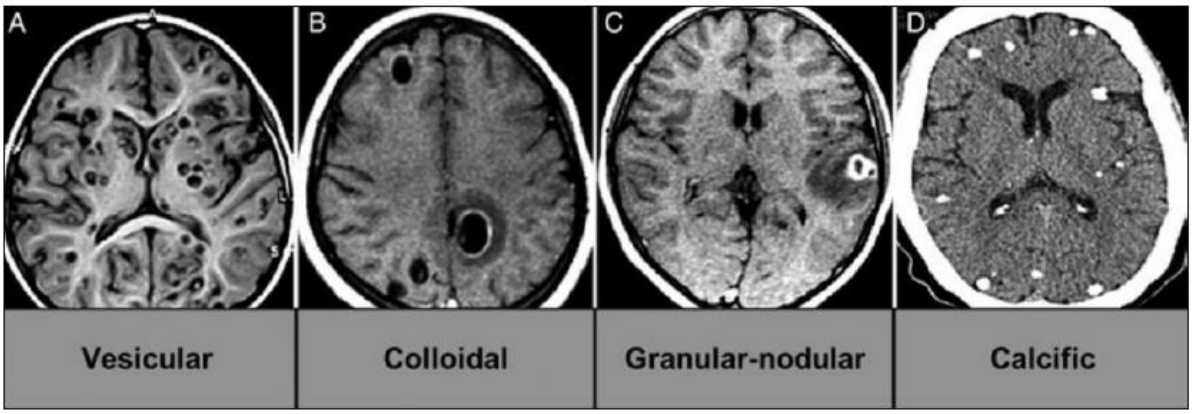

Figure 1.3 Stages of cysticerci development in parenchymal NCC. An MRI scan of A) vesicular/viable cysticerci, B) colloidal cysticerci, and C) degenerating cysticerci in the granular-nodular stage D) CT scan of calcified cysticerci (Images acquired from Carpio and Romo 2014, and de Lange, Mahanty, and Raimondo 2018).

1.3 WHAT CAUSES SEIZURES IN NEUROCYSTICERCOSIS?

1.3.1 Epilepsy, seizures, and neurocysticercosis

As previously highlighted, many NCC patients present with epileptic seizures (Carpio & Romo, 2014). However, there remains debate whether seizures secondary to NCC constitute epilepsy because the two are not always synonymous. The International League Against Epilepsy (ILAE) has suggested epilepsy be defined as “two or more unprovoked seizures occurring at least 24 hours apart” (Carpio & Romo, 2014; Fisher et al., 2005; Thurman et al., 2011) of which unprovoked seizures may arise as a consequence of a demonstrated pre-existing condition. Epilepsy, according to the ILAE, can be broadly attributed to three etiological categories: genetic, structural/metabolic, or unknown (Carpio & Romo, 2014; Thurman et al., 2011). The structural/metabolic causes of epilepsy include the concurrent manifestation of structural or metabolic abnormalities with seizures. Here, the cause of epilepsy is predominantly associated with the condition that has the closest and most direct relationship to its onset (Carpio & Romo, 2014). For instance, in NCC, this may be patients with calcified cysts who present with seizures (Carpio, 2013; Carpio & Romo, 2014; Thurman et al., 2011).

Epileptic seizures, on the other hand, are defined by the ILAE as a “transient occurrence of signs and/or symptoms due to abnormal excessive or synchronous

neuronal activity in the brain" (Carpio & Romo, 2014; Thurman et al., 2011). It is, however, essential to note that epileptic seizures, even recurrent ones, do not always constitute epilepsy. In NCC, patients who experience seizures in response to the inflammatory response elicited by degenerating cysts in the transitional stage could be classified as having acute symptomatic seizures, which are isolated seizures associated with acute conditions (Carpio & Romo, 2014). Conversely, seizures occurring in patients with viable cysts or inactive calcified cysts may be classified as presenting with recurrent unprovoked or remote seizures, i.e., epilepsy (Carpio, 2013; Carpio & Romo, 2014). Because of the heterogeneous presentation of symptoms in NCC, it is essential to differentiate between acute and unprovoked seizures in patients for better prognostic and treatment outcomes.

1.3.2 Possible mechanisms for seizure occurrence in neurocysticercosis

The pathophysiological mechanisms underlying seizure development in NCC are multifactorial and not fully understood. Most studies have focused on the hypothesis that seizure occurrence in NCC results from host immune and inflammatory responses to transitional and degenerating cysts. However, it has been demonstrated that seizures can also occur during the viable cyst stage, where there are very minimal host immune responses (Garcia & Del Brutto, 2017). For example, Naidoo et al. (1987) found that 12.9% of the 70 patients in his imaging study of NCC patients presenting with seizures had only viable cysts. Some researchers have hypothesised that seizures occur during the viable cyst stage because viable cysts elicit short-term host inflammatory episodes and then return back to a non-inflamed status (Garcia & Del Brutto, 2017). In addition, seizures have also been reported in patients with calcified non-inflamed cysts, with some patients displaying peri-calcification oedema around lesions, hypothesised to be the result of host inflammatory responses to residual antigens in the calcified cyst (Garcia & Del Brutto, 2017; Nash et al., 2008). The occurrence of seizures during what are asymptomatic anti-inflammatory periods in NCC highlights that they may not always be the consequence of the host's inflammatory responses. For example, it is conceivably possible that the cysts themselves, under certain conditions, could release some pro-seizure substances.

There is, however, substantial evidence that seizures in NCC are the result of host inflammatory responses to degenerating cysts. This is characterised by the release of

pro-inflammatory cytokines such as TNF-α and IL-1β in response to antigens produced by transitionary cysts, moving the overall inflammatory phenotype to a Th1 response (Prodjinotho et al., 2020). This pro-inflammatory response leads to changes in BBB integrity, resulting in the infiltration of peripheral immune cells such as T and B lymphocytes, macrophages, and eosinophils to the site of cyst lesions (Carpio et al., 1998; Prodjinotho et al., 2020). Additionally, it leads to the formation of perilesional oedema associated with increased intracranial pressure, which in turn increases seizure susceptibility (Flisser et al., 1986; Prodjinotho et al., 2020; White et al., 1992). A large body of evidence suggests that seizure presentation in NCC is primarily mediated by changes in the Th1/Th2 axis (as mediated by T cells) (Carpio et al., 2021; Clinton White, 2019; Prodjinotho et al., 2020; Toledo et al., 2018; White et al., 1992, 1997). Additionally, studies have identified potential genetic variations in inflammatory genes, particularly in the Toll-like receptor 4 (TLR4) gene (Steyn et al., 2022; Verma et al., 2010). This receptor plays a role in regulating the balance between Th1 and Th2 immune responses and genetic variations may make certain NCC patients more susceptible to seizures.

Alongside the inflammatory response observed in transitional cysts is the release of the neuropeptide Substance P (SP) by neurons, endothelial cells, and immunocytes (Robinson et al., 2012). SP has been implicated in seizure generation in NCC as it has been associated with the release of Th1 cytokines such as interleukin 2 (IL-2) and interleukin 18 (IL-18) in lesions surrounding dying cysts (Prodjinotho et al., 2020; Restrepo et al., 2001; Robinson et al., 2012). Robinson et al. (2012) found that SP produced within cyst granulomas caused seizures in brain biopsies of patients with NCC and in rodent models of NCC. They also observed severe seizures in rats after intrahippocampal injection with both SP alone and SP from granulomas from *Taenia*-infected wild-type mice (Robinson et al., 2012). Additionally, studies from mice deficient with an SP precursor do not develop acute seizures in response to injected granulomas, highlighting that SP percussor (and SP) is needed for seizure generation (Robinson et al., 2012). Taken together, this highlights the possible role and involvement of SP in seizure generation in NCC.

The overall observation that seizures in NCC can occur at any stage throughout infection, sometimes with very little or no contribution from host inflammatory

responses, suggests that the mechanisms underlying seizures in this disease are highly complex and multifactorial. What is clear, however, is that there is a link between inflammation and seizure development.

1.3.3 Inflammation: Cause or consequence of epilepsy?

Epilepsy is the third most common neurological disorder, affecting 50 million people worldwide (Vezzani et al., 2011). The relationship between seizures and inflammation is complex, with evidence suggesting seizures could cause inflammation and vice versa. There is substantial clinical and experimental evidence supporting the hypothesis that inflammatory mechanisms in the brain underlie the pathogenesis of seizures and epilepsy. For example, experimentally induced seizures in rodents trigger a robust inflammatory response in the epileptic focus (Oprica et al., 2003; Turrin et al., 2004; Vezzani & Granata, 2005). Likewise, in rodent models of epilepsy, members of the TLR family, which mediate bacterial and parasitic recognition in the brain, are upregulated by seizures in microglia and astrocytes, leading to an increase in the transcription of inflammatory mediators, including pro-inflammatory cytokines, chemokines and major histocompatibility complex I and II (MCH I & MCH II) (Turrin et al., 2004; Vezzani & Granata, 2005). The first clinical evidence of the relationship between seizures and inflammation comes from clinical studies that demonstrated that steroids and other anti-inflammatory treatments displayed anticonvulsant properties in treating epilepsies that were resistant to treatment (Vezzani & Granata, 2005; Wheless et al., 2007; Wirrell et al., 2005). Likewise, brain tissue from patients with drug-resistant epilepsies, Rasmussen encephalitis, and patients with temporal lobe epilepsy all show an increased expression of pro-inflammatory molecules in neuroglia (Crespel et al., 2002; Pardo et al., 2004; Vezzani & Granata, 2005).

Experimental evidence for inflammation causing seizures was demonstrated in a rodent model of induced hyperthermia for studying febrile seizures, where the core temperature of rodents was increased to mimic fever (Baram et al., 1997; Lee et al., 2019). Here, they reported that pups displayed behaviours such as biting, tonic stiffness, and falling over, which are behaviours commonly observed in rodents administered with pro-convulsants (Baram et al., 1997; Lee et al., 2019). It has been further demonstrated that in this model, there was increased release of pro-inflammatory cytokines, activation of both microglia and astrocytes in the

hippocampus, and an increase in prostaglandins such as prostaglandin-endoperoxide synthase 2 (COX-2), all of which increase seizure susceptibility (Baram et al., 1997; Dubé et al., 2010). Likewise, in an *in vivo* model of epilepsy using intraperitoneal injections of kainic acid (KA), researchers found that seizure occurrence was significantly increased when KA was co-injected with lipopolysaccharide (LPS), a component of the outer member of Gram-negative bacteria and a powerful pro-inflammatory stimulant (Dubé et al., 2010; Hu et al., 2022). LPS has been shown to increase the body temperature of rodents' mimicking fever conditions (Hu et al., 2022; Lee et al., 2019). More importantly, LPS can elicit an inflammatory response that is characterised by the activation of microglia and astrocytes and the increase in the release of pro-inflammatory cytokines and chemokines (Hu et al., 2022; Lee et al., 2019; Papageorgiou et al., 2016), which are mechanisms that have been demonstrated to increase seizure susceptibility. Taken together, these findings demonstrate that there are instances where inflammation can increase seizure susceptibility. However, in most models, inducing inflammation alone does not cause seizures but rather adds to the myriad of mechanisms that increase the likelihood of seizures occurring.

A growing body of evidence suggests that inflammation is a consequence of seizures. For example, a rodent model of temporal lobe epilepsy using KA injection in the hippocampus of rats increased the number of cells that were positive for IL-1β, IL-6 and TNF-α, which are all markers for inflammation (Chen et al., 2017; Lee et al., 2019). They additionally found that KA promotes astrogliosis, another marker of inflammation (Lee et al., 2019). Another study demonstrated that KA injections disrupt the integrity of the BBB, resulting in perivascular oedema and increased infiltration of peripheral immune cells into the brain (Chen et al., 2017). Likewise, models that have induced seizures using the cholinergic agonist pilocarpine in rodents have found increased levels of inflammatory markers such as IL-1β, TNF-α, Nuclear Factor Kappa-light-chain-enhancer of activated B cells (NF-κB) and COX-2 in rat hippocampi, indicating inflammation (Ali et al., 2018). Additionally, models of seizures and hyperexcitability induced by serum albumin injections have also been shown to provoke BBB dysfunction and disrupt K^+ buffering in astrocytes (Frigerio et al., 2012; Lee et al., 2019). These injections also increased astrogliosis and the release of IL-1β, indicative of inflammation (Frigerio et al., 2012; Lee et al., 2019). Together, these findings

suggest that brain inflammation occurs after the induction of seizures, eliciting a response that could exacerbate seizure severity and frequency.

In the context of neurocysticercosis, the interrelationship between inflammation and seizures becomes especially pertinent, and it is clear it is not simple cause-and-effect. Instead, it is a multifaceted interplay where inflammation can initiate seizures and result from the body's response to seizure activity. With that, however, as seizures and inflammation tend to occur far later in the progression of the disease, there remain gaps in our understanding of the neuroinflammatory mechanisms occurring in the viable asymptomatic stage of NCC. A significant yet largely unexplored aspect is the function of innate immune cells in the brain during this stage of the disease. The following section will explore the classical neuroinflammatory events in the brain under parasitic invasion with an emphasis on the role that microglia and astrocytes play during the neuroimmune response to *Taenia* infection.

1.4 THE NEUROIMMUNE RESPONSE TO NEUROCYSTICERCOSIS

1.4.1 Glial cells mediating the neuroinflammatory response to parasitic infections

Historically, the brain was considered an immunologically privileged or inert zone (Barker & Billingham, 1978; Forrester et al., 2008; Louveau et al., 2015), a concept centred on keeping adaptive immune responses and inflammation highly regulated. Several factors contributed to this belief, including the presence of a BBB that restricts the entry of a majority of peripheral immune cells and systemic antibodies into the brain and the absence of lymphatic drainage, which would limit immune cell trafficking in and out of the brain. Moreover, there was the belief that the brain possesses a limited number of specialised antigen-presenting cells such as dendritic cells, and an abundance of anti-inflammatory molecules, including transforming growth factor-beta (TGF-β) and IL-4 that inhibit pro-inflammatory immune responses (Barker & Billingham, 1978; Forrester et al., 2008; Hubbard & Binder, 2016; Louveau et al., 2015). However, recent research has dramatically expanded our understanding of neuroimmunology. For example, a specialised and functional waste and antigen-clearing glymphatic system has recently been identified in the brain (Jessen et al., 2015). Moreover, under certain conditions, such as brain infections and

neuroinflammation, activated peripheral immune cells can traverse the BBB (Prodjinotho et al., 2020). Additionally, resident immune cells such as microglial cells and astrocytes become activated in brain injury or invasion, exhibiting not only an inflammatory cascade but also the capacity for antigen presentation (Matejuk & Ransohoff, 2020), underscoring the brain's multifaceted immune response capabilities. Therefore, while the brain is a site of regulated immune surveillance, it is not entirely isolated from the systemic immune response. This interconnectedness means that peripheral immune events can have profound implications for CNS health and disease. The concept of brain immune privilege has thus been replaced by a classical model of neuroinflammation with intricate immune responses mediated by innate immune cells within the CNS (Hubbard & Binder, 2016). The next section will cover the classical inflammatory responses that occur in the brain under parasitic invasion.

The first line of defence in the CNS is microglia cells, the resident and most abundant macrophage in the brain (Jurga et al., 2020). The role of microglia in the adult brain is to maintain brain homeostasis by monitoring the microenvironment for danger signals and eliciting a corresponding inflammatory response upon their detection (Guo et al., 2022; Jurga et al., 2020). However, these cells are multitasking and have also been shown to participate in synaptic pruning, remodelling, and plasticity, as well as tissue and neuronal repair (Du et al., 2017).

Microglia have unique cell surface pattern recognition receptors (PRRs), including toll-like receptors (TLR) and chemokine receptors (CR) that can uniquely recognise both pathogen-associated molecular patterns (PAMPs) and damage-associated molecular patterns (DAMPs) invading the brain microenvironment (Du et al., 2016; Jurga et al., 2020). The recognition of PAMPs, such as parasites, leads to the classical activation (M1) of these cells and initiates the activation of inflammatory signalling pathways that eventually lead to the increase in the transcription and release of pro-inflammatory molecules (Guo et al., 2022; Huuskonen et al., 2005; Jurga et al., 2020; Papageorgiou et al., 2016). These include pro-inflammatory cytokines such as IL-6, TNF-α, and IL-1β and chemokines such as chemokine ligand 5 (CCL5) (Guo et al., 2022; Huuskonen et al., 2005; Jurga et al., 2020; Papageorgiou et al., 2016). These cytokines and chemokines work together to function as messenger molecules to activate nearby

inflammatory cells, propagating the inflammatory response (Guo et al., 2022; Huuskonen et al., 2005; Jurga et al., 2020; Papageorgiou et al., 2016). M1 activation of microglial cells also features transcriptomic changes, changes in antigen presentation, morphological changes, as well an increase in the release of reactive oxygen species and nitric oxide (NO), all of which ultimately contribute to the severity of the inflammatory response (Delbridge et al., 2020; Papageorgiou et al., 2016). While M1 activation is essential in eliciting the initial pro-inflammatory response to fight infection, it has been demonstrated that prolonged uncontrolled release of pro-inflammatory molecules can be neurotoxic to the brain microenvironment (Guo et al., 2022; Jurga et al., 2020). As such, microglial activation is highly polarised, with some cells becoming alternatively activated (M2), taking on an anti-inflammatory phenotype that offers neuroprotection by inhibiting M1 inflammation and repairing any damage to the CNS (Guo et al., 2022; Jurga et al., 2020).

The activation of microglial cells is also accompanied by changes in their morphology. During homeostatic conditions, microglia are in a ramified morphology, displaying a small soma with extended processes that offer protective surveillance to the brain microenvironment (Lier et al., 2021). Upon activation, microglia change into an activated morphology where their ramifications shorten, and the size of the soma increases; here, their primary function is phagocytosis and antigen presentation (Lier et al., 2021). When activated, microglia can also take on an ameboid morphology where they become fully rounded, displaying only the soma with no ramifications and adapting a purely phagocytotic function (Lier et al., 2021). On occasion, activated microglia can lose their function entirely and take on a dystrophic morphology as observed in Alzheimer's (AD) disease, where they display signs of swelling or thinning of processes and an overall loss of ramification and function (Lier et al., 2021). Because of these diverse phenotypic presentations, changes in microglial morphology have in the past been used as a marker for their activation (Hovens et al., 2014; Papageorgiou et al., 2016; Sugama et al., 2007); however, this is not always systematic as morphological changes occur on a continuum and are not always apparent in some cells. As a result, more sophisticated methods such as transcriptomics and tracking the protein expression and cellular signalling of inflammatory markers have been used instead, as done in this thesis.

Astrocytes, the most abundant glia in the CNS, are the second line of defence during parasitic brain invasion. (Giovannoni & Quintana, 2020). Their primary function under physiological conditions is to maintain brain homeostasis for optimal neuronal functioning (Giovannoni & Quintana, 2020; Reid & Kuipers, 2021). They do this by maintaining the BBB integrity, refining synapses, and regulating the extracellular balance of fluids, ions, and neurotransmitters (Giovannoni & Quintana, 2020; Reid & Kuipers, 2021). Though participating in a myriad of support functions in the homeostatic brain, astrocytes are critical regulators of neuroinflammation during injury and brain invasion. Much like microglia, astrocytes have PRRs on their cell surfaces that can recognise PAMPs and launch an appropriate response, leading to reactive astrogliosis (Reid & Kuipers, 2021).

Two types of reactive astrocytic phenotypes have been identified, A1 and A2, which seem to parallel M1/M2 phenotypes in microglia (Reid & Kuipers, 2021). A1 astrocytes are pro-inflammatory, releasing pro-inflammatory cytokines and chemokines (Liddelow et al., 2017; Reid & Kuipers, 2021). A2 astrocytes, on the other hand, display anti-inflammatory neuroprotective functionality promoting CNS repair after pathology, much like M2 microglia (Liddelow et al., 2017; Reid & Kuipers, 2021). Reactive astrocytes also display morphologically different phenotypes to astrocytes in physiological conditions. Reactive astrocytes generally increase in size as marked by the increase in the structural protein glial fibrillary acidic protein (GFAP), increasing the number of processes and how far they extend in a morphology that is characteristically “bushy” (Reid & Kuipers, 2021; Schiweck et al., 2018).

Microglia-astrocyte crosstalk is essential during neuroinflammation. Microglial-derived cytokines, for example, regulate astrocytic activation, moving them towards an A1 phenotype that can themselves release pro-inflammatory cytokines (Linnerbauer et al., 2020; Matejuk & Ransohoff, 2020; Saijo & Glass, 2011; Sofroniew, 2015). This further amplifies the inflammatory response by acting not only on other astrocytes but also on microglia, promoting their activation in a positive feedback loop. While microglia are recruited and activated quite quickly following parasitic invasion, astrocytes are activated shortly after that, forming an astrogliosis scar that helps contain inflammatory cells in one area and preventing their spread to healthy tissue (Linnerbauer et al., 2020; Matejuk & Ransohoff, 2020; Sofroniew, 2005). It has,

however, been demonstrated in mouse models treated with the inflammatory activator LPS that there is a significant increase in harmful neurotoxic molecules when M1 and A1 cells are activated at the same time, which is why M2 and A2 activation is also essential (Saijo & Glass, 2011; Sofroniew, 2005). Additionally, it has also been demonstrated that the activation of astrocytes outlasts that of microglia in the brain (Sofroniew, 2005). Thus, A2 astrocytes are activated far longer than M2 microglia and work to significantly antagonise M1 and A1 neurotoxicity to return the brain to homeostasis (Sofroniew, 2005).

1.4.2 Do neurons have inflammatory capacity?

As the basic functional units of the CNS, it is often debated whether neurons are active participants in the neuroinflammatory response elicited by pathology in the brain. Literature has demonstrated that neurons express PRRs on their cell surface, such as TLRs, which, in an inflammatory environment, can become activated by cytokines derived from innate immune cells (Lafon et al., 2006; Ma et al., 2006). This activation initiates a cascade of inflammatory signalling pathways leading to the release of neuronal-derived inflammatory mediators such as pro-inflammatory cytokines and chemokines (Lafon et al., 2006; Ma et al., 2006). These neuronal-derived cytokines modulate the activation of microglia and astrocytes, further exacerbating the inflammatory response (Bartfai & Schultzberg, 1993). While neurons do not seem to play a role in actively combating and ameliorating inflammation as microglia and astrocytes, they can contribute to the inflammatory response by releasing inflammatory factors that modulate the activation of immune-competent glial cells.

1.4.3 The role of microglia and astrocytes in *Taenia* infection

As previously highlighted, the viable cyst stage of *Taenia* infection is predominantly asymptomatic with minimal inflammatory response from the host (De Lange et al., 2018; White et al., 1992). As a result, most research characterising host inflammatory responses to *Taenia* infection has focused on the symptomatic stages of infection (i.e., transitional and calcified cyst stages) with a strong emphasis on peripheral immune cells that regulate the Th1/Th2 axis (Prodjinotho et al., 2020; White, 1997, 2000). For example, one study that used histology and immunohistochemistry to characterise the immune cell types surrounding granulomas in human brain specimens histologically confirmed with NCC found that the predominant cell types are plasma cells, B and T

lymphocytes, macrophages, and mast cells (Restrepo et al., 2001). With that, however, others have reportedly found activated microglia and astrocytes surrounding mature granulomas in transitional and calcified cysts in NCC, where they are hypothesised to contribute to the high production of pro-inflammatory cytokines along with the present peripheral immune cells (Fleury et al., 2003, 2016; Prodjinotho et al., 2020; Restrepo et al., 2001). Another study utilised a porcine model of NCC in which activated *T. solium* oncospheres were implanted in the cerebral subarachnoid space of pigs. Here, they reported high expression of mature and immature astrocytes, as well as markers of activated astrocytes in tissue close to transitional cysts four months post-infection (Fleury et al., 2015). Additionally, pro-inflammatory cytokines produced during the transitional and calcified cyst stages of NCC infection have been demonstrated to increase microglial and astrocytic proliferation and gliosis (Prodjinotho et al., 2020). One study that used immunohistochemistry to examine the immunopathological changes caused by viable and dead *Taenia* parasite in a porcine model of NCC found increased expression of the astrocytic marker fibrillary acidic protein (GFAP) in both viable and dead stages of disease (Sikasunge et al., 2009). They additionally observed extensive astrogliosis and that astrocytic end feet formed glial scars around the dead *Taenia* parasite (Sikasunge et al., 2009). A critical observation is that gliosis has been highly implicated in epileptiform activity, the most prominent symptom at this stage of the infection (Prodjinotho et al., 2020). With this, however, debate remains on whether gliosis is a cause or consequence of seizures in NCC. Studies that have induced conditional widespread astrocytic gliosis without any other pathologies in mice have found that they developed spontaneous recurrent seizures (Patel et al., 2019; Robel et al., 2015). Another study that virally induced astrocytic gliosis in rodent hippocampus also found that it caused neuronal hyperexcitability (Ortinski et al., 2010; Patel et al., 2019). Additionally, chronic astrogliosis has also been linked to hyperexcitability, affecting the ionic balance of K^+ in the brain and potentially contributing to epileptogenesis (Losi et al., 2012; Patel et al., 2019), all of which suggest that gliosis could be a cause of seizures. Contrary to these reports, another study that looked at astrogliosis in a mouse model of temporal lobe epilepsy where mice were treated with pilocarpine for seizures did not find a correlation between seizure frequency and reactive gliosis (Buckmaster et al., 2017). Finding instead that seizure frequency was more correlated with the loss of GABAergic

interneurons in the hippocampus than with gliosis (Buckmaster et al., 2017; Patel et al., 2019). While this debate remains, gliosis present in transitional and calcified cyst stages may be a key contributor to seizure generation in NCC, a phenomenon that may shift microglia and astrocytes towards M1 and A1 inflammatory phenotypes to parallel the overall Th1 response present during this stage of infection.

With that, however, how these innate immune glial cells respond during the viable cyst stage of NCC remains largely unexplored. What is interesting is that peripheral immune cells such as eosinophils and T and B lymphocytes have been observed surrounding viable cysts (Fleury et al., 2016; White, 2000). Additionally, viable cysts have been demonstrated to produce excretory-secretory products that exert significant immunoregulatory effects on the surrounding peripheral innate immune cells by shifting them toward Th2 phenotype (Fleury et al., 2016; Prodjinotho et al., 2020; White, 2000). This process increases the production of anti-inflammatory cytokines, creating an environment favourable for cyst survival while limiting the progression of the disease. Thus, Prodjinotho et al. (2020) have postulated that it is conceivable that these excretory-secretory products may also be regulating microglial and astrocytic function at this stage of the disease. Though yet to be elucidated, this hypothesis raises critical immunological questions and gaps yet to be addressed. These include whether viable cysts attenuate the microglial and astrocytic cells towards an M2 and A2 phenotypes to parallel the general Th2 response present at this stage of infection or whether these glial cells do not become activated at all and remain in a ramified and non-reactive phenotype. What is increasingly clear is that these cell types, as critical players of inflammatory processes in the brain, likely play a key role in the neuroinflammatory response in the viable stage of NCC infection. Thus, to address some of these gaps, aspects of this thesis characterised the neuroimmune response to *Taenia* infection. This was done by explicitly tracking the changes in the activation of microglia and astrocytes in a model of viable NCC. The next section will cover how the signalling of inflammatory transcription factors can be utilized to track microglial and astrocytic activation in the brain.

1.5 INFLAMMATORY TRANSCRIPTION FACTORS AS FUNCTIONAL READOUTS TO TRACK THE ACTIVATION OF MICROGLIA AND ASTROCYTES IN THE BRAIN

In order to investigate the neuroinflammatory processes in NCC one would have to experimentally induce inflammation in the brain. One way of doing this, as done in this thesis and as demonstrated by many others, is by exposure to an immunogenic agent such as LPS (Lu et al., 2008; Papageorgiou et al., 2016). LPS is a potent TLR4 ligand and has been shown to activate both microglia and astrocytes through inflammatory signalling pathways that lead to the transcription of target inflammatory genes (Acaz-Fonseca et al., 2019; Herden et al., 2015; Poltorak et al., 1998; Zimmermann et al., 2015). Additionally, activation of these inflammatory signalling pathways leads to the translocation of transcription factors usually present in the cytoplasm under physiological conditions into the nucleus; these include NF-κB, signal transducer and activator of transcription 3 (STAT-3), and nuclear factor for interleukin 6 (NF-IL6) (Rummel, 2016). As such, this nuclear translocation can be a useful tool for systematically measuring both neuroinflammation and glial cell activation and the subsequent downstream releasable factors and the resulting transcriptomic changes as confirmation of this inflammatory response.

NF-κB

The NF-κB signalling pathway is activated by a diverse range of stimuli, from microbial derivatives like LPS to pro-inflammatory cytokines such as TNF-α and IL-1β (Park & Hong, 2016). The pathway's activation often begins at the cell surface receptors, notably TLRs (Lu et al., 2008; Park & Hong, 2016; Rummel, 2016). Upon receptor engagement, the intracellular signalling cascade is set in motion, leading to the activation of the IκB kinase (inhibitor of NF-κB) complex (Gilmore, 2006; Hayden & Ghosh, 2004; Park & Hong, 2016). This complex, composed of IKKα and IKKβ catalytic subunits, when activated, phosphorylates the inhibitor IκB that holds NF-κB in the cytoplasm (Gilmore, 2006; Hayden & Ghosh, 2004; Park & Hong, 2016). The phosphorylation of IκB by IKK flags it for degradation, freeing NF-κB to translocate into the nucleus (Gilmore, 2006; Hayden & Ghosh, 2004; Park & Hong, 2016). Here, it drives up the transcription of genes regulating pro-inflammatory cytokines such as IL-

6 and IL-18, chemokines such as RANTES, and adhesion molecules such as I-CAM (Gilmore, 2006; Hayden & Ghosh, 2004; Park & Hong, 2016).

STAT-3

STAT-3 has been shown to play a role in neuroinflammation, cell growth, and cell proliferation (Bromberg & Wang, 2009; Rummel, 2016). STAT-3 activation is mediated via the Janus kinase/signal transducer and activator of transcription (JAK/STAT) inflammatory signalling pathway, which is activated by cytokines, growth factors, and hormones (Bromberg & Wang, 2009; Levy & Darnell, 2002; O'Shea & Plenge, 2012). Upon the binding of cytokines or growth factors to their respective receptors, an associated JAK becomes activated through autophosphorylation (Levy & Darnell, 2002). Activated JAKs, in turn, catalyse the phosphorylation of specific tyrosine residues on the receptor itself, creating docking sites for STAT molecules (Bromberg & Wang, 2009; Levy & Darnell, 2002; O'Shea & Plenge, 2012). STAT-3, once docked, gets phosphorylated by the JAK. This phosphorylation triggers its dimerization, allowing two STAT-3 molecules to bind together (Levy & Darnell, 2002). The formed dimer undergoes a conformational change enabling its translocation to the nucleus (Bromberg & Wang, 2009; Levy & Darnell, 2002; O'Shea & Plenge, 2012). Inside the nucleus, the dimerized STAT-3 binds to specific DNA sequences, driving the transcription of target genes (Bromberg & Wang, 2009; Rummel et al., 2005). These include pro-inflammatory cytokines such as IL-6, as well as chemokines such as CXCL1 and CCL2 (Levy & Darnell, 2002). What is of note is that the activation of STAT3 differs among cell types, with a pronounced activation observed in astrocytic cells relative to microglial cells, as demonstrated through immunohistochemical staining (Rummel, 2016).

NF-IL6

NF-IL6 is a relatively newly discovered transcription factor and has important roles in a multitude of cellular processes, most notably inflammation, where it has been implicated in the neurotoxic effects of microglia (Poli, 1998; Ramji & Foka, 2002; Rummel, 2016). NF-IL6 is activated via TLR by agonists and distinct cytokines, a pattern of expression that is evident in microglial cells subjected to systemic LPS exposure (Damm et al., 2011, 2012; Rummel, 2016). Elevated NF-IL6 activation is observed in contexts ranging from traumatic brain injuries to settings characterized by

heightened neuronal activity and psychological stress (Rummel, 2016). The modulation of NF-IL6 is an intricate process influenced by multiple inflammatory signalling cascades, these include the NF-κB pathway, the JAK/STAT pathway and the mitogen-activated protein kinase (MAPK) pathway (O'Shea & Plenge, 2012; Ramji & Foka, 2002; Rummel, 2016). For example, the MAPK signalling pathway is often initiated by extracellular stimuli such as growth factors and cytokines (e.g., TNF-α and IL-1) (Keshet & Seger, 2010; Seger & Krebs, 1995). This leads to a cascade of phosphorylation events involving a series of kinases: an upstream MAP kinase kinase kinase (MAP3K), MAP kinase kinase (MAP2K), and the MAPK itself (Keshet & Seger, 2010; Seger & Krebs, 1995). These kinases activate sequentially, amplifying the signal at each step. The culmination is the phosphorylation and activation of MAPK, which can activate cytoplasmic NF-IL6 (Keshet & Seger, 2010; Seger & Krebs, 1995). Upon activation, cytoplasmic NF-IL6 is phosphorylated and translocated into the nucleus, where it upregulates the transcription of pro-inflammatory genes such as the cytokine IL-6 (Akira et al., 1990; Schneiders et al., 2015).

There is constant crosstalk between the inflammatory signalling pathways that feature these transcription factors. This is observed by more than one pathway regulating their activation and by the fact that these transcription factors converge in regulating the same or closely related inflammatory genes. Fuchs et al. (2013), for example, found a colocalization between STAT-3 and NF-IL6 and between NF-κB and NF-IL6 in PAMP-stimulated cell cultures. This highlights that these factors may be activated simultaneously, which could amplify the release of inflammatory molecules. More importantly, the nuclear translocation of these transcription factors presents a systematic way of measuring inflammation and the activation of inflammatory cells. This thesis takes advantage of this neuroinflammatory signalling and uses NF-IL6 nuclear translocation as a marker for microglial and astrocytic activation in an inflammatory challenge and in response to *Taenia* infection.

1.6 CURRENT MODELS FOR STUDYING DISEASE PROCESSES IN NEUROCYSTICERCOSIS

The major challenge in studying the neuroinflammatory mechanisms in neurocysticercosis is that there are limited experimental models of the disease. To date, the study of human NCC is commonly done in symptomatic patients using mostly neuroimaging and serological techniques (Carpio & Romo, 2014; De Lange et al., 2018). However, an undeniable drawback to this is that it is very difficult to control for important variables, such as the onset of the disease and the stage at which the disease has progressed (De Lange et al., 2018). Therefore, developing models that accurately recapitulate host-pathogen interactions whilst affording improved experimental control is essential for studying the disease. There are two facets to modelling human NCC, the first being the ability to accurately model the disease-causing cestode species (*T. solium*), and the second is modelling the host (Humans). It is thus challenging to model host-pathogen interactions at the correct stage of the disease. Here, I briefly describe some of the most commonly utilised *in vivo* and *in vitro* models to study the pathogenesis of NCC.

1.6.1 Tapeworm species used to study neurocysticercosis

The definitive cestode for investigating disease processes in NCC is *T. solium,* the disease-causing parasite in humans, whose lifecycle involves humans as definitive hosts and pigs as intermediate hosts (De Lange et al., 2018). The obvious limitation of using *T. solium* is that it is highly infectious to humans, and its utilisation within a laboratory context requires stringent biosafety measures. As a result, most studies that utilise *T. solium* are reported from naturally infected patients or pigs.

The closely related cestode, *Taenia crassiceps* (*T. crassiceps*), is thus commonly used within the laboratory setting. In the life cycle of *T. crassiceps*, wild canines are the definitive hosts of the parasite, and small mammals such as rodents are the intermediate hosts (De Lange et al., 2018). As such, it rarely infects humans (De Lange et al., 2018; Tsai et al., 2013). *T. crassiceps* is an attractive model organism as it shares the same genus and a robust antigenic and genetic similarity to the human disease-causing *T. solium* (De Lange et al., 2018; Tsai et al., 2013). Additionally, the ORF strain of *T. crassiceps* can divide asexually in the peritoneum of its intermediate

rodent hosts, making it easy to maintain a colony in the laboratory environment (Willms & Zurabian, 2010). A drawback to using a species that is not the disease-causing species in humans is that the transferability of findings to humans is not certain. There is always a possibility of species-specific immune responses not being accurately replicated in the model.

Another organism that is reasonably easy to use within the laboratory setting is *Mesocestoides corti (M. corti*), which infects canines and felines as definitive hosts and small mammals and reptiles as intermediate hosts (De Lange et al., 2018). *M. corti* have also been shown to divide asexually in their intermediate hosts, making colony maintenance possible (Alvarez et al., 2010). However, a significant drawback to using this species is that it is a different genus than *T. solium,* which increases the likelihood of substantial antigenic differences between the two (Matos-Silva et al., 2012). Additionally, in its natural life cycle, *M. corti* does not naturally enter or infect the CNS of its hosts, which is an essential aspect of *Taenia* infection and significantly limits the transferability of findings (De Lange et al., 2018).

All in all, *T. crassiceps* is likely the most attractive species to use in modelling NCC, providing a balance between sufficient similarity to *T. solium* and ease of use within the laboratory setting.

1.6.2 *In vivo* models of neurocysticercosis

Many *in vivo* studies investigating disease mechanisms in NCC utilise imaging techniques, brain tissue samples and serology in naturally infected NCC patients. However, a significant challenge with this approach is the lack of experimental control of variables such as stage of infection, type of infection, and even presenting symptoms. As such, many studies have attempted to control for these variables by injecting *T. solium* oncospheres into its intermediate pig host (De Aluja et al., 1996; Deckers et al., 2008; Fleury et al., 2015; Verástegui et al., 2000). Previously, most porcine models have used oral infection of *T. solium* eggs; however, this infection route often requires an extremely high number of eggs/inoculum and produces very variable and low rates of infection, especially in brain tissue (De Aluja et al., 1996; Deckers et al., 2008; Verástegui et al., 2000). This makes it difficult to study some of the basic and fundamental neuroimmune questions in NCC. Whilst naturally infected pigs may help overcome some of these shortcomings (Fleury et al., 2015), there

remain too many uncontrolled variables to make it an effective model. More recently, researchers have injected activated oncospheres directly into the carotid arteries of pigs, recapitulating how the oncospheres enter the brain via the BBB, and this model has yielded more than 66.6% success rate in recreating a cyst burden in the CNS that is similar to the human infection (Alroy et al., 2018). This model could be crucial in studying the pathogenesis of NCC, especially because the wild-type CNS infection also occurs through vascular structures.

Much research on NCC has also been done in *in vivo* rodent models via intracranial injection of *Taenia* larvae into the brains of mice and rats (Garza et al., 2010; Matos-Silva et al., 2012; Stringer et al., 2003). However, because of how large larvae from *T. crassiceps* and *T. solium* are, it is generally quite challenging to inject them directly into rodent brains. This is because injecting into the brain parenchyma of rodents would on its own cause injury and inflammation, making studying the neuroimmune responses to the parasite difficult. As such, homogenate made from the larvae of parasites is sometimes applied to *ex vivo* brain tissue (Garza et al., 2010). *In vivo* models of NCC may, however, recapitulate disease processes better, especially neuroimmune mechanisms in response to cestode infection. Cardona et al. (1999), for example, demonstrated that recruitment of infiltrating peripheral immune cells in extra parenchymal brain regions in an *in vivo* rodent model of NCC occurs as soon as two days post-infection. *In vivo* studies in mice intracranially injected with *T. crassiceps* have also demonstrated essential aspects of NCC, including that tissue surrounding cysts contains inflammatory infiltrating cells, collagen, and perivascular infiltrate (Verastegui et al., 2015). In addition, one *in vivo* study has shown that injections with cyst granuloma extracts cause seizures in the host; another demonstrated that it is the Substance P in the granuloma extracts that causes seizures (De Lange et al., 2018; Garza et al., 2010; Matos-Silva et al., 2012; Stringer et al., 2003).

Genetically altered animal models are another avenue that could prove crucial in studying the mechanisms of disease progression in NCC. While this is currently a hugely underexplored area in the study of NCC, there is the capacity to develop and help exploration of unelucidated questions in the disease. A research group pioneering some of this research was successfully able to transfect a pcDNA3.1/NT-GFP-TOPO plasmid into *T. crassiceps* cysts, making them express green fluorescent protein

(GFP) that they could then visualise and track through fluorescence microscopy (Moguel et al., 2015; Steyn et al., 2022). This could be important as it would allow for *in vivo* localisation of the parasite. With that, such genetic models also make it possible to elucidate and characterise signalling pathways and even investigate protein-protein interactions in the disease (Moguel et al., 2015; Quinzo et al., 2022). Developing transgenic animals sensitive to cysticerci could also be crucial to investigating this disease's pathogenesis.

While *in vivo* models have been important in highlighting essential aspects of inflammatory responses in NCC, they do not allow for cell-type specific tracking of innate immune competent cells. In addition, they do not allow for the observation of innate immune responses in isolation from peripheral adaptive immune responses.

1.6.3 *In vitro* models of neurocysticercosis

Many *in vitro* studies have been done to investigate disease processes in NCC. Firstly, serum from NCC patients has been analysed for cytokines and other inflammatory markers. These have been instrumental in highlighting that asymptomatic NCC patients present with high levels of Th2 anti-inflammatory cytokines in their serum, whereas symptomatic patients present with high levels of Th1 pro-inflammatory cytokines (Verma et al., 2011). In addition, histological analyses have also been done on human brain tissue from NCC patients, where it has been demonstrated that lesions associated with NCC present with oedema, gliosis, and fibrosis (Ericson Dametto, 2016; L'Ollivier et al., 2012).

Cultured cell lines derived from human and animal nervous tissue have also been utilised to investigate cellular and molecular mechanisms in NCC (Amit et al., 2011; Chile et al., 2016; Palma et al., 2019; Prasad et al., 2009; Uddin et al., 2005, 2010). One study, for example, stimulated human-derived astrocytes and monocytes with *T. solium* larvae to investigate its regulation of chemokine secretion and found that there was rapid accumulation of CCL2 and CXCL8 in astrocytes as soon as 1-hour post-treatment (Uddin et al., 2005). Another study that treated human-derived lymphocytes with various extracts of *T. solium* larvae found that only cyst fluid elicited an inflammatory response as characterised by increased lymphocyte proliferation (Amit et al., 2011).

To the best of my knowledge, no study has utilised *in vitro* models that have allowed for the tracking of cell-type specific inflammatory responses of microglia and astrocytes during *Taenia* infection at the same time. Thus, aspects of this thesis employ the organotypic brain slice culture system that preserves all innate glia and neurons to investigate inflammatory mechanisms in this infection.

1.7 ADDRESSING GAPS IN THE CURRENT UNDERSTANDING OF NCC

Although much research has been done to investigate cellular and inflammatory mechanisms in NCC, there are still multiple gaps in the literature that prevent a comprehensive understanding of this infection. Most studies investigating the inflammatory mechanisms in this disease use serum from naturally infected patients who present with seizures. As such, most work has mainly investigated inflammatory responses in patients with transitional and calcified cysts, with minimal work investigating processes during the viable/vesicular stage. Additionally, no current *in vitro* model allows for the tracking of cell-type specific inflammatory responses of innate resident CNS cells in isolation from the peripheral immune response.

Therefore, I set out to establish *in vitro* models of neuroinflammation using both rodent and human organotypic brain slice cultures to investigate inflammatory mechanisms in NCC (**Aim 1 and 3**). Applying *T. crassiceps* homogenate prepared from viable larvae to rodent organotypic brain slice cultures (**Aim 2**) allowed me to model the vesicular/viable stage of the disease. These models allowed me to explore cell-type specific inflammatory responses of microglia, astrocytes, and neurons, using both inflammatory markers and pro-inflammatory cytokines release. I also explored whether *T. crassiceps* larvae affect the transcription of inflammatory genes in both microglia and astrocytes.

1.8 AIMS

Aim 1: To establish the rodent-derived organotypic brain slice culture system as an *in vitro* model for studying neuroinflammatory signalling in the brain.

Aim 2: To investigate the neuroimmune response to *Taenia* infection using mouse organotypic brain slice cultures.

Aim 3: To establish a translational *in vitro* human brain-based slice culture system for studying neuroinflammatory signalling in the brain.

1.9 OBJECTIVES

Aim 1: To establish the rodent-derived organotypic brain slice culture system as an *in vitro* model for studying neuroinflammatory signalling in the brain.

1.1 Characterize the composition and distribution of microglia, astrocytes, and neurons in organotypic brain slice cultures.

1.2 Measure the activation of microglia, astrocytes, and neurons in organotypic brain slice cultures in response to an inflammatory challenge.

1.3 Measure concentrations of pro-inflammatory cytokines released in culture medium by organotypic brain slice cultures following an immunogenic agent.

1.4 Investigate gene expression changes of key inflammatory genes in microglia and astrocytes in response to an immunogenic challenge.

1.5 Confirm the protein expression of genes upregulated following an inflammatory challenge in microglia and astrocytes using immunofluorescence staining.

Aim 2: To investigate the neuroimmune response to *Taenia* infection using mouse organotypic brain slice cultures.

2.1 Determine whether *Taenia* larvae exert a cytotoxic effect on microglia and astrocytes in organotypic brain slice cultures.

2.2 Measure how *Taenia* larvae affect microglial and astrocytic activation in organotypic brain slice cultures.

2.3 Measure how *Taenia* larvae attenuate concentrations of pro-inflammatory cytokines released in culture medium by organotypic brain slice cultures.

2.4 Determine the active anti-inflammatory agent in *Taenia* larvae using size exclusion fractionation and chromatography.

2.5 Investigate how *Taenia* larvae alter gene expression of key inflammatory genes in microglia and astrocytes.

Aim 3: To establish a translational *in vitro* human brain-based slice culture system for studying neuroinflammatory signalling in the brain.

3.1 Characterize the composition of microglia, astrocytes, and neurons in human acute and untreated organotypic brain slice cultures.

3.2 Measure the differences in the activation of microglia, astrocytes, and neurons between human acute slices and untreated human organotypic brain slice cultures.
3.3 Quantify the concentrations of the pro-inflammatory cytokine IL-6 released in the culture medium by human organotypic brain slice cultures over a 7-day culture period.
3.4 Measure the activation of microglia, astrocytes, and neurons in human organotypic brain slice cultures following an immunogenic challenge.
3.5 Quantify the concentrations of pro-inflammatory cytokines released in culture medium by human organotypic brain slice following an inflammatory challenge.

CHAPTER 2

MATERIALS AND METHODS

All reagents used were procured from Sigma-Aldrich (Merck) unless otherwise stated.

All animal handling, care and procedures were performed as prescribed by the South African National Standard (South African Bureau of Standards, 2008) and as authorised by the University of Cape Town Animal Ethics Committee (Protocols: AEC 019/025, AEC 022/018, AEC 018/010, AEC 021/026). Animal rooms were maintained between 20 – 24 °C, a lux of 100 – 300, and animals had unlimited access to food and water. Human brain tissue was obtained from patients undergoing epilepsy neurosurgery at Red Cross War Memorial Children's Hospital or Mediclinic Constantiaberg in Cape Town, South Africa, and use was authorised by the University of Cape Town Human Research Ethics Committee (Protocol: HREC 016/2018).

2.1 *TAENIA* MAINTENANCE AND PREPARATION OF WHOLE CYST HOMOGENATE

2.1.1 Intraperitoneal infection of *T. crassiceps* larvae

T. crassiceps larvae (ORF strain), which were donated by Dr Siddhartha Mahanty (NIH, Maryland, USA), were propagated *in vivo* by serial intraperitoneal infection of 5 – 8 week-old female C57BL/6 mice. In short, 20 small and motile larvae were selected into a 1 ml syringe and injected into the mouse intraperitoneally using a 20-gauge needle (B&M Scientific); 8 mice were injected every 12 weeks to maintain the *T. crassiceps* colony. After 12 weeks, mice were euthanised using halothane overdose, followed by cervical dislocation as a secondary confirmation of death. Larvae were harvested by peritoneal lavage and rinsed six times in phosphate-buffered saline (PBS; pH 7.4; Whitehead Scientific). A select number of these larvae were then used to re-infect a new set of 8 mice, and the rest were stored at -80 °C for use in subsequent experiments. During the 12-week period in which the colony mice were infected, they were monitored daily for welfare and weighed weekly to track changes in their body weight.

2.1.2 Preparation of *T. crassiceps* whole cyst homogenate

***T. crassiceps* whole cyst homogenate** was prepared by Dr Anja de Lange. Immediately after harvesting, *T. crassiceps* larvae were frozen at -80 °C. On preparation day, the larvae were thawed (thereby lysing the cells) and suspended in PBS containing a protease inhibitor cocktail (1% vol/vol) in a ratio of 1:3 (larvae volume: PBS volume). The larvae were then homogenised on ice using an electronic tissue homogeniser (Polytron, PT 2500E, Kinematica) and a 40 ml Dounce glass tissue grinder. The resulting mixture was centrifuged at 3100 *g* for 20 minutes at 4 °C (5810 R, Eppendorf). The liquid supernatant (between the white floating layer and the solid pellet) was then collected and sterilised through a 0.22 µm size filter (Millex-GV syringe filter). The supernatant was aliquoted and stored at -80 °C for later use in experiments as *T. crassiceps* homogenate.

Ammonium sulphate-treated *T. crassiceps* whole cyst homogenate (50% AS > 100 kDa *T. crassiceps* homogenate). For bulk precipitation of proteins, 6 ml of whole cyst *T. crassiceps* homogenate at a concentration of 1.7 mg/ml was gradually saturated with ammonium sulphate on ice. The saturation was increased to a concentration of 50% by adding ammonium sulphate in increments, ensuring thorough mixing between each addition. Proteins were then precipitated by centrifugation at 3000 *g* for 30 minutes, and the residual homogenate was resuspended in 1000 µL of PBS. To remove impurities and salts, desalting was performed using Millipore Amicon-Ultra 0.5 centrifugal filters (100 kDa MWCO), as per the manufacturer's instructions. To ensure sterility, the solutions were further filtered through a 0.22 µm filter (Millex-GV syringe filter).

The protein concentrations of both the ***T. crassiceps* whole cyst homogenate** and **50% AS > 100 kDa *T. crassiceps* homogenate** were subsequently assessed using a bicinchoninic acid (BCA) assay kit (BCA protein assay kit, Merck) as per manufacturers' instructions.

2.2 ORGANOTYPIC BRAIN SLICE PREPARATION AND TREATMENT

2.2.1 Mouse hippocampal organotypic brain slice preparation

Hippocampal organotypic brain slices were prepared from 6 - 8 day-old C57BL/6 mice; a detailed protocol for organotypic culturing can be found in our published paper by Awala et al. 2023. Briefly, mouse brains were extracted after cervical dislocation and immediately placed in ice-cold (4 °C) dissection medium containing Earle's balanced salt solution (EBSS) supplemented with 6.1 g/l of 4-(2-hydroxyethyl)-1-piperazineethanesulfonic acid (HEPES), 6.6 g/l of D-glucose and 5 µM of saturated sodium hydroxide. The brain was separated by hemisphere, and the hippocampi were dissected out and sectioned into 350 µM slices using a McIlwain tissue chopper (Brinkmann, Mickle). Cold dissection medium was then used to rinse and separate the slices from each other. The slices were quality controlled for intact architecture and structural integrity using a light microscope and then placed onto Millicell-CM cell culture inserts in a 6-well plate (6 slices were plated on each culture insert). These slices were maintained in culture medium (1.2 ml per well) containing (vol/ vol): 50% minimum essential medium (MEM) with Glutamax, 23% EBSS, 25% heat-inactivated horse serum (Biochrom), 2% B27 and 6.5 g/l D-glucose. Slices were stored in a humidified incubator at 37 °C and 5% CO_2 with medium change every 2 to 3 days.

2.2.2 Acute and cortical human organotypic brain slice preparation

Acute and cortical organotypic human brain slices were prepared from cortical brain tissue obtained from patients undergoing epilepsy surgeries at the various collaborating hospitals in and around Cape Town. Patients were required to provide written informed consent to participate in the study. All tissue resected and collected was excess tissue from the anterior medial temporal cortex that had to be removed as part of a temporal lobectomy. The tissue utilised was not from the epileptic focus, displayed no structural abnormalities and was neither gliotic nor necrotic, as stipulated in Verhoog et al. (2013). Immediately after resection, tissue was placed in ice-cold 1X choline artificial cerebrospinal fluid (aCSF) slicing solution consisting of (in mM): 110 choline chloride, 26 $NaHCO_3$, 10 D-glucose, 11.6 sodium ascorbate, 7 $MgCl_2$, 3.1 sodium pyruvate, 2.5 KCL, 1.25 NaH_2PO_4, and 0.5 $CaCl_2$. The aCSF was cooled and bubbled with carbogen (95% O_2, 5% CO_2) for 30 minutes before use. The tissue was

then transported to the Raimondo lab facilities within the recommended transition time of approximately 10-15 minutes (Mohan et al., 2015). Cortical brain slices of 250 µm thickness were then prepared using a Compresstome. Some of the sectioned brain slices were immediately fixed with ice-cold 4% paraformaldehyde (PFA) for 16 hours at 4 °C in preparation for immunofluorescence staining (as acute slices). The remaining brain slices were plated and cultured on Millicell-CM cell culture inserts in 6-well plates (2 slices were plated on each culture insert) for use as human organotypic brain slice cultures. These slices were maintained in human culture medium (1.2 ml per well) consisting of 100 ml of heat-inactivated horse serum, 1 mg/ml of insulin and (in mM): 30 HEPES, 13 D-glucose, 15 $NaHCO_3$, 1 ascorbic acid, 2 $MgSO_4$. $7H_2O$, 1 $CaCl_2$. $2H_2O$, 0.5 GlutaMax. Slices were stored in a humidified incubator at 37 °C, and 5% CO_2 with culture media changed and collected every two days for subsequent cytokine analysis.

2.2.3 Treatment of mouse hippocampal and human organotypic brain slices

Six days post-culture, rodent brain slices were treated with whole cyst *T. crassiceps* homogenate alone or concurrently with LPS to elicit an inflammatory response. Treatment was administered via the culture medium. There were four experimental groups for these experiments: 1) an untreated control group, which received fresh culture medium and served as an experimental control; 2) an LPS (10 ng/ml) treatment group, which served as a positive control for inflammation; 3) a whole cyst *T. crassiceps* homogenate group (200 µg/ml) to model the viable *Taenia* infection; 4) and finally a co-treatment of both LPS (10 ng/ml) and whole cyst *T. crassiceps* homogenate (200 µg/ml) to investigate the potential immunomodulatory effects of *Taenia* larvae on inflammation.

For inflammatory characterisation of human organotypic brain slice cultures (hOBSCs), slices were treated in two experimental groups: 1) a control group that received fresh culture medium; or 2) an LPS (10 ng/ml) treatment group. Slices were treated for 24 hours, after which the medium was collected for cytokine analysis, and tissue was utilised for either immunofluorescence staining or single nucleus RNA-sequencing experiments.

2.3 IMMUNOFLUORESCENCE STAINING

2.3.1 Mouse hippocampal organotypic brain slices

After the 24-hour treatment period, brain slices were collected from culture and immediately fixed with 4% PFA at 4 °C for 20 minutes. The brain slices were then permeabilised for 3 x 10 minutes in a wash buffer (0.3% Triton X- 100 in PBS) before blocking for 4 hours in a blocking buffer (5% bovine serum albumin (BSA), 1% Triton X-100 in PBS). After blocking, brain slices were incubated in primary antibodies solution overnight at 4 °C. Primary antibodies used for this study, and their dilutions are described in **Table 2.1**. Following primary antibody incubation, brain slices were rinsed with wash buffer three times for 10 minutes and thereafter incubated with secondary antibody solution for 5 hours at room temperature. Secondary antibodies used for this study and their dilutions are described in **Table 2.1**. After three successive 10-minute rinses with wash buffer, brain slices were incubated with nuclear stain (Hoechst) for 15 minutes, followed by a final 10-minute rinse in PBS. Slices were then mounted on slides with an aqueous mounting medium (Mowiol), coverslipped, and stored at 4 °C pending microscopic analysis.

2.3.2 Acute and cortical human organotypic brain slices

The staining procedure for human acute and organotypic brain slices required slices to be fixed for either 16 hours or 20 minutes with 4% PFA at 4 °C, respectively. This was followed by overnight permeabilization in a wash buffer (1% Triton X-100 in PBS). Brain slices were then blocked for 4 hours at room temperature with a blocking buffer (5% BSA, 1% Triton X-100 in PBS). After blocking, brain slices were incubated in primary antibody solution overnight at 4 °C. Primary antibodies used for this study, and their dilutions are as described in **Table 2.1**. The rest of the staining procedure follows the same protocol as that of rodent OBSCs, as detailed in the previous section (i.e., **Section 2.3.1**).

Table 2.1 Antibodies used in immunofluorescence staining experiments

Target	Antibody	Dilution in blocking buffer	Manufacturer & catalogue number
	Primary antibodies:		
Microglia	IBA1 (rabbit monoclonal)	1:250	Abcam (ab178846)
Microglia	IBA1 (goat polyclonal)	1:250	Nuvos Biological (nb100-1028)
Astrocytes	S100β (rabbit monoclonal)	1:250	Abcam (ab52642)
Astrocytes	S100β (mouse polyclonal)	1:250	Thermo Fisher (ma125005)
Astrocytes	GFAP (goat polyclonal)	1:250	Abcam (ab53554)
Neurons	NeuN (rabbit monoclonal)	1:250	Abcam (ab177487)
NF-IL6	C/ebpβ (mouse monoclonal)	1:2000	Santa Cruz Biotechnology (sc-7962)
Timp1 protein	Timp1 (rabbit monoclonal)	1:250	Thermo Fisher (pa589507)
Ccl5 protein	Ccl5 (rabbit monoclonal)	1:250	Thermo Fisher (710001)
Pik3ap1 protein	Pik3ap1 (rabbit monoclonal)	1:250	Thermo Fisher (bs-13675r)
Lcn2 protein	Lcn2 (rabbit monoclonal)	1:250	Thermo Fisher (pa5-79590)
	Secondary antibodies:		
	Donkey anti-rabbit Alexa Fluor 488	1:250	Abcam (ab150073)
	Donkey anti-rabbit Alexa Fluor 647	1:250	Abcam (ab150075)
	Donkey anti-goat Alexa Fluor 488	1:250	Abcam (ab150129)
	Donkey anti-mouse Alexa Fluor 647	1:250	Abcam (ab150107)
	Donkey anti-mouse Cy^3	1:250	Jackson ImmunoResearch (715-165-150)
	Other: Hoechst nuclear marker	1:5000	Thermo Fisher (62249)

Key: IBA1= Ionized calcium-binding adaptor molecule 1; S100β=S100 calcium-binding protein beta; GFAP= Glial fibrillary acidic protein; NeuN= Neuronal nuclei, C/ebpβ= CCAAT/enhancer binding protein beta; NF-IL6= transcription factor nuclear factor interleukin 6; Timp1= Tissue inhibitor of metalloproteinase 1; Ccl5= Chemokine ligand 5; Pik3ap1= Phosphoinositide 3-kinase adapter protein 1, Lcn2= Lipocalin 2.

2.4 IMAGING AND QUANTIFICATION

2.4.1 Imaging of mouse hippocampal organotypic brain slices

An LSM 880 airyscan confocal microscope (Carl Zeiss, Zen SP 2 Software) with 20X, 40X, and 63X objectives (Zeiss) was used to acquire images from immunofluorescence-stained mouse brain slices. Data was collected from the cornu armmonis 3 (CA3), a hippocampal region associated with seizure generation and epileptogenesis (Barbarosie & Avoli, 1997; Song et al., 2018; Zhang et al., 2017). To locate the CA3 region, a full slice tile scan was performed on the Hoechst channel using the 20X objective. Using the position function, two positions/regions were selected in the CA3 region on the full slice tile scan. A detailed z-stack with a 0.7914 µm z-interval was then performed on the two selected regions at 40X magnification, capturing the region from the top to the bottom of the slice (these z-stacks ranged from about 18 – 23 µm in thickness and were 212.5 x 212.5 µm in area). This was done using the channel with the glia as a guide (either the Alexa Fluor 488 channel or the Alexa Fluor 647 channel) to ensure that the entire selected z-plane was imaged from top to bottom. These 40X z-stack images were transferred into the ImageJ software (National Institutes of Health, USA) for cell counts and quantification of activation. High-resolution images illustrating the morphology of microglia (IBA1), astrocytes (S100β), and neurons (NeuN) were obtained using the 63X oil objective.

2.4.2 Imaging of human acute and organotypic brain slices

Both human acute and organotypic brain slices were imaged using an LSM 880 airyscan confocal microscope (Carl Zeiss, Zen SP2 software) with 40x and 63x objectives (Zeiss). Because of the considerably larger size of these slices, a two-layer z stack (with a 10 µm z-interval) with a 3 x 3 tile scan was performed on two regions on each slice at 40X magnification (each region being 616 x 616 µm in area). Again, this was performed using the channel with the major glia stain as a guide (either the Alexa Fluor 488 or Alexa Fluor 647 channel). These 40X z-stack images were

transferred into the ImageJ software for cell counts and activation quantification. High-resolution images illustrating the morphology of microglia (IBA1), astrocytes (GFAP), and neurons (NeuN) in human acute and hOBSCs were obtained using the 63X oil objective.

2.4.3 Cell counts and activation analyses in ImageJ

We used a custom-built ImageJ cell counter macro (script) to quantify cell numbers and conduct colocalization analyses to determine cell activation. Briefly, each channel was assigned a channel number: Hoechst (blue channel), IBA1/S100β/GFAP/NeuN (green channel), and NF-IL6 (red channel) as channels 1, 2, or 3, respectively. Important constants were set, including a minimum and maximum cell size of 16 and 160 μm^2, respectively. The number of Hoechst-stained cells in each image was then determined using Huang's method of thresholding (Huang & Wang, 1995), which ultimately was used to determine what the macro recognises as a cell. This was followed by conversion for masking, de-speckling, watershed segmentation, and particle analysis. The macro then determined which cells were positive for certain markers. For instance, cells were designated as NF-IL6 positive if more than 40% of their nucleus area was red (based on the colocalization with the Hoechst staining). Similarly, a cell was classified as a 'green cell', i.e., microglia, astrocyte, or neuron, if more than 65% of its Hoechst area/nucleus was green.

The macro facilitated counting the total number of cells in each image (total Hoechst positive cells), red cells (NF-IL6 positive cells), green cells (IBA1/S100β/GFAP/NeuN positive cells), and red positive green cells (which are IBA1/S100β/GFAP/NeuN positive cells that colocalize with the nuclear red/NF-IL6 signal). Overall, this image analysis pipeline allowed us to quantify cell populations with different marker expressions in both rodent and human tissue in a standardized, non-biased, and automated manner.

2.4.4 Mean fluorescence intensity analysis in ImageJ

For the validation experiments, where I triple stained cell type-specific markers for glia together with genes that were upregulated in response to LPS (as per snRNA-sequencing findings), I used the Z-axis profile function in ImageJ to visualise potential differences in protein expression between the various treatment groups. This function

allows for the effective measurement of the overall mean fluorescence intensity of pixels between images, where increases in mean fluorescence intensity represent increases in the protein expression of the stained gene.

2.5 SINGLE NUCLEUS RNA-SEQUENCING

The single nucleus RNA-sequencing datasets were generated through the 10X Genomics interface (*Chromium Next GEM Single Cell V(D)J Reagent Kits v1.1 with Feature Barcode Technology for Cell Surface Protein*, 2021). For each condition (control, *T. crassiceps* homogenate, LPS, and LPS and *T. crassiceps* homogenate), thirty-six OBSCs were treated for 24 hours and stored at -80 °C. On the day of the experiment, samples underwent a nuclei isolation step where they were homogenised using a micro tissue grinder and lysed in a cell-lysis buffer (Nuc-101 kit, Merck). Samples were then incubated on ice, centrifuged for 5 minutes, and the supernatant removed. The pellet was resuspended in more lysis buffer and centrifuged once more, after which the residual pellet was resuspended in a nuclear suspension buffer (1% BSA, 0.1% RNAse inhibitor). The cell viability was assessed using trypan blue staining with a target viability set at less than 5%. The samples were then made up to 2 ml, filtered through a 40 µm filter and the number of nuclei was counted using a haemocytometer. Nuclei solutions were then diluted to achieve the target number of nuclei (700—1000/µl) required for sequencing.

snRNA-sequencing runs were conducted according to the Chromium Next GEM 3' Single Cell 3 Reagent Kits v3.1 user guide. For each run, between 6000 – 10000 nuclei were targeted. The samples were diluted using nuclease-free water, to which a Master Mix was added (59.1% RT Reagent B, 7.5% Template Switch Oligo, 6.3% Reducing Agent B, and 27.4% RT Enzyme C). This combination of the diluted nuclear suspension and Master Mix was then loaded into the first row of wells on the 10X Genomics Single cell 3'chip. The corresponding wells in the second row were filled with Gel Beads, and the third row with Partitioning Oil. The remaining unused wells of the chip were filled with a 50% glycerol solution. The 10X Gasket was then attached to the chip and placed into the 10X Genomic Chromium Controller. This device uses microfluidics to capture individual nuclei within oil droplets and attach barcoded beads for subsequent nuclei identification. Subsequent steps included reverse transcription within the droplets to convert RNA into cDNA and barcode attachment to the cDNA

transcripts. This was followed by the construction of cDNA libraries, which involved PCR amplification of cDNA, size selection of transcripts, adaptor ligation for sequencing, and index addition for sample-specific demultiplexing with Illumina (Illumina Inc., USA). Following quality control checks post-library construction, the samples were sequenced using the Illumina Novaseq 6000 S2 flow cell according to manufacturer recommendations. Finally, the raw base calls were demultiplexed to produce individual FastQ files for each sample.

Sequenced data was further computationally analysed by Ms Teresa Steyn in the following abridged manner. The data, mapped to a mouse reference transcriptome from 10X Genomics, was filtered to remove poor-quality nuclei and potential doublets utilising various doublet-identifying tools such as DoubletFinder (McGinnis et al., 2019) and Scrublet (Wolock et al., 2019). The datasets were then normalised, the variance stabilised, and samples were integrated with other pre-existing datasets from our lab. A Principal Component Analysis (PCA) helped group cells, forming 30 different cell clusters. These clusters were annotated via automated tools and manual inspections, along with a label transfer method using the Allen Institute Mouse Brain atlas. The clusters were then tested for differential gene expression between control and LPS groups using the DESeq2 package (Love et al., 2014), with an adjustment for batch variations, and differentially expressed genes were ranked according to their Log2FoldChange.

2.6 ENZYME-LINKED IMMUNOSORBENT ASSAYS (ELISAs)

The concentrations of pro-inflammatory cytokines interleukin-6 (IL-6) and tumour necrosis alpha (TNF-α) released by brain slices in culture medium (for both mice and human OBSCs) were assessed using sandwich enzyme-linked immunosorbent assays (ELISAs). In short, after a 24-hour treatment period, culture medium from each well was collected. ELISA plates (Nunc Maxisorp 96-well plate, Thermo Fisher) were then coated with capturing antibodies (human/mouse IL-6 and TNF-α, R&D systems) and incubated at room temperature overnight. The plates were washed three times with a wash solution (1 % Tween in PBS), after which they were incubated in a blocking buffer (4% BSA, 0.02% NaN_3 in PBS) at 4 ºC overnight. After three more washing steps, the plates were subsequently incubated with the samples (culture medium) and

prepared cytokine standards (Recombinant human/mouse IL-6 and TNF-α, R&D systems) overnight at 4 ºC. Following another three rounds of washing, the detection antibodies (Human/mouse Biotinylated IL-6 and TNF-α, R&D systems) were added and incubated at 37 ºC for 1 hour. This was followed by a final set of three washes and 1-hour incubation with streptavidin-alkaline phosphatase (SaV-AKP, Ascendis Medical). Finally, the plates were incubated with phosphatase substrate in the dark for 30 minutes. The plates were then read using a microplate reader (GloMax Discover, Promega). Cytokine data was exported to GraphPad Prism (Version 9) for subsequent analysis. A detailed protocol for the detection of these cytokines was developed by Dr Anja De Lange and is available online (De Lange et al., 2020).

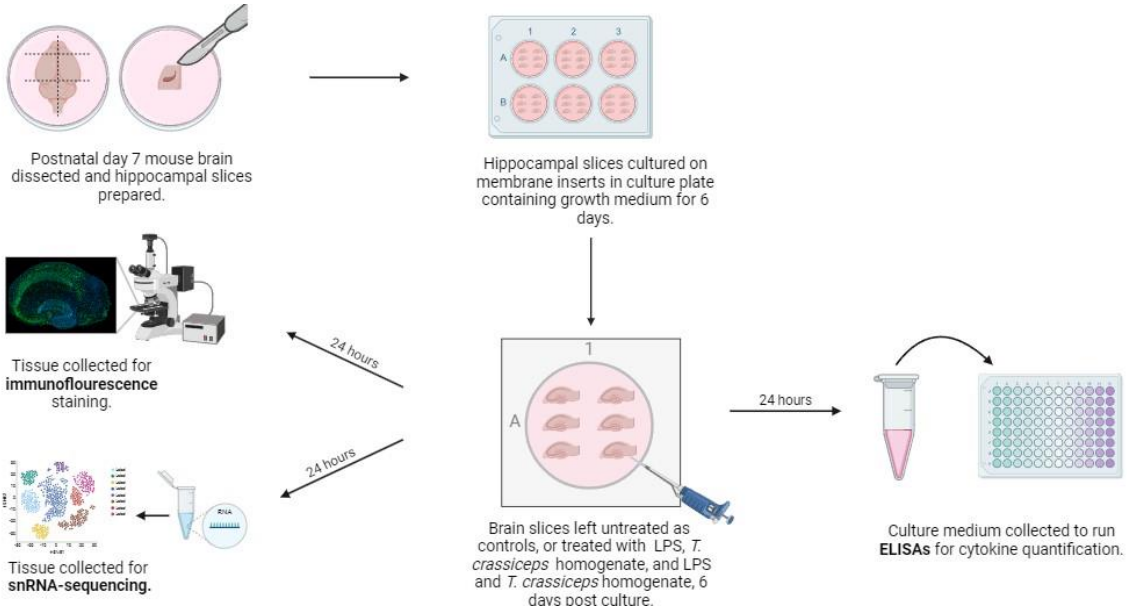

Figure 2.1 Modelling acute immune activation and *Taenia* infection in mouse hippocampal organotypic brain slice culture. Illustration of our experimental setup showing hippocampal organotypic brain slices prepared from post-natal day 7 mice and cultured for 6 days. Slices were treated for 24 hours with either regular growth medium (CTR), 10 ng/ml LPS (LPS), 200 ug/ml *T. crassiceps* homogenate (Hom); or both 10 ng/ml LPS and 200 ug/ml *T. crassiceps* homogenate (LPS+Hom). Slices were either used the snRNAseq experiments or fixed in 4% PFA for the immunofluorescent staining experiments. Enzyme-linked immunosorbent assays (ELISAs) were carried out on the growth media to measure the concentrations of interleukin-6 (IL-6) and tumor necrosis factor alpha (TNF-α).

2.7 SIZE EXCLUSION CHROMATOGRAPHY

The **50% AS > 100 kDa *T. crassiceps* homogenate** prepared in **Section 2.1.2** was subjected to size exclusion chromatography (SEC) for further separation. This was done in collaboration with Dr Jeremy Woodward, who ran the homogenate through the TSKgel G5000PWxl column (Tosoh Bioscience) specifically designed for separating high molecular weight compounds of up to 1000 kDa. The protein solution was injected into the column, and elution was monitored. This process separates proteins according to their sizes, and larger proteins, due to their inability to penetrate the porous structure of the resin beads within the column, were eluted earlier from the column. In contrast, smaller proteins, which can permeate into the bead pores, were eluted later. This process effectively enabled the separation of proteins in our *Taenia* homogenate (50% AS > 100 kDa *T. crassiceps* homogenate) so that, in the end, about 62 different fractions were obtained (based on their size). These were later used to treat rodent OBSCs to try and characterise the active anti-inflammatory agent in *Taenia larvae*.

2.8 DATA ANALYSIS AND STATISTICS

Data was analysed and graphed using Microsoft Excel 2019 and GraphPad Prism v9. Adobe Illustrator vCS6 was used for figure generation.

Both parametric and non-parametric tests were used to analyse data in this study. The parametric test utilized was a one-way analysis of variance (ANOVA) with Tukey's Multiple Comparisons test, where data was presented as the mean and standard error of the mean (SEM). The non-parametric tests used were the Mann- Whitney U test (where data was presented as the mean and SEM) and Kruskal- Wallis ANOVA with Dunn's multiple comparisons tests (where data was presented as the median and interquartile range). The confidence interval for all the statistical analyses was 95%; as such, only the differences where $p \leq 0.05$ were considered statistically significant.

In the immunofluorescence experiments, 'N' represents the number of brain slices, while 'n' signifies the number of imaged regions per brain slice. This distinction is important for accurately interpreting the data and understanding the scope of our analysis. The number of imaged regions per slice ('n') provides a more detailed analysis of the variability and specific characteristics within individual slices, allowing us to assess the consistency and heterogeneity of the fluorescence staining across different areas of the same slice. We thus chose to use the Standard Error of the Mean (SEM) to quantify the variability of our measurements.

In our immunofluorescence/microscopy analysis, we utilized N = 3 brain slices to ensure precise and high-resolution examination of specific regions, also allowing for the maintenance of consistent and controlled experimental conditions. For the soluble pro-inflammatory cytokine analysis using ELISAs, an N of up to 40 was reported owing to the fact that we could pool data from various experiments.

Throughout this thesis, cell count/ cell activation, cytokine, and snRNA-sequencing data from control and LPS conditions presented in Chapter 3 were later also presented in Chapter 4 for comparison with the *T. crassiceps* homogenate, and LPS and *T. crassiceps* homogenate treatment groups.

CHAPTER 3

ESTABLISHING AN *IN-VITRO* MOUSE MODEL FOR STUDYING INFLAMMATORY SIGNALLING IN THE BRAIN

3.1 INTRODUCTION

Central nervous system (CNS) infections are debilitating and have an incredibly high burden of mortality and morbidity (Robertson et al., 2019). Many of these infections, such as the parasitic disease neurocysticercosis, are known to be accompanied and worsened by an inflammatory milieu (Cangalaya et al., 2016; Toledo et al., 2018). Yet, there is still limited knowledge on the neuroinflammatory mechanisms in this infection, and especially how various immune competent glia respond and contribute to inflammation. This is mainly because there is a lack of reliable experimental models to accurately track and measure cell-type specific inflammatory changes at the molecular level in these infections.

In vivo animal models of neuroinflammation have been the gold standard for investigating inflammatory brain mechanisms (Nazem et al., 2015). While these have been important in highlighting the intricate interactions between different cell types and inflammatory mediators such as cytokines, chemokines and infiltrating peripheral immune cells during neuroinflammation (Lyman et al., 2014), they make it challenging to gain information on cell-type specific neuroinflammatory changes. Additionally, these *in vivo* models do not permit the study of innate immune responses in isolation and separate from the adaptive immune system. Cell cultures and cell lines of innate cells have thus been used as an alternative to overcome some of these challenges; however, the sequential passage of cell lines has been implicated in genetic and phenotypic differences in cells in these models (Kaur & Dufour., 2012). Gosselin et al. (2017), for example, observed fast and extensive alterations in gene expression after 6 hours in a primary culture of microglial cells. As such, there remains a need for neuroinflammatory models that allow the tracking of specific cell types and potentially their interactions during inflammatory conditions. Therefore, this chapter aimed to use

an *in vitro* mouse model of neuroinflammation to investigate cell-type specific inflammatory responses in the brain.

To address this, I used mouse hippocampal organotypic brain slice cultures (OBSCs), which preserve all innate glia and neurons (Croft et al., 2019). OBSCs have previously been used to study neuroinflammation in the brain by application of pro-inflammatory stimulants, where they have revealed important aspects of the inflammatory response, including morphological changes of glial cells, cytokine release, and even transcriptomic changes during an inflammatory challenge (Bernardino et al., 2008; Chong et al., 2018; Delbridge et al., 2020; Huuskonen et al., 2005; Papageorgiou et al., 2016). Nonetheless, it was essential to further establish and verify this model system in my hands.

I confirmed the presence and intact morphology of microglia, astrocytes, and neurons in OBSCs using immunofluorescence staining. LPS-challenged OBSCs were then used to mimic an inflammatory environment and observe changes in glial activation. I found that LPS increased the activation of both microglia and astrocytes in OBSCs. This activation was observed by the colocalization of IBA1 and S100β signalling with the inflammatory transcription factor NF-IL6. LPS treatment also increased the concentrations of pro-inflammatory cytokines IL-6 and TNF-α released by OBSCs in the culture medium. Finally, I found that LPS induced an upregulation of key inflammatory genes, including *Cebpβ* (NF-IL6), *Timp1* and *Ccl5*, in both microglia and astrocytes, which I confirmed at the protein level using immunofluorescence staining. My findings are relevant for validating and showing that OBSCs present a useful tool for studying neuroimmune responses in the brain. More importantly, I show that this model has the capacity for tracking cell-type specific neuroinflammatory changes.

3.2 HIPPOCAMPAL ORGANOTYPIC BRAIN SLICE CULTURES DISPLAY PRESERVED HIPPOCAMPAL ARCHITECTURE AND RETAIN MICROGLIAL, ASTROCYTE, AND NEURONAL POPULATIONS.

To confirm the presence of major innate cell types, I performed immunofluorescence staining on untreated mouse hippocampal OBSCs using various antibodies to specifically target microglia (IBA1), astrocytes (S100β), and neurons (NeuN). These were all counter-stained with Hoechst nuclear marker, which stains all nuclei in the

slice. To visualise the architecture of the hippocampus, a detailed full slice tile scan was performed on the confocal microscope at 20X magnification. This showed preserved slice architecture with easy identification of both the dentate gyrus and Cornu Ammonis (CA) regions **(Fig. 3.1 A)**. To visualise the morphology of the various cell types, a higher magnification of 63X was used to image the various stains, and that showed preserved morphology and populations of microglia, astrocytes, and neurons **(Fig. 3.1 B-C).** Microglial cells can be observed in a ramified morphology, and astrocytes in a nonreactive phenotype.

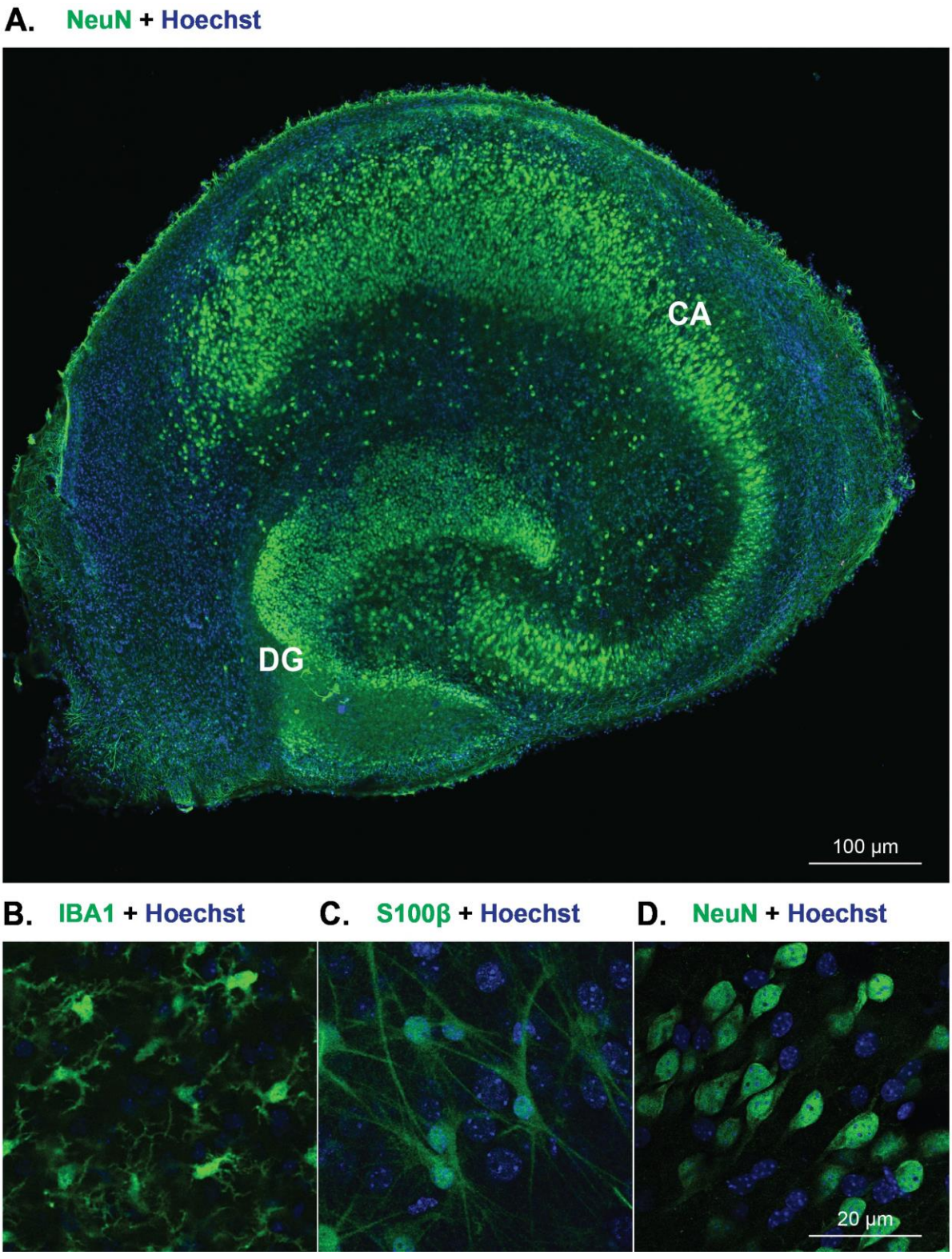

Figure 3.1 Hippocampal organotypic brain slice cultures display preserved hippocampal architecture and retain microglial, astrocyte, and neuronal populations. **A**) A confocal microscope tile scan image taken at 20X magnification displaying the well-preserved architecture of an entire hippocampal organotypic brain slice culture stained with the neuronal marker NeuN (green) and Hoechst nuclear marker (blue). The Cornu Ammonis (CA) region and the dentate gyrus (DG) are easily identifiable. **B**) Microglia stained with IBA1 and Hoescht nuclear marker visualised at 63X. **C**) Astrocytes stained with S100β and Hoechst

nuclear marker also visualised at 63X on the confocal microscope. **D**) Neurons stained with NeuN and Hoechst nuclear marker visualised at 63X on the confocal microscope. Organotypic brain slice cultures retain populations of all resident cell types with morphologically intact phenotypes.

3.3 RESIDENT BRAIN CELL TYPES ARE DIFFERENTIALLY DISTRIBUTED AT DIFFERENT DEPTHS OF OBSCS; HOWEVER, THEIR DISTRIBUTION AND RELATIVE DENSITY ARE UNAFFECTED BY LPS.

While imaging the various cell-type specific stains, I observed that microglia formed a dense sheath at the top of the slice (on the air-exposed side); however, this dense aggregation of cells is not present elsewhere throughout the slice. I was thus curious how the various cell types were distributed across the slice and whether their relative distribution was affected by treatment with the pro-inflammatory stimulant LPS. To assess this, I took detailed z-stacks at 40X magnification in two separate regions of the CA3 in each slice on the confocal microscope. This z-stack spanned from the top (sheath layer) to the bottom of the slice. This was done for both untreated control and LPS-treated slices to investigate whether there was an LPS-dependent change in cell distribution. Using our cell counter macro in ImageJ, I analysed the total proportion of cells in three different layers throughout the slice, 0 µm (sheath), 5 µm, and 10 µm depths.

During this analysis, an interesting and unexpected observation was that OBSCs decreased significantly in thickness from the initial 350 µm during slice culture preparation to only about 12 – 23 µm at 6 days post-culture. The slices seem to spread out to cover a larger surface area, decreasing their overall thickness while in culture. As a result, the deepest depth that was analysed for these experiments was ~10 µm.

In terms of cell distribution, I found that microglia form a sheath at the top of the slice (0 µm) **(Fig 3.2 A),** which may be the result of microglial cell migration or proliferation as a response to the trauma of cutting during slice culture preparation. This sheath layer (0 µm) had the highest proportion of microglial cells (51%); however, this distribution was unaffected by the LPS treatment **(Fig 3.2 B)** (N = 3, p = 4686, Mann-Whitney U test). In addition, microglial proportions decreased with slice depth, with the 10 µm layer having the lowest average proportion of cells, with only 8% of total cells

being microglia. In general, the furthest layers from the microglial sheath had the lowest proportion of microglial cells, and there was no LPS-dependent change in this distribution.

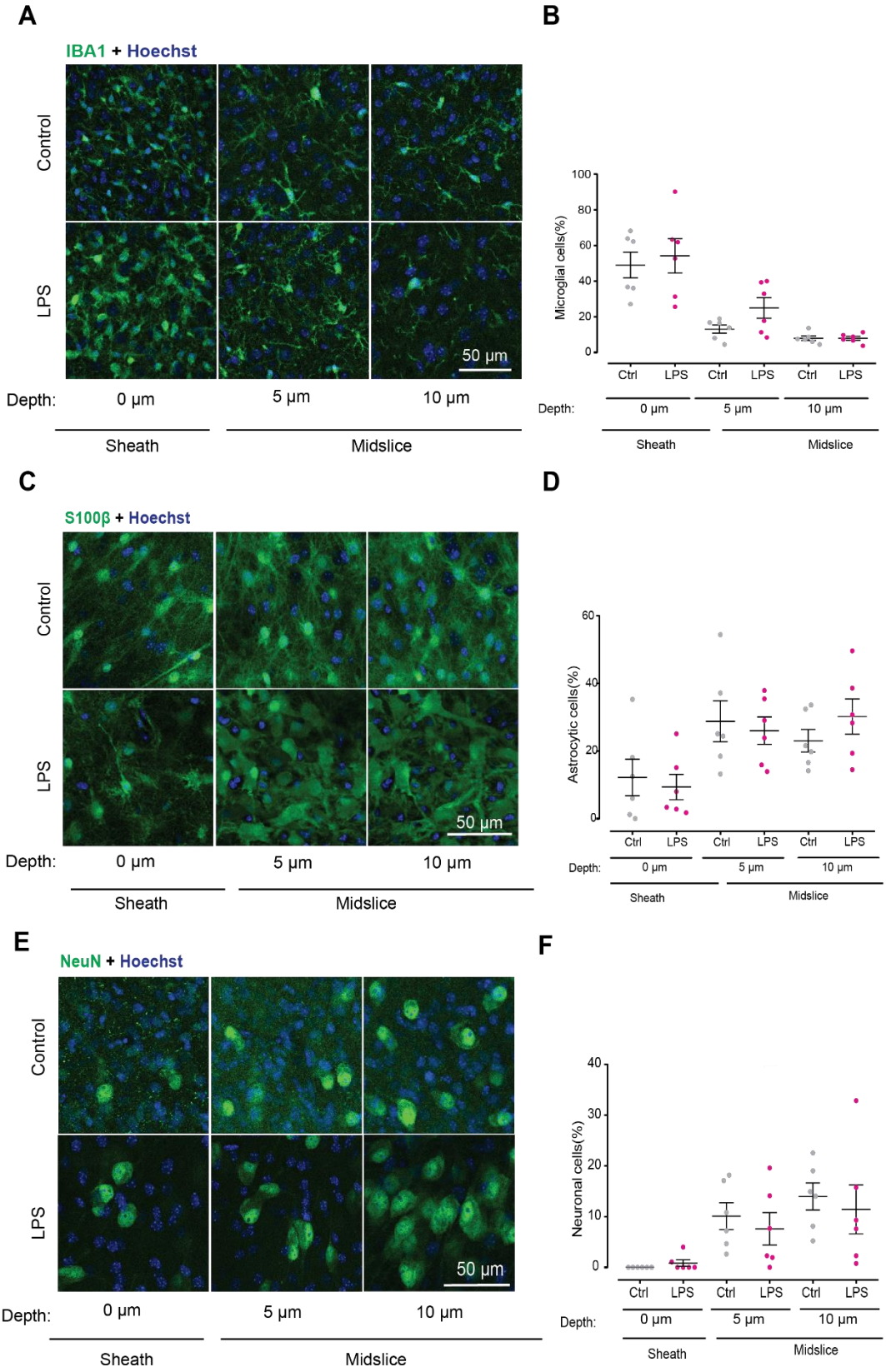

Figure 3.2 Resident brain cell types are differentially distributed at different depths of OBSCs; however, their distribution and relative density are unaffected by LPS treatment. A) Representative confocal microscope images of IBA1 (microglia) and Hoechst stained OBSCs from controls and LPS-treated slices at 0 µm, 5 µm and 10 µm depths. Images

obtained from a z-stack (with a z-interval of 0.7914 µm) imaged at 40X magnification in the CA3 region of the hippocampus. **B)** Population data of microglia (as a proportion of all cells) collected from the three different depths. Microglia form a sheath at the top of the slice and decreased with slice depth; however, the proportion of cells that were microglia was unaffected by LPS treatment. **C)** Representative confocal microscope images of OBSCs stained with S100β (astrocytes) and Hoechst nuclear marker. **D)** Population data of astrocytes (as a proportion of all cells) collected from the three different slice depths. The proportion of cells that were astrocytes increased with slice depth and this distribution was not affected by LPS treatment. **E)** Representative confocal microscope images of OBSCs stained with NeuN (neurons) and Hoechst. **F)** Population data of neurons (as a proportion of all cells) display an increase with slice depth, with 10 µm depth having the highest proportion of cells. There was no LPS-dependent change in the proportion of cells that were neurons. Values with means ± SEM, each data point represents an imaged z-stack region (N = 3 slices imaged per condition).

The proportion of cells that were astrocytes increased with slice depth, with the lowest proportion (12.2% of total cells) found at the sheath layer (0 µm) (**Fig. 3.2 C**). The highest proportion of astrocytes was observed just below the sheath (5 µm), where 20.8% of cells were astrocytes **(Fig. 3.2 D)**. I observed no LPS-induced change in the proportions and distribution of astrocytes with slice depth.

The proportion of neurons also increased with slice depth **(Fig. 3.2 E-F),** with the highest proportion (13% of total cells) found at the 10 µm layer. The sheath layer had the lowest proportion of cells that were neurons, with 0% in controls and 0.8% in the LPS-treated slices. There was no LPS induced change in neuronal cell distribution across the slice.

Knowledge of the distribution of the major cell types across the brain slice was important for informing my subsequent cell type specific analyses. Having seen that the cell types were unevenly and differentially distributed across the brain slice, all subsequent analyses for microglial cells were done at the sheath layer (0 µm), astrocytes at the 5 µm layer, and finally, neurons were analysed at the 10 µm layer.

3.4 LPS ACTIVATES MICROGLIA AND ASTROCYTES IN ORGANOTYPIC BRAIN SLICE CULTURES.

LPS is the cell wall component of gram-negative bacteria and a powerful TLR4 ligand (Krasovska & Doering, 2018; Papageorgiou et al., 2016). TLR4 are expressed on the cell surface of microglia, astrocytes and neurons. The consequence of LPS binding to these receptors triggers an inflammatory cascade resulting in phenotypic changes and activation of these cells. This in turn increases the release of inflammatory mediators

such as the pro-inflammatory cytokines IL-6 and TNF-α. I therefore used LPS as an immunogen for assessing inflammatory activation of microglia and astrocytes.

To assess glial activation and track inflammation, I employed dual immunofluorescence staining for measuring the activation of NF-IL6, a pro-inflammatory transcription factor that mediates a cell's inflammatory response to an immunogen. NF-IL6 is a cytoplasmic protein that only gets translocated into the nucleus upon activation by inflammatory stimulants such as LPS (Rummel, 2016). I co-stained this with cell-type specific markers for microglia (IBA1), astrocytes (S100β) and neurons (NeuN). Thus, in the stained OBSCs, a nuclear colocalization between the primary cell-type markers and NF-IL6 indicates activation of that cell. Colocalization analyses were done using our cell counter macro in ImageJ.

My results show a strong NF-IL6 immunoreactivity in the LPS-treated slices **(Fig. 3.3 A).** Additionally, there was a strong nuclear colocalization between IBA1 and NF-IL6 in the LPS group, which was indicative of activation of those microglial cells **(Fig. 3.3 A)**. There was minimal observable NF-IL6 immunoreactivity in controls and low colocalization with IBA1, highlighting that the cells in that condition were not in an inflammatory state **(Fig. 3.3 A).** Compared to controls, with an average of 2.6% of activated microglia, the average proportion of activated microglia was 46% in the LPS-treated slices **(Fig. 3.2 B),** constituting an inflammatory response ($N = 6$, $p < 0.0001$, Mann-Whitney U test).

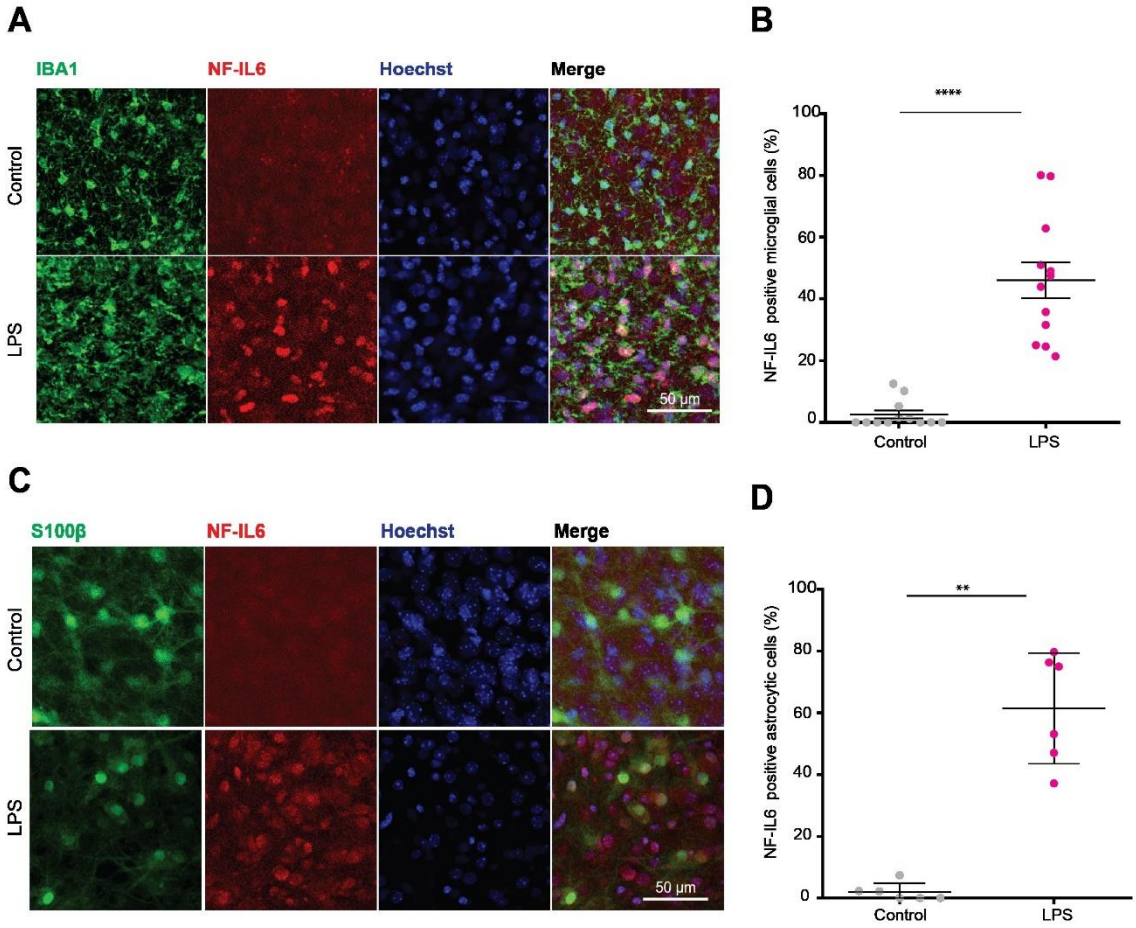

Figure 3.3 LPS activates microglia and astrocytes in organotypic brain slice cultures. **A)** Representative images taken on the confocal microscope (at 40X magnification) of a co-stain of microglia (IBA1), the inflammatory transcription factor NF-IL6, and Hoechst nuclear marker in control (untreated) and LPS-treated OBSCs. Cell activation was determined by the nuclear colocalization of IBA1 and NF-IL6. **B)** Population data of the proportion of microglia that were activated in controls and LPS-treated slices. LPS induced an inflammatory response in microglial cells, as indicated by the increase in the proportion of cells that were activated. **C)** Representative confocal microscope images of OBSCs stained with S100β to label astrocytes, NF-IL6, and Hoechst. As before, a nuclear colocalization of S100β and NF-IL6 is indicative of activated astrocytes. **D)** Population data of the proportion of activated astrocytes in controls and LPS-treated slices. Values with means ± SEM, ***p*≤ 0.001; **** *p* ≤0.0001; Mann- Whitney U test; each data point represents an imaged z-stack region (N = 6 slices for IBA1, N = 3 slices for S100β).

Figure **3.3 C & D** shows that there was a significantly higher colocalization between the astrocytic marker (S100β) and the inflammatory biomarker NF-IL6 in LPS-treated OBSCs (61.4%) compared to controls (2%) (N=3; p = 0.0022, Mann Whitney U test). Taken together, I have shown that we can elicit an inflammatory response in OBSCs by treating them with an immunogen (LPS) and we can measure this response at the protein level by tracking the translocation of NF-IL6 into the nucleus and colocalizing that with markers for microglia and astrocytes.

3.5 NEURONS CONSTITUTIVELY EXPRESS NF-IL6 IN MOUSE ORGANOTYPIC BRAIN SLICE CULTURES.

Literature has demonstrated that neurons may have inflammatory capacity (Gruol, 2015; Jüttler et al., 2002). I wanted to explore whether we can track this via the cell activation of neurons in response to an immunogenic challenge (LPS) using NF-IL6 as a functional read-out. I observed high constitutive expression of NF-IL6 in untreated controls slices **(Fig 3.4 A)**. This expression was strongly colocalized with the neuronal marker NeuN **(Fig 3.4 A);** an average of 69% of neurons in controls showed NF-IL6 expression. Similarly, the LPS treated slices also displayed high levels of NF-IL6 expression, with an average of 88% of NeuN-positive cells colocalizing with NF-IL6. Control and LPS treated slices were not significantly different from each other (**Fig. 3.4 B)** (N = 3, p = 0.1429, Mann Whitney U test).

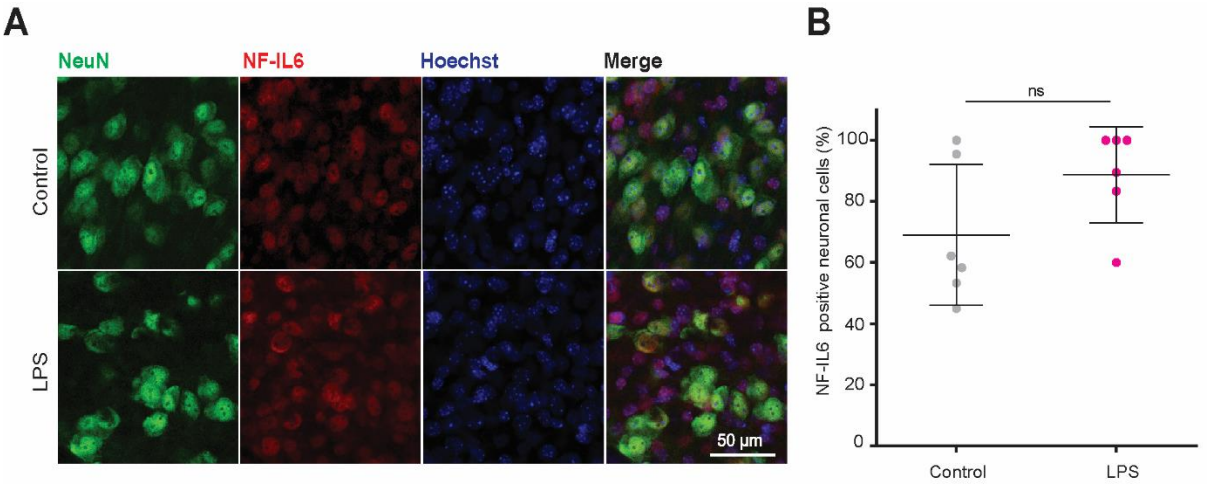

Figure 3.4 Neurons constitutively express NF-IL6. A) representative confocal images (taken at 40X magnification) of a co-stain of neurons (NeuN), NF-IL6, and Hoechst nuclear marker in untreated control and LPS-treated OBSCs. Constitutive expression of NF-IL6 is observed in control treated slices, as highlighted by the colocalization between NeuN and NF-IL6. **B)** Population data showing the proportion of neurons that were NF-IL6 positive, indicating high proportions of activated neurons in both controls and LPS-treated OBSCs. Values with means ± SEM; each data point represents an imaged z-stack region (N = 3 slices, $p = 0.1429$, Mann- Whitney U test; ns = not significant).

3.6 LPS INDUCES THE RELEASE OF PRO-INFLAMMATORY CYTOKINES IL-6 AND TNF-α IN MOUSE ORGANOTYPIC BRAIN SLICE CULTURES.

In **Figure 3.3,** I demonstrated that LPS induced an inflammatory response in microglia and astrocytes. Additionally, I established that one way that we can track this inflammatory response is by measuring the activation of these innate cells by dual immunofluorescence staining of innate glial markers with the inflammatory transcription factor NF-IL6. Knowing that activated glia cells release pro-inflammatory cytokines in response to an inflammatory challenge (Akira et al., 1990; Gruol, 2015; Wang et al., 2015) and that the nuclear translocation of NF-IL6 drives up the transcription of genes regulating downstream releasable factors (Rummel, 2016), we decided to use enzyme-linked immunosorbent assays (ELISAs) to measure the concentrations of pro-inflammatory cytokines released by OBSCs in the culture medium. To do this, we stimulated OBSCs with 10 ng/ml of LPS in medium for 24 hours, six days post culture, after which we collected the medium to measure the concentrations of IL-6 and TNF-α released by OBSCs. We compared these LPS-

treated slices to untreated controls. These experiments were done collaboratively with Dr Anja de Lange, A post-doctoral research fellow in the Raimondo lab.

Figure 3.5 A-B shows that LPS induced a significant increase in the release of IL-6 and TNF-α, as compared to untreated control slices *(*IL-6: $p \leq 0.0001$, Mann-Whitney U test; TNF-α: $p \leq 0.0001$, Mann-Whitney U test). This confirms that there was indeed inflammation occurring in the LPS treated OBSCs, further substantiating the findings in **Fig. 3.3**.

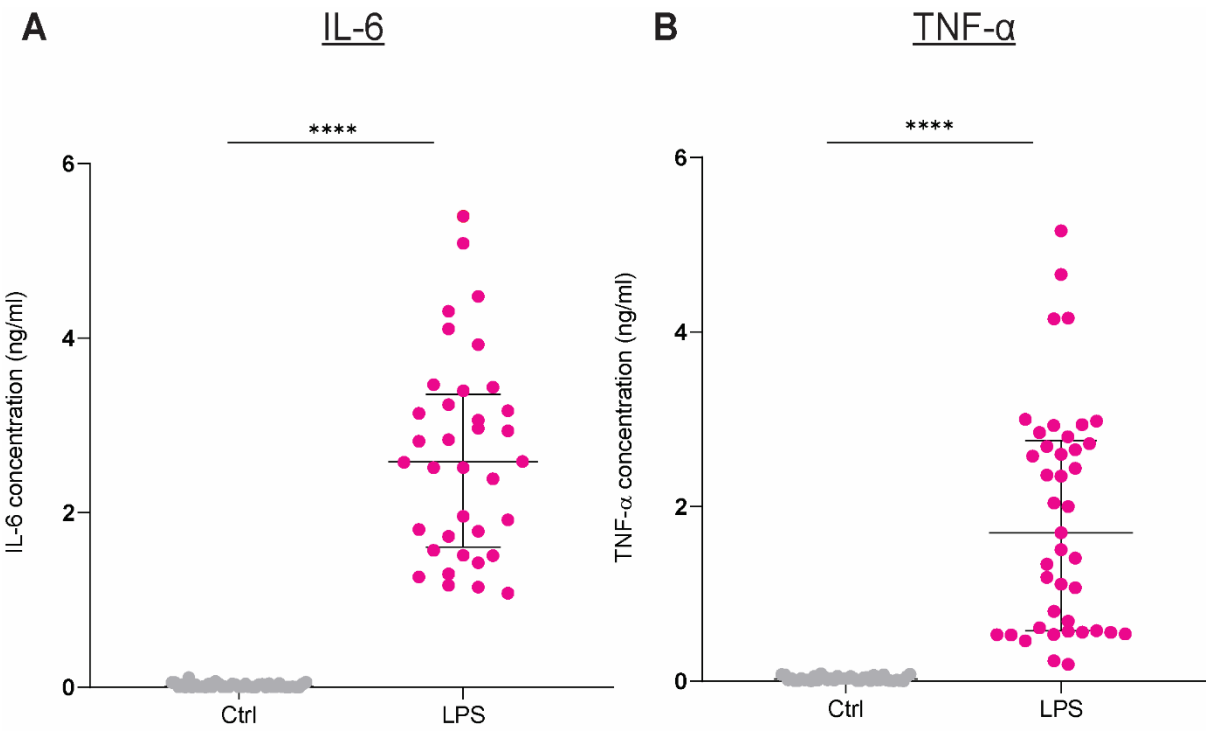

Figure 3.5 LPS induces the release of pro-inflammatory cytokines IL-6 and TNF-α in OBSCs. A) The concentration of pro-inflammatory cytokine IL-6 released by OBSCs in the culture media, showing a strong LPS response after 24 hours in treatment as compared to controls. **B)** The concentration of the pro-inflammatory cytokine TNF-α released by OBSCs in culture media, also displaying a substantial increase in response to LPS treatment as compared to untreated controls. Values with median ± IQR, **** $p \leq 0.0001$; Mann-Whitney U test; for IL-6: N = 36 - 41, for TNF-α: N = 40 - 41.

3.7 SINGLE NUCLEUS RNA-SEQUENCING ENABLES CELL TYPE IDENTIFICATION ACCORDING TO GENE EXPRESSION.

Thus far, I have demonstrated various ways that we can track and confirm inflammatory responses in immune competent glia in the brain. One of those ways was tracking the protein expression of the inflammatory transcription factor NF-IL6; another was measuring releasable inflammatory molecules such as pro-inflammatory cytokines IL-6 and TNF-α. Another more advanced method we utilised was tracking gene expression changes of key inflammatory genes in response to LPS challenge using single nucleus RNA-sequencing (snRNA-sequencing). In collaboration with other members of the Raimondo lab, OBSCs from post-natal day 7 mice were prepared, some slices were left untreated to serve controls and other were treated with 10 ng/ml of LPS. I then dissociated nuclei from the slices in lysis buffer, and a snRNA-sequencing pipeline using the 10X Genomics platform was initiated. Single-nucleus RNA sequencing libraries from treated tissue were generated by Dr Raimondo, Mr Josh Selfe, and Ms Teresa Steyn using the 10X Genomics platform. Ms Steyn then went on to carry out computational processing and analysis to integrate and cluster the datasets for the identification of cell-type populations. Up to 10 different cell clusters were identified, including microglia, astrocytes, inhibitory neurons, and excitatory neurons **(Fig 3.6 A).** To validate the cell clusters, I visualized the average expression of known cell-type specific markers **(Fig. 3.6 B).** Microglial-specific markers such as *Tmem119* and *P2ry12* were observably highly expressed in the microglial cells as compared to other cell types. Likewise, astrocyte specific markers such as *Gfap* and *Aqp4* were highly expressed in astrocytes.

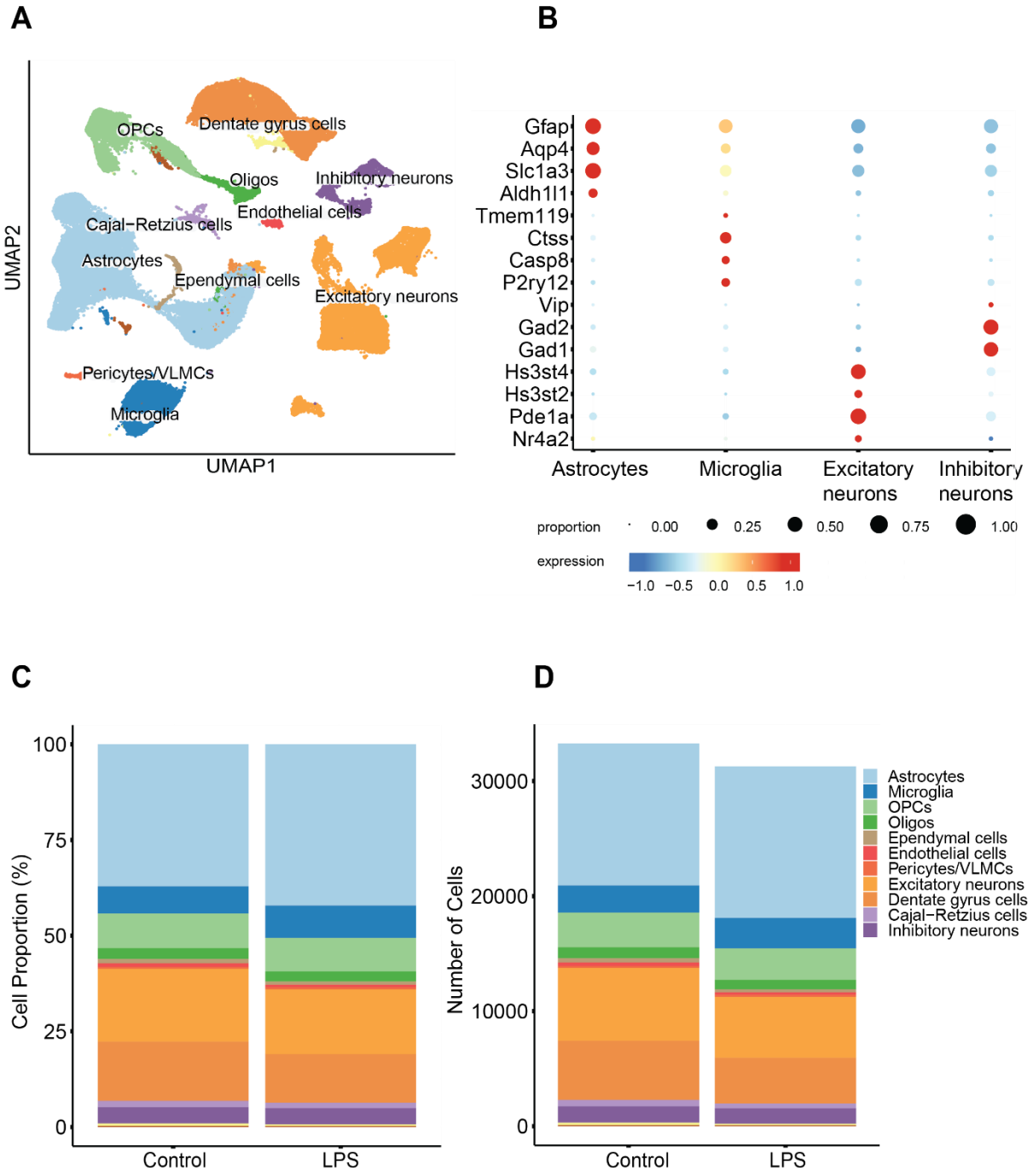

Figure 3.6 Single nucleus RNA-sequencing enables cell-type identification according to gene expression. A) Uniform Manifold Approximation and Projection (UMAP) plot of annotated clusters where both microglia and astrocytes can be visualised. **B)** Bubble plot displaying the expression of cell-type specific markers to validate the annotated cell clusters. **C)** Cell proportions in the different clusters display no changes in response to LPS treatment. **D)** The absolute number of cells in each cluster in control and LPS conditions.

I was also interested in whether there was an LPS-dependent change in the number of cells (as determined by the number of nuclei in each cell type cluster) and their proportions (as a function of the total number of nuclei), this also served as a measure of possible proliferation in the different cell types. There were no significant changes in the proportion of cells between controls and LPS for any of the cell types identified in our snRNA-sequencing dataset **(Fig 3.6 C & D)**. This, to an extent, substantiates the findings we observed in **Figure 3.2,** where we observed no LPS dependent change in cell proportions of microglia, astrocytes, and neurons.

3.8 LPS TRIGGERS AN UPREGULATION OF INFLAMMATORY GENES IN MICROGLIA AND ASTROCYTES.

I was interested in whether there were gene expression changes of major inflammatory genes in microglia and astrocytes in response to an immune challenge (LPS). To this end, I looked at the top 20 differentially expressed inflammatory genes in microglia and astrocytes (using DESeq2) between control and LPS-treated OBSCs. In microglia, there was a strong upregulation of inflammatory genes such as *Timp1, Ccl5* and *Lcn2* that were expressed at low levels in control OBSCs **(Fig 3.7 A).** All of these are critical genes involved in inflammation and its regulation in the brain, this highlights an inflammatory response in the LPS-treated group**.** There was also a strong upregulation of inflammatory genes in astrocytes; there was an upregulation of genes such as *Mmp3, Timp1* and *Ccl5* **(Fig 3.7 B)**. Furthermore, there was a strong upregulation of the NF-IL6 encoding gene (*Cebpβ)* in response to LPS treatment in both microglia and astrocytes **(Fig 3.7 A & B).** This further confirms that LPS induces inflammation in OBSCs which we can track in immune-competent resident brain cells at both the protein and gene expression level.

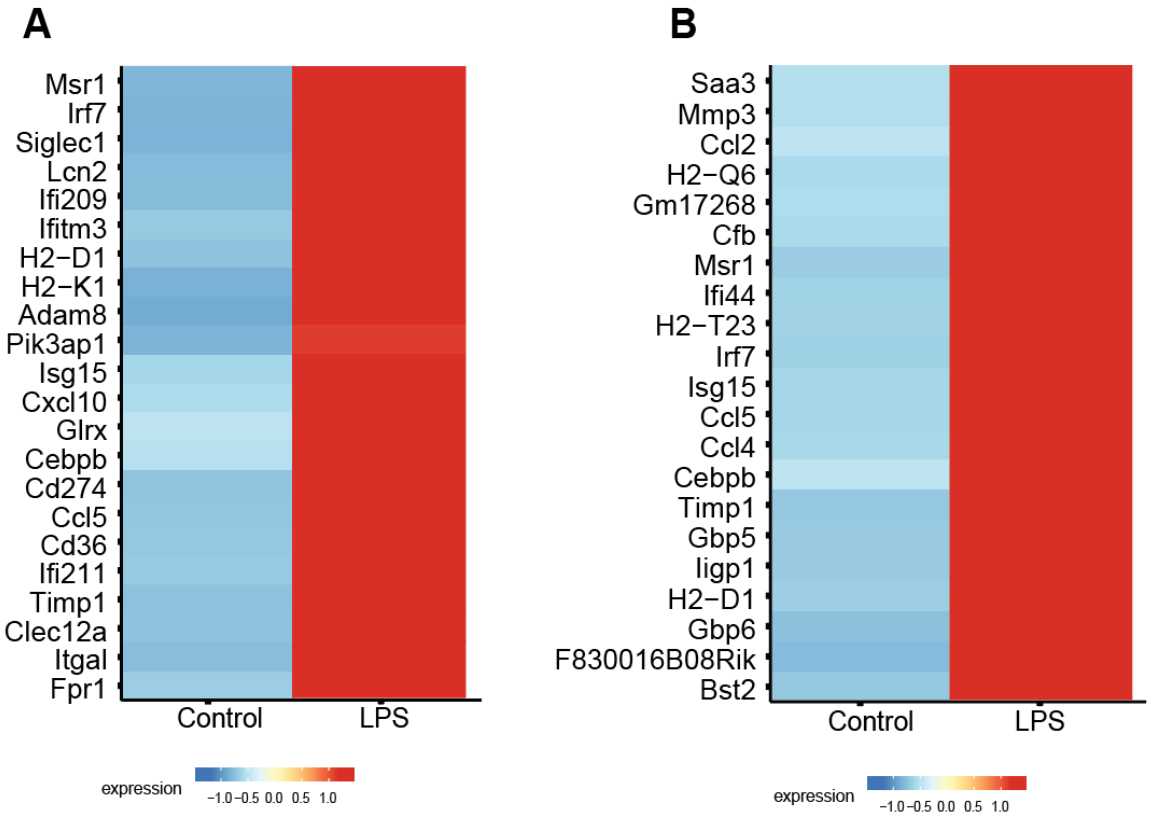

Figure 3.7 LPS triggers an upregulation of inflammatory genes in microglia and astrocytes A) Heatmap showing the average expression of the top 20 differentially expressed inflammatory genes in microglia in control and LPS treated OBSCs. All 20 genes show a strong upregulation in response to LPS, highlighting an inflammatory response in this cell type. **B)** Heatmap showing the average expression of the top 20 differentially expressed genes in astrocytes, also comparing controls to LPS-treated OBSCs. As in microglia, all 20 genes are strongly upregulated in response to LPS in astrocytes.

3.9 USING IMMUNOFLUORESCENCE STAINING TO EXPLORE THE PROTEIN EXPRESSION OF INFLAMMATORY GENES UPREGULATED IN RESPONSE TO LPS TREATMENT.

I further wanted to explore the protein expression of some of the inflammatory genes upregulated in response to LPS treatment (as observed in **Fig 3.7**). I additionally wanted to investigate which cell type, microglia or astrocytes, was expressing the protein and to what extent. To this end, I chose four genes (based on their differential expression) that were upregulated in response to 10 ng/ml of LPS treatment: *Timp1, CCL5, Pik3ap1, and Lcn2*. Our snRNA-sequencing results confirmed that *Timp1, CCL5* and *Lcn2* were significantly upregulated in response to LPS in both microglia and astrocytes; however, *Pik3ap1* was microglial specific and only significantly upregulated within this cell type. To visualise the average protein expression of these genes, I carried out triple immunofluorescence staining on untreated control and LPS-treated OBSCs, where I stained for both microglia (IBA1) and astrocytes (S100β) simultaneously with one of the genes of interest, and Hoechst nuclear marker. I then visualised the average protein expression of these genes at three different slice depths (0 µm, 10 µm, and 20 µm) by quantifying and comparing the mean fluorescence intensity of the staining signal between the two treatment groups.

3.9.1 *TIMP1* PROTEIN EXPRESSION IS UPREGULATED BY LPS TREATMENT.

At the protein level, *Timp1* was constitutively expressed in untreated control OBSCs **(Fig 3.8A).** When the protein expression was quantified by the mean fluorescence intensity (MFI) of the staining signal, there was significant upregulation of *Timp1* expression in response to LPS treatment at all recorded slice depths **(Fig 3.8 B).** The most significant difference in MFI was observed at the 10 µm layer, where a Mann-Whitney U test found a significant difference between controls (44.9 RFU) and LPS-treated slices (77 RFU) (n = 10 -12, $p \leq 0.0001$, Mann- Whitney U test). At the sheath layer (0 µm), the MFI for controls (44.1 RFU) was also significantly different from that of the LPS group (70.6 RFU) (n = 9-12, $p = 0.0110$, Mann- Whitney U test).

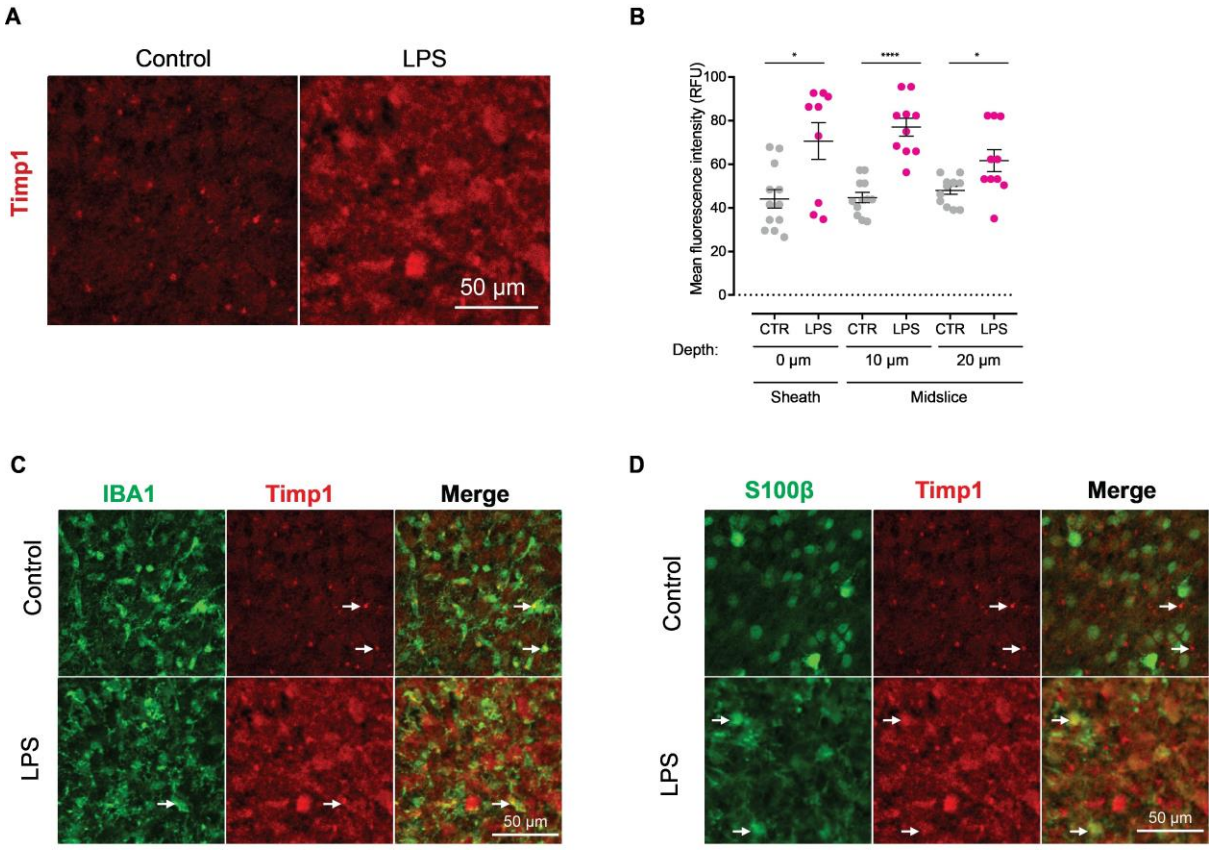

Figure 3.8 *Timp1* protein expression is upregulated by LPS treatment. Untreated control or LPS-treated OBSCs were triple labelled for microglia (IBA1), astrocytes (S100β), and *Timp1*. **A)** *Timp1* protein expression visualised by mean fluorescence intensity comparing a control and LPS-treated slice. **B)** Population data of *Timp1* mean fluorescence intensity (protein expression) quantified at three different slice depths. LPS treatment significantly increased *Timp1* protein expression at all recorded depths. **C)** A detailed visualisation of *Timp1* and IBA1 staining in a control and LPS-treated slice. Cytoplasmic *Timp1* appears to colocalize with microglial processes (arrows). **D)** A detailed visualisation of *Timp1* and S100β staining comparing an untreated control slice to an LPS-treated OBSC. Values with mean ± SEM, * $p \leq 0.01$, **** $p \leq 0.0001$; Mann-Whitney U test; n = 9 -12 imaged regions. *NB: As this was a triple stain, images depicting the Timp1 signal in A, C and D are the same as the same region of the slice was imaged to visualise all three stains.*

The *Timp1* protein expression appeared cytoplasmic and colocalized with the IBA1 stain, specifically the primary processes of microglial cells **(**see arrows in **Fig 3.8 C).** In response to LPS treatment, the *Timp1* fluorescence intensity increased and became more generalised, colocalizing with both IBA1 and S100β positive cells **(**see arrows **Fig 3.8 C & D)**. With that, however, some *Timp1*-positive cells did not colocalize with either IBA1 or S100β, highlighting that they could be colocalized with other cell types, perhaps neurons **(Fig 3.8 C & D).**

3.9.2 THE *CCL5* PROTEIN IS PRIMARILY EXPRESSED IN ASTROCYTES HOWEVER, DISPLAYS NO OBSERVABLE LPS-DEPENDENT UPREGULATION IN ITS EXPRESSION.

Our snRNA-sequencing results highlighted that *Ccl5* was upregulated in response to LPS in both microglia and astrocytes. However, at the protein level, there were no substantial differences in the *Ccl5* immunoreactivity between untreated controls and LPS-treated OBSCs **(Fig 3.9 A).** When the MFI was quantified to visualise the average protein expression between the two treatment groups, the sheath layer had an MFI of 19.03 RFU for controls, which was not significantly different to the 17.9 RFU reported in the LPS-treated slices **(Fig 3.9 B)** (n = 12, p = 0.7020, Mann- Whitney U test). Likewise, the deepest recorded layer (20 µm) had an MFI of 15.6 RFU for controls, which was not significantly different from the 14.8 RFU recorded in the LPS group (n = 11 -12, p = 0.3687, Mann- Whitney U test).

The *Ccl5* protein was predominantly expressed in astrocytes, with significant colocalization between S100β and *Ccl5* and very negligent colocalization with IBA1 **(**see arrows **Fig 3.9 C & D).** In addition, the *Ccl5* staining appeared to be nuclear and was constitutively expressed in untreated control OBSCs **(Fig 3.9 C & D)**.

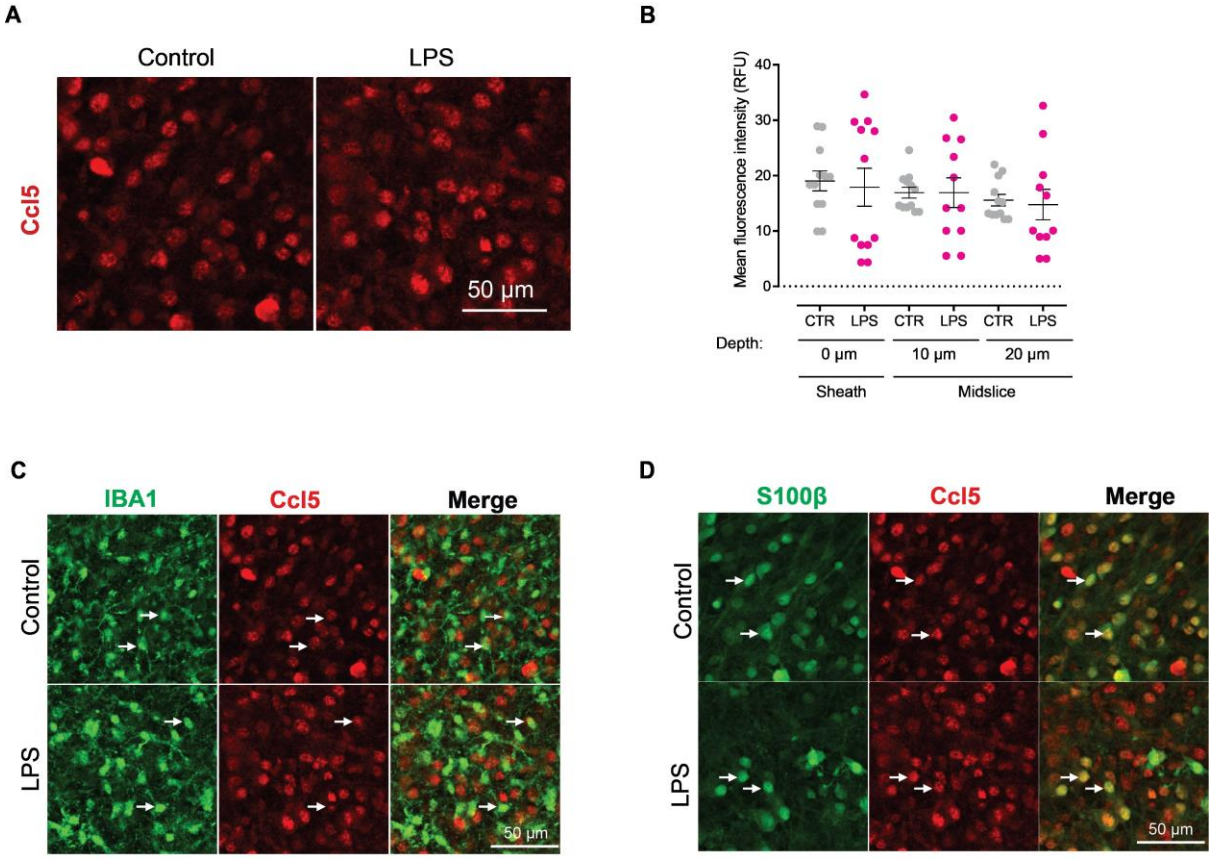

Figure 3.9 The *CCL5* protein is primarily expressed in astrocytes; however, displays no observable LPS-dependent upregulation in its expression. Untreated control or LPS-treated OBSCs were triple labelled for microglia (IBA1), astrocytes (S100β), and the inflammatory protein *Ccl5.* **A)** *Ccl5* protein expression visualised by mean fluorescence intensity comparing a control and LPS-treated slice. *Ccl5* was constitutively expressed in untreated controls with no obvious dissimilarities in immunoreactivity when compared to LPS-treated slices. **B)** Population data of *Ccl5* mean fluorescence intensity quantified at three different slice depths displaying no LPS-dependent changes in expression at all recorded depths. **C)** A detailed visualisation of *Ccl5* and IBA1 staining in a control and LPS-treated slice. **D)** Confocal microscope images of *Ccl5* and S100β staining in an untreated and LPS-treated OBSC. *Ccl5* was highly colocalized with the S100β signal, indicating that it was highly expressed in astrocytes. Values with mean ± SEM, Mann-Whitney U test; n = 11 -12 imaged regions. *NB: As this was a triple stain, images depicting the Ccl5 signal in A, C and D are the same as the same region of the slice was imaged to visualise all three stains.*

3.9.3 *PIK3AP1* IS PREDOMINANTLY LOCALIZED WITHIN MICROGLIAL CELLS AND EXHIBITS A DIFFUSE PATTERN OF EXPRESSION IN RESPONSE TO LPS TREATMENT.

The *Pik3ap1* protein was constitutively expressed in untreated control slices, with a diffuse pattern of expression when slices were treated with LPS **(Fig 3.10A).** When the signal was quantified, there were no LPS-dependent differences in MFI at any of the analysed layers **(Fig 3.10 B)**. For example, the sheath layer had an MFI of 43 RFU for controls and 42.8 RFU for LPS (n = 12, p = 0.9372, Mann- Whitney U test). Similarly, the 10 µm layer had an average MFI of 52.7 RFU in controls, which was not significantly different to the 52.3 RFU reported in the LPS group (n = 12, $p \geq 0.9999$, Mann- Whitney U test).

In agreement with our snRNA-sequencing findings, *Pik3ap1* was predominantly expressed by microglial cells, this was evident in the untreated control slices, as demonstrated by the colocalization between the IBA1 and *Pik3ap1* staining **(Fig 3.10 C & D).** When homing in further on the *Pik3ap1* signal, the staining was not nuclear rather, it stained just outside/adjacent to the nucleus, and almost always within microglial cells **(**see arrows in **Fig 3.10 C & D).**

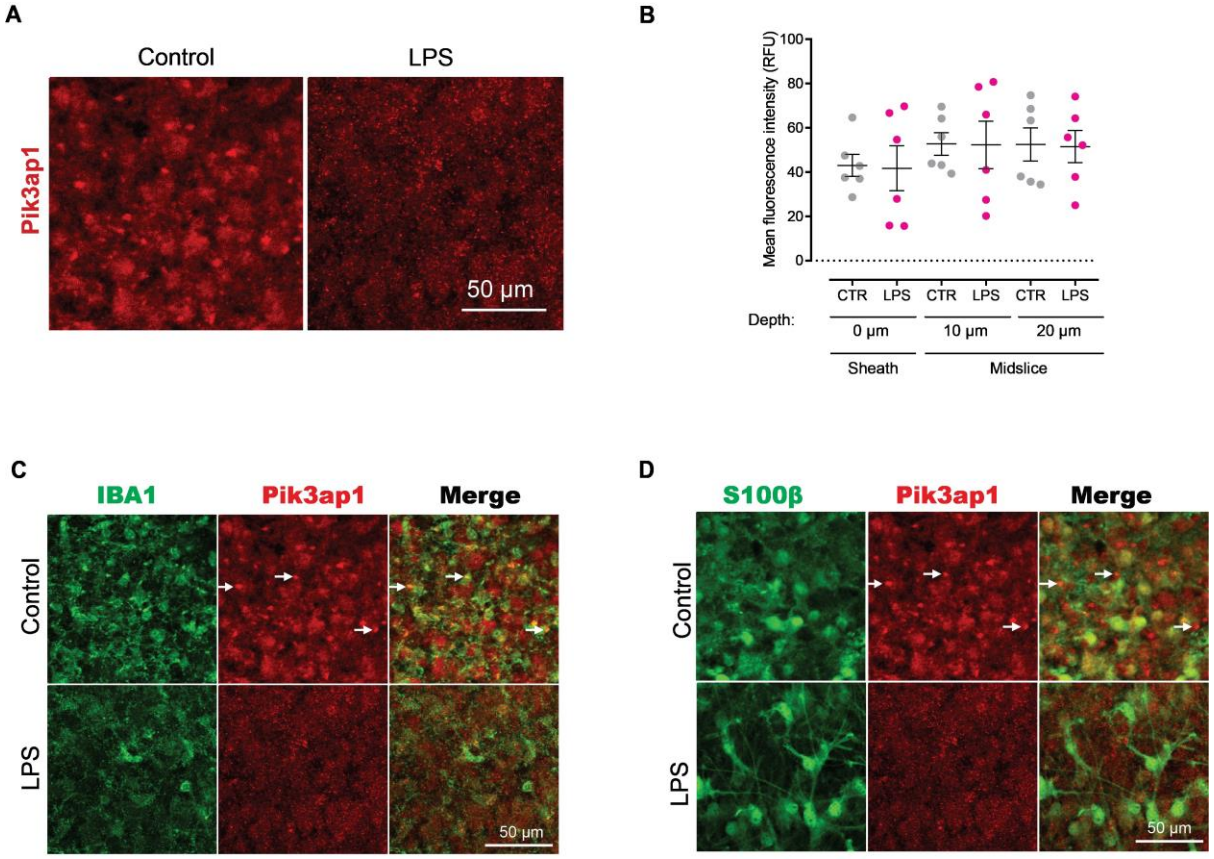

Figure 3.10 *Pik3ap1* is predominantly localised within microglial cells and exhibits a diffuse pattern of expression in response to LPS treatment. Untreated control or LPS-treated OBSCs were triple labelled for microglia (IBA1), astrocytes (S100β), and the inflammatory protein *Pik3ap1*. **A)** *Pik3ap1* immunoreactivity visualised by mean fluorescence intensity comparing a control and LPS-treated slice*. Pik3ap1* was constitutively expressed in untreated controls; however, its expression was significantly more diffuse in slices treated with LPS. **B)** Population data displaying no significant differences in the mean fluorescence intensity between controls and LPS-treated OBSCs at 3 all depths of the slice. **C)** A detailed visualisation of *Pik3ap1* and IBA1 staining in a control and LPS-treated slice. *Pik3ap1* colocalized with the IBA1 signal, indicating that it is highly expressed in microglia compared to astrocytes (see arrows). **D)** Shows *Pik3ap1* and S100β staining comparing an untreated control slice to an LPS-treated OBSc. Values with mean ± SEM, Mann-Whitney U test; n = 6 imaged regions. *NB: As this was a triple stain, images depicting the Pik3ap1 signal in A, C and D are the same as the same region of the slice was imaged to visualise all three stains.*

3.9.4 THE *LCN2* PROTEIN EXHIBITS PROMINENT CYTOPLASMIC LOCALIZATION WITHIN ASTROCYTES AND DOES NOT EXHIBIT UPREGULATION IN RESPONSE TO LPS TREATMENT.

At the protein level, *Lcn2* was constitutively expressed in control slices, where its staining was significantly colocalized with astrocytes with very negligible microglial colocalization (see arrows **Fig 3.11 A, C, & D).** When the expression was quantified, there was no LPS-dependent increase in the *Lcn2* protein expression at any of the recorded slice depths as measured through the MFI of the staining **(Fig 3.11 B).** The sheath layer displayed the most variability in MFI between the two treatment groups, with 35.6 RFU for controls and 53.2 RFU for LPS; however, a Mann- Whitney U test did not find these differences significant (n = 3, p = 0.2000, Mann- Whitney U test). At the 10 µm layer, controls had a slightly higher MFI (26.8 RFU) than LPS slices (22.8 RFU). However, these were also not significantly different (n = 3, $p \geq 0.9999$, Mann-Whitney U test).

The *Lcn2* staining was cytoplasmic and appeared to stain reactive astrocytes. This is particularly evident in the LPS-treated slices where the *Lcn2* stain surrounds the predominantly nuclear S100β stain **(Fig 3.11C&D).**

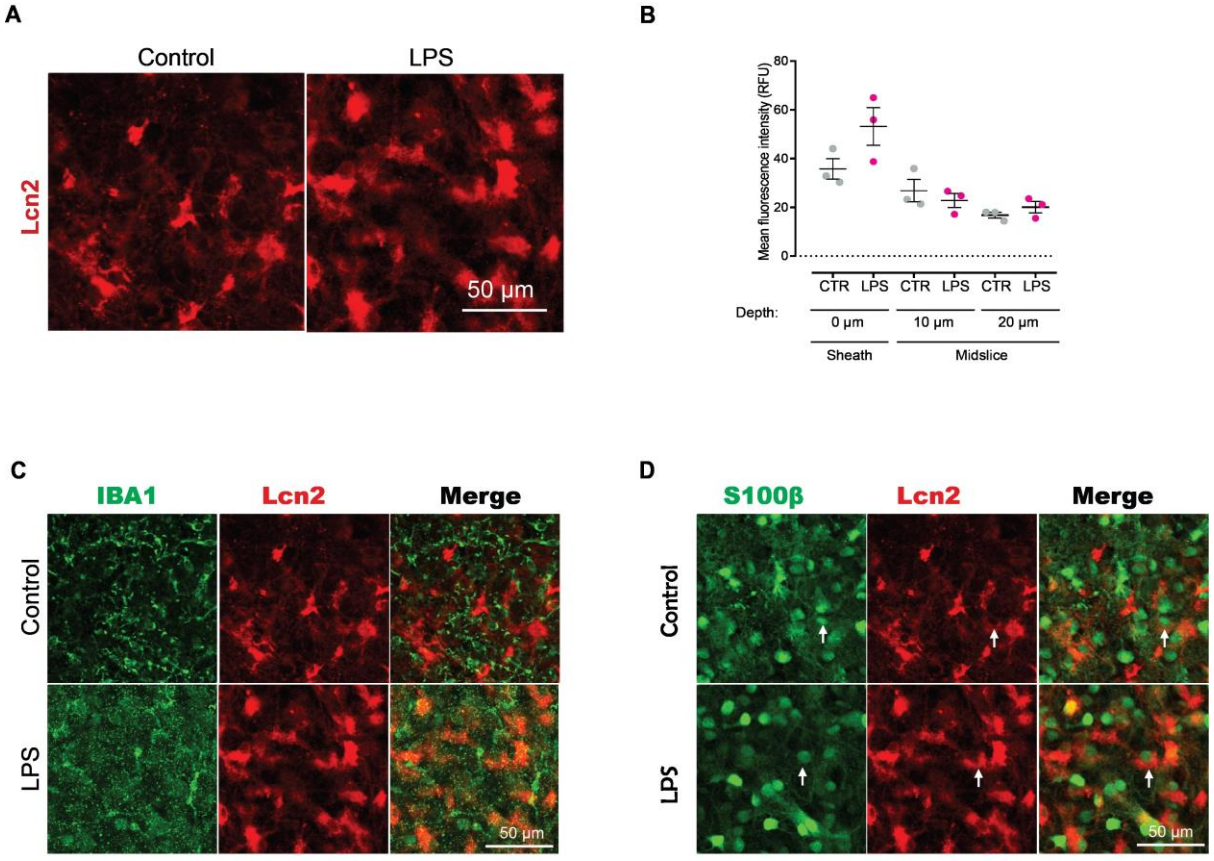

Figure 3.11 The *Lcn2* protein exhibits prominent cytoplasmic localization within astrocytes and does not exhibit upregulation in response to LPS treatment. Untreated control or LPS-treated OBSCs were triple labelled for microglia (IBA1), astrocytes (S100β), and the *Lcn2* protein. **A)** *Lcn2* protein expression visualised by mean fluorescence intensity comparing a control and LPS-treated slice. *Lcn2* displayed constitutive expression in controls, with no evident differences in immunoreactivity when compared to LPS-treated slices. **B)** Population data displaying no significant differences in the mean fluorescence intensity between controls and LPS-treated OBSCs at all recorded slice depths. **C)** A detailed visualisation of *Lcn2* and IBA1 staining in a control and LPS-treated slice. **D)** A detailed visualization of Lcn2 and S100β staining. *Lcn2* was highly colocalized with the S100β signal and appears to be staining the processes of reactive astrocytes. Values with mean ± SEM, Mann-Whitney U test; n = 3 imaged regions. *NB: As this was a triple stain, images depicting the Lcn2 signal in A, C and D are the same as the same region of the slice was imaged to visualise all three stains.*

3.10 DISCUSSION

Infections of the central nervous system disproportionately impact low and middle-income populations. Numerous conditions, including neurocysticercosis, have been shown to be accompanied by, and/or worsened by neuroinflammation. However, the mechanistic events occurring in these conditions have been challenging to study because of the scarcity of models of neuroinflammation that enable the monitoring of cell-type specific reactions within an inflammatory environment. In this chapter, I used mouse hippocampal organotypic brain slice cultures (OBSCs) to investigate cell type-specific inflammatory responses in the brain.

In the first experiment, I showed that all major cell types, microglia, astrocytes, and neurons are present and display intact morphology in OBSCs by staining for them with cell-type specific markers, an observation that has been previously reported in literature (Awala et al., 2023; Coleman et al., 2020; Delbridge et al., 2020; Huuskonen et al., 2005; Mewes et al., 2012; Papageorgiou et al., 2016). Furthermore, I also showed that using confocal microscopy, we can visualise the intact morphology of the entire hippocampal slice, where we are able to observe the morphology and architecture of both the dentate gyrus and Cornu Ammonis (CA) regions.

Next, I wanted to investigate the distribution of the various innate cell types across OBSCs and ascertain whether this was at all changed or affected by treatment with the pro-inflammatory stimulant LPS at 10 ng/ml. I found that glia and neurons are differentially and unevenly distributed across OBSCs. I found that at the surface of slices, at the “sheath layer”, most cells were microglia. This is likely a response to the trauma and injury of slice sectioning during culture preparation, as it has been demonstrated that brain injury induces M1 classical activation of microglial cells, and this phenotypic change is accompanied by directional migration of cells towards the site of injury (Guo et al., 2022; He et al., 2016; Lively & Schlichter, 2013; Matejuk & Ransohoff, 2020). While microglia make up the first line of defense following injury, astrocytes may also be recruited shortly after taking on a reactive phenotype and forming an astrogliosis scar. This astrogliosis scar is made up of a thick layer of astrocytic processes and is essential for confining inflammatory cells in one region and preventing their spread to ‘healthy’ brain tissue (Guo et al., 2022; Matejuk &

Ransohoff, 2020). In support of this, I observed that the highest relative density of astrocytes was found in the layers just below the sheath layer (5 µm) **(Fig 3.2 C& D)**.

Importantly, in my experiments, it is also unlikely that LPS induced migration of glial cell types between layers as their relative densities stayed constant following treatment. A logical question from these experiments would be why the microglial sheath forms exclusively on one side of the slice (the air exposed side) when both sides of the slice were sectioned. I hypothesize that while both sides experience the injury from slicing, the recovery conditions are different. The side in contact with the culture medium has immediate access to nutrients, and potentially protective factors in the medium, which can help mitigate some of the injury-induced stresses. On the other hand, the air-exposed side lacks this direct contact, potentially leading to increased cellular stress or slower recovery, which might attract more microglia. Additionally, microglia may be sensing the dual stresses of slicing and air exposure on one side, and they might be migrating to set up a sort of protective or reparative front on the air-exposed side. Given the observed tissue spreading and significantly reduced thickness while in culture, it is also possible that gravitational and physical/mechanical stresses, related to the slice's spatial orientation, may also have influenced the uneven pattern of microglial reaction. These hypotheses could, however, be confirmed more definitively in the future with time-lapse 2-photon imaging of live GFP-labelled microglia in the CX3CR1-GFP transgenic mouse line to track microglial migration dynamics (Eme-Scolan & Dando, 2020; Eyo et al., 2016; Frenger et al., 2021; Kokona et al., 2017). In addition, at least in my model system, LPS does not appear to induce proliferation of any glial cell type. Future studies could confirm this more definitively using alternative methods such as Bromodeoxyuridine (BrdU) incorporation or Ki-67 staining.

LPS is a pathogen-associated molecular pattern (PAMP) that stimulates TLR4 on the cell surface of innate immune cells (He et al., 2021; Herden et al., 2015; Lu et al., 2008; Park & Lee, 2013; Poltorak et al., 1998). The recognition of LPS by TLR4 initiates a cascade of inflammatory signalling pathways that elicits the translocation of cytoplasmic inflammatory transcription factors into the nucleus to drive up the transcription of an array of inflammatory genes. My results show that LPS significantly induced activation of inflammatory signalling in both microglia and astrocytes, as

shown in **Fig. 3.3**. This aligns with observations made by Papageorgiou et al. (2016), who demonstrated that chronic TLR4 activation by LPS induces activation and reactive phenotypes in microglia cells. Though it is important to note that this study only looked at microglial activation and used morphological changes as a measure of glial activation, in contrast, the current study uses the nuclear translocation of the inflammatory transcription factor NF-IL6 in both microglia and astrocytes, adding to these findings. We found a robust, reproducible activation of the transcription factor in both cell types which further supports the usefulness of NF-IL6 and other transcription factors as a functional readout for neuroinflammation. These concepts are fully discussed and reviewed by Rummel et al. (2016).

Interestingly, these experiments also showed that at 6 days post-culture, control microglia in the sheath layer did not express high levels of NF-IL6 and could be considered “non-activated”. This suggests that microglia are able to mitigate the initial inflammatory response post-sectioning (Chong et al., 2018; Huuskonen et al., 2005) and return back to a resting non-inflammatory morphology and a predominantly non-activated state. These findings are substantiated by Huuskonen et al. (2005), who characterized cytokine release in untreated OBSCs over 7 days in culture and observed that slices recover from the injury of culture preparation as soon as 4 days post-culture as highlighted by the substantial decrease in IL-6 and TNF-α in culture medium.

I also sought to find out whether we can track changes in neuronal activation using NF-IL6 as a functional readout. While neuronal cells have been demonstrated to produce inflammatory molecules such as the pro-inflammatory cytokine IL-6 under pathological conditions highlighting their capacity to attenuate inflammatory responses (Bartfai & Schultzberg, 1993; Gruol, 2015; Jüttler et al., 2002; Ringheim et al., 1995), I found that NF-IL6 was constitutively expressed in neuronal cells, finding it at detectable levels in both control and LPS-treated slices. While this could be a clear limitation of this experiment, as it demonstrates that NF-IL6 is not an ideal measure of inflammation in neurons, it also raises the question of whether NF-IL6 may take on functions other than inflammation in neuronal cells, which requires further exploration. In the periphery, for example, NF-IL6 plays a key role in regulating the differentiation and proliferation of various cell types including adipocytes (Guo et al., 2015) and

hematopoietic stem/progenitor cells in bone marrow (Sato et al., 2020), pointing to its diverse role in the body. In terms of tracking inflammation in neurons, it could be worth considering using a different functional readout, such as inflammatory transcription factors NF-κB or STAT3, which have also been shown to be expressed in neurons (Bromberg & Wang, 2009; Mattson & Meffert, 2006; Rummel, 2016).

It has been demonstrated that the nuclear translocation of NF-IL6 during an inflammatory challenge increases the transcription of inflammatory genes that regulate downstream releasable factors, including that of the pro-inflammatory cytokine IL-6 (Rummel, 2016); thus, I measured the concentrations of IL-6 and TNF-α released by OBSCs in culture medium. I found that LPS caused a significant increase in the levels of both these pro-inflammatory cytokines as compared to controls. These findings were consistent with previously recorded data that showed that TLR4 activation by LPS induces the release of pro-inflammatory cytokines, including IL-6 and TNF-α in OBSCs (Huuskonen et al., 2005; Lu et al., 2008; Papageorgiou et al., 2016; Poltorak et al., 1998; Qureshi et al., 1999), validating the immunofluorescence findings and confirming that there was inflammation in these OBSCs.

Next, we explored gene expression changes in microglia and astrocytes in response to LPS challenge using snRNA-sequencing. We confirmed the computationally grouped cell clusters by quantifying the average expression of known cell-type specific markers. Microglial-specific marker genes such as *Tmem119*, a transmembrane protein that is expressed in resident non-ramified (resting) microglia (Mercurio et al., 2022; Ruan & Elyaman, 2022), were highly expressed in microglial cells as compared to other cell types. Likewise, *Gfap*, an intermediate filament protein that is highly expressed within astrocytic processes (Brenner, 2014; Messing & Brenner, 2020), and *Aqp4*, a water channel expressed in astrocytic end feet, especially at the BBB where it has been implicated in water transport across the BBB (Szu & Binder, 2016), where both highly expressed in astrocytes confirming our cluster annotations.

I also further investigated whether there were LPS-dependent changes in the proportion of nuclei clustered in each cell type (especially in the microglia and astrocytes clusters), partly to substantiate the findings in **Fig 3.2,** where I comprehensively looked at cell distributions of various cell types. Here I did not observe stark differences in the proportion of cells between clusters; however, the

minute differences that were observed can be attributed to the fact that the cell counts in **Fig 3.2** were done solely in the CA3 region of the hippocampus, whereas in the snRNA-sequencing experiments, full hippocampi slices were utilised. It is then plausible that there may be some differences in the cell proportions.

In response to LPS treatment, there was a global upregulation of inflammatory genes in both microglia and astrocytes that were expressed at low levels in control slices. I visualised this expression by looking at the top 20 differentially expressed inflammatory genes between control and LPS-treated slices in both microglia and astrocytes. Here I observed genes such as *CCL5,* an inflammatory chemokine being upregulated in both microglia and astrocytes. Interestingly, many of these upregulated genes in both cell types were mediated by the same or closely related inflammatory signalling pathways. *CCL5,* for example, is regulated by the PI3K/AKT, NF-κB, and the JAK/STAT inflammatory signalling pathways (Zeng et al., 2022). Interestingly, the *Timp1* gene, which was also upregulated in both microglia and astrocytes, is also activated via the NF-κB and the JAK/STAT signalling pathways (Bommarito et al., 2011; Rummel, 2016). Furthermore, most of these inflammatory signalling pathways are in extensive crosstalk with one another. For instance, Zhang et al. (2012) found that in a rat model of myocardial infarction, the production of STAT 1 (by the JAK/STAT signalling pathway) and NF-κB worked synergistically to increase the transcription of pro-inflammatory cytokines.

Additionally, the activation of most of these signalling pathways leads to the release of the same inflammatory molecules by immune cells. The release of IL-6 and TNF-α, for example, is mediated by an array of pathways, including the JAK/STAT, NF-κB, as well as the NF-IL6 signalling pathway. The release of these inflammatory modulators by the activation of highly related inflammatory signalling pathways suggests that there is crosstalk between microglia and astrocytes to carry out inflammatory functions in the brain. Bidirectional crosstalk between microglia and astrocytes in inflammation has been well described in the literature (Linnerbauer et al., 2020; Matejuk & Ransohoff, 2020; Rostami et al., 2021), and thus it is not surprising that very closely related immune pathways are activated in both cell types. The findings from these experiments are also in line with reports from Delbridge et al. (2020), who used snRNA-sequencing to investigate transcriptomic changes in microglial cells in OBSCs

in response to LPS treatment. The author observed a robust upregulation of inflammatory genes comparable to what is observed *in vivo* following intraperitoneal LPS injections. Our study has gone further to show that LPS induces an upregulation of inflammatory genes in both microglia and astrocytes.

Another gene of interest upregulated in response to LPS treatment was the *Cebpβ* gene, which encodes for NF-IL6; the transcription factor we used as our functional readout for tracking inflammation at the protein level in OBSCs. This gene was upregulated in both microglia and astrocytes and corroborated the findings we observed in our immunofluorescence staining experiments.

Based on the transcriptomic findings, I explored the protein expression of some of the inflammatory genes upregulated in response to LPS treatment. I used immunofluorescence staining to validate the protein expression of *Timp1*, *Ccl5*, and *Lcn2,* which were upregulated in both microglia and astrocytes at the transcriptomic level. I also visualised the expression of *Pik3ap1*, an inflammatory gene that was upregulated by LPS predominantly in microglial cells. All of these genes function and contribute to inflammation in various ways. *Timp1*, for example, is a matrix metalloproteinases (MMP) inhibitor and prevents excessive tissue damage in inflammation (Ries, 2014). During an inflammatory challenge, MMP expression can become dysregulated, which may result in tissue and cell damage, as well as apoptosis, all of which are processes that can further exacerbate inflammation (Cabral-Pacheco et al., 2020). *Timp1* regulates the inflammatory response by antagonising MMP function preventing excessive tissue damage and chronic inflammation (Ries, 2014; Schoeps et al., 2023). Likewise, *Pik3ap1* is involved in modulating inflammation by linking TLR signalling to the PI3K-Akt inflammatory signalling pathway, a process that limits TLR signalling in macrophages and prevents neurotoxicity during inflammation (Hamerman et al., 2016).

Intriguingly, I observed that the snRNA-sequencing findings did not always parallel the protein expression of these genes. Only *Timp1* displayed a consistent finding of upregulation in response to LPS; the rest displayed no significant differences in protein expression between controls and LPS treated slices. In some cases, I observed high protein expression in both untreated controls and LPS-treated OBSCs, e.g., in *Ccl5*. There are possible reasons why a gene transcribed at low levels (as observed in the

expression of these genes in controls in the snRNA-sequencing findings) can still result in high protein expression. One of these could be that once the genes are transcribed, the mRNA could be undergoing post-transcriptional modification, which stabilises it and helps with efficient protein translation (Nachtergaele & He, 2017). Additionally, some genes possess regulatory elements within their mRNA sequences, including specific motifs that enhance ribosomal translation efficiency, which means they can be translated efficiently even with low mRNA levels (Nachtergaele & He, 2017). This is quite interesting because for some of these stains, i.e., in controls of *Timp1* and *Pik3ap1* **(Fig 3.8 B & Fig 3.10 B),** we observed distinctive cytoplasmic staining that was always adjacent to the nucleus. We hypothesised that this might be staining the cell's protein synthesis machinery, including ribosomes and lysosomes containing transcribed and translated proteins awaiting post-translational modification and subsequent release to their functional sites upon activation. Notably, the lysosomal localisation can be attributed to the antibody's ability to target both the active and non-active forms of the protein, which share a similar sequence for antibody binding.

With that, however, this dataset needs to be expanded on by increasing the sample sizes as well as by using a different way of analysing our immunofluorescence images. These experiments used the mean fluorescence intensity to quantify differences in protein expression, and while this was informative, we could not conduct definitive colocalization analyses; perhaps creating a colocalization macro in ImageJ would be more informative.

There were some limitations to my model system, one of which was that only one immunogenic agent (LPS) was tested to elicit an inflammatory response in the OBSCs. With this, however, literature has demonstrated that other immunogenic agents such as polyriboinosinic-polyribocytidylic acid (poly I:C), which activates TLR3 and zymosan (TLR2), also exert their functions on TLRs much like LPS, activating inflammatory signalling pathways such as NF-κB and increasing the release of pro-inflammatory molecules (Field et al., 2010; Frasnelli et al., 2005; Wang et al., 2014). Additionally, imaging data recorded in this chapter was done solely in the CA3 region of the hippocampus; this was done because this model system was established to investigate inflammatory mechanisms in NCC where seizures are the most common

symptoms, and the CA3 region has been implicated in epileptogenesis in the brain (Song et al., 2018; Zhang et al., 2017). To further characterise this model, different hippocampal regions may be imaged; this may also help findings of cell distributions and proportions align more with the cell proportions observed in the snRNA-sequencing findings.

In summary, whilst previous work has used OBSCs as a model system to study neuroinflammation, in this chapter, I have extended this by performing thorough immunohistochemical analysis and snRNA-sequencing to characterise LPS-induced protein and gene expression changes in different glial cell types. I have thus demonstrated that OBSCs present a reliable tool for investigating cell-type specific inflammatory responses of innate immune cells in isolation from adaptive immune responses in the brain.

CHAPTER 4

INVESTIGATING *TAENIA* MODULATION OF NEUROINFLAMMATION

4.1 INTRODUCTION

The parasitic infection neurocysticercosis (NCC) is the leading cause of adult-acquired epilepsy in the world (Carpio, 2002; Carpio & Romo, 2014). In endemic regions, NCC infection has been associated with 30% of all epilepsy cases, burdening community health heavily (Carpio, 2002; Carpio & Romo, 2014; Del Brutto, 2012; Gripper & Welburn, 2017). The most common clinical manifestation of NCC is epileptic seizures, which occur in up to 80% of all symptomatic cases (Steyn et al., 2022; World Health Organisation, 2016).

Intriguingly, seizure occurrence in NCC is primarily associated with the degenerative transitional and calcified stages of the parasite, which occur months or even years post-initial infection (Carpio et al., 2021; De Lange et al., 2018). Additionally, seizures present concurrently with neuroinflammation in this disease, which has prompted the widely believed hypothesis that it is the neuroinflammation caused by the dead or degenerating cysts that elicit seizures in NCC (Steyn et al., 2022; Stringer et al., 2003). Paradoxically, during the viable cyst stage (vesicular cyst stage) that occurs immediately post-infection and for a period of months to years, patients present with no symptoms, displaying no seizures and, in turn, no neuroinflammation. In line with that, literature has shown that asymptomatic NCC patients tend to present higher serum levels of anti-inflammatory cytokines, whereas symptomatic patients display high levels of pro-inflammatory cytokines, which is indicative of neuroinflammation (Prasad et al., 2009; Verma et al., 2011). This underscores the existence of neuroinflammatory alterations in the progression of this disease. With that, the mechanisms of how viable cysts are able to exist and evade host innate immune responses for such extended periods of time, prompting no inflammatory response from the host, remain unclear. Particularly unknown is how innate immune cells such as microglia and astrocytes respond during the infection. Thus, this chapter aimed to investigate how viable *Taenia* larvae modulate neuroinflammation by looking at

changes in the activation of microglia and astrocytes, exploring gene expression changes and measuring the release of pro-inflammatory cytokines.

To investigate this, I utilised mouse hippocampal organotypic brain slice cultures (OBSCs) and subjected them to four comparable treatments: **1)** untreated control slices; **2)** LPS-treated slices to induce an inflammatory response and act as a positive control for inflammation; **3)** to simulate the viable stage of cestode infection, slices were treated with the viable larvae (homogenate) of *T. crassiceps*, a cestode closely related to the human disease-causing *T. solium;* and **4)** finally, to examine the potential immunomodulatory effects of viable *Taenia* larvae on neuroinflammation, I treated slices with both LPS and *T. crassiceps* homogenate simultaneously.

I used double immunofluorescence staining to visualise various cell-type specific markers for either microglia (IBA1) or astrocytes (S100β) together with the inflammatory transcription factor NF-IL6. This allowed me to determine inflammatory activation in both cell types in all treatment groups. I ascertained that *T. crassiceps* homogenate on its own does not exert a cytotoxic effect on glia in OBSCs by comparing the total proportion of cells that were glia in untreated control versus *T. crassiceps* homogenate-only treated slices. In terms of inflammatory mechanisms, I found that *T. crassiceps* homogenate suppresses the LPS-induced microglial and astrocytic activation, suppresses pro-inflammatory cytokine release as measured through ELISAs, and prevents LPS-induced upregulation of key inflammatory genes. From this data, I concluded that *Taenia* larvae suppress the brain's pro-inflammatory responses mediated by microglia and astrocytes, and this may explain why the parasite can persist and develop in the brain with minimal symptoms in the host.

4.2 *TAENIA CRASSICEPS* WHOLE CYST HOMOGENATE DOES NOT EXERT A CYTOTOXIC EFFECT ON GLIA AND DOES NOT AFFECT GLIAL DISTRIBUTION ACROSS OBSCS.

To model viable NCC infection, I used 200 µg/ml of whole cyst homogenate made from the viable larvae of *T. crassiceps* to treat OBSCs (see **Chapter 2.1.2**). Before I could begin characterising inflammatory processes in response to treatment, I first ascertained whether the *T. crassiceps* whole cyst homogenate had a cytotoxic effect on glia. To do this, I used immunofluorescence staining to compare the total proportion

of cells, which were either microglia (IBA1) or astrocytes (S100β) in untreated control versus *T. crassiceps* homogenate-treated OBSCs. I quantified these proportions at three different depths of OBSCs: 0 µm (sheath), 5 µm, and 10 µm. Quantification was done on z-stacks acquired on the confocal microscope at 40X magnification; cell counts were done using our cell counter macro in ImageJ.

My results show that microglial cells formed a sheath at the top of the slice (0 µm) in both control and *T. crassiceps* homogenate-treated slices. The total proportion of cells that were microglia at this layer was 49% for controls and 44.4% for *T. crassiceps* homogenate **(Fig 4.1 A & B).** A Mann-Whitney U test did not find these results significantly different (N = 3, p = 0.5887, Mann-Whitney U test). As demonstrated in **Chapter 3**, overall microglial distribution decreased with slice depth, with the lowest proportions of cells that were microglia being recorded at 10 µm. Morphologically, microglia can be observed in a ramified morphology in both control and *T. crassiceps* homogenate-treated slices, especially in the deeper slice layers **(Fig 4.1 A**). There was additionally no significant *T. crassiceps* homogenate-dependent decrease in the total proportion of microglial cells at any of the recorded layers. This highlighted that the viable larvae homogenate was not inducing the death of microglial cells in the slices.

The proportion of cells that were astrocytes increased with slice depth, with the highest proportion of cells being recorded at the 5 µm layer where controls had an average of 28.8% and the *T. crassiceps* homogenate treated slices had an average of 38.8%, which was not significantly different (N = 3, p = 0.2403, Mann-Whitney U test). Overall, for all depths recorded, the average proportion of cells that were astrocytes tended to be slightly higher in the *T. crassiceps* homogenate group; however, a Mann- Whitney U test found the differences as not significant.

The findings that treating OBSCs with *T. crassiceps* homogenate does not decrease the proportion of cells which are either microglia or astrocytes indicates that the homogenate likely does not exert a specific cytotoxic effect on glial cells. Subsequent cell count analyses for microglia were done at the sheath layer (0 µm) and at 5 µm for astrocytes.

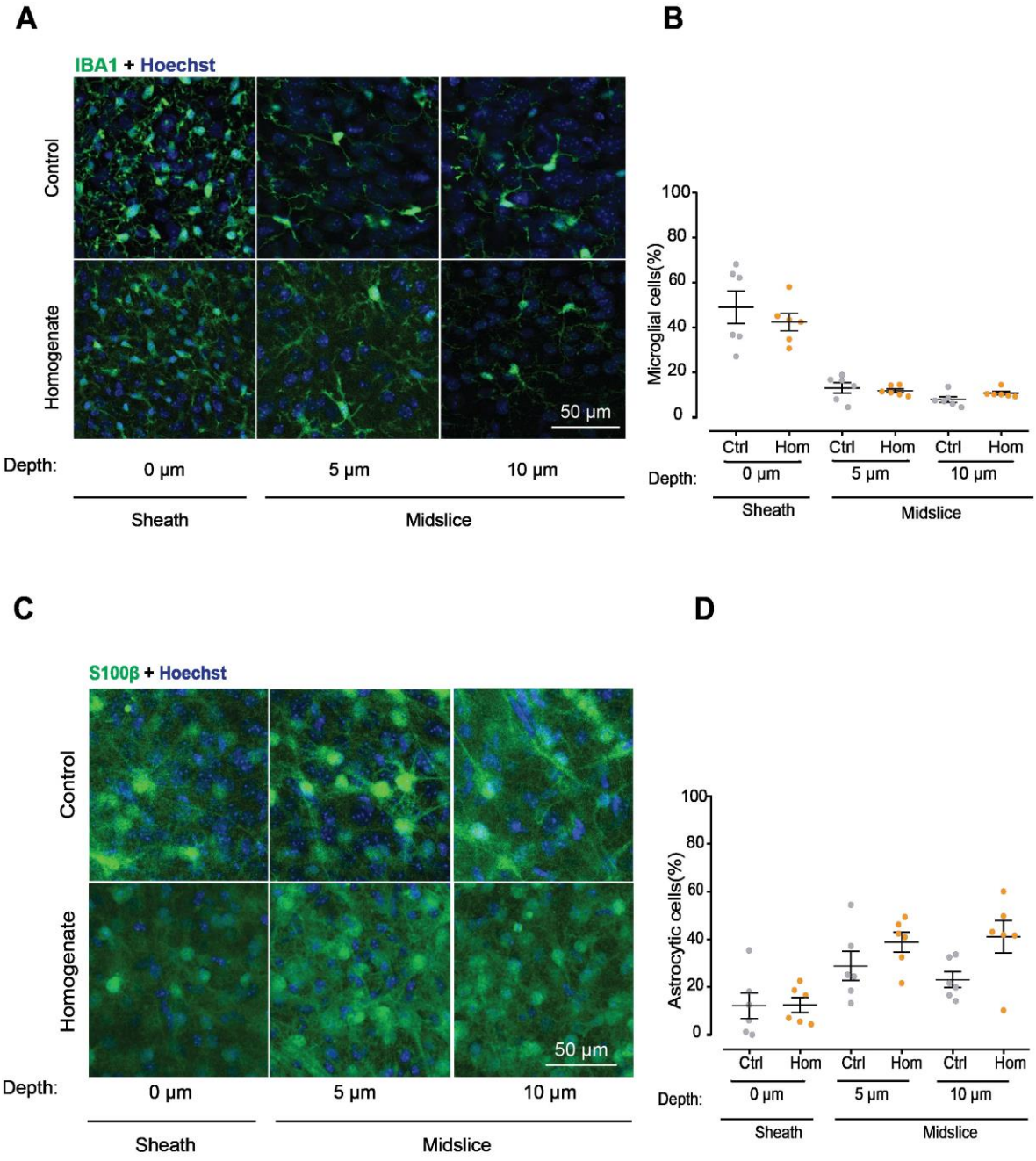

Figure 4.1 *T. crassiceps* whole cyst homogenate does not exert a cytotoxic effect on glia and does not affect glial distribution across OBSCs. A) Representative confocal microscope images of IBA1 (microglia) and Hoechst stained OBSCs from untreated controls and *T. crassiceps* whole cyst homogenate treated slices at 0 µm, 5 µm and 10 µm slice depths. Images were obtained from a z-stack taken in the CA3 region of the hippocampus at 40X magnification. **B)** Population data of the total proportion of microglial cells collected from the three different slice depths. **C)** Representative confocal microscope images of slices stained with S100β to mark astrocytes along with Hoechst nuclear marker. **D)** Population data of astrocytes as a proportion of all cells collected from the three different depths. The proportion of astrocytes increased with slice depth and did not display a homogenate-dependent decrease. Values with means ± SEM, each data point represents an imaged z-stack region (N = 3 slices per condition).

4.3 *TAENIA CRASSICEPS* WHOLE CYST HOMOGENATE SUPPRESSES LPS-INDUCED GLIAL ACTIVATION IN OBSCS.

To investigate how *T. crassiceps* homogenate was modulating inflammation in the brain, I measured how the homogenate altered LPS-induced inflammatory activation in microglia and astrocytes. This was accomplished by co-staining for cell-type specific markers for microglia (IBA1) and astrocytes (S100β) and the inflammatory transcription factor NF-IL6. Nuclear colocalization between the respective markers and NF-IL6 would indicate the activation of that specific cell type, thereby signifying an inflammatory response. Four different conditions were stained and compared; to elicit an inflammatory response in OBSCs, I treated slices with 10 ng/ml of LPS for 24 hours; these were compared to untreated control slices and to slices treated with 200 ug/ml of *T. crassiceps* homogenate which served as a viable cestode model of NCC. To investigate the potential immunomodulatory effects of *Taenia* larvae on glial cell activation and inflammation, I co-treated some slices with both LPS (at 10 ng/ml) and *T. crassiceps* homogenate (200 ug/ml) together for 24 hours. I then took detailed z-stacks at 40x magnification on the confocal microscope and did colocalization analyses using a cell counter macro in ImageJ.

My results show low NF-IL6 immunoreactivity in untreated controls and *T. crassiceps* homogenate-only treated slices. There was also low colocalization between NF-IL6 and IBA1 in both groups, with a total proportion of activated microglial cells for controls (2.2%) not being significantly different to that of the *T. crassiceps* homogenate group (1%) **(Fig 4.2 A & B)** (N = 6, p = 0.9823, one-way ANOVA with Tukey's test). LPS treatment, however, increased the observable NF-IL6 immunoreactivity and the proportion of activated microglial cells to 46.7%, as measured through NF-IL6 and IBA1 colocalization. This increase was significantly different from both controls and *T. crassiceps* homogenate (Control vs LPS: N = 6, $p \leq 0.0001$; *T. crassiceps* homogenate vs LPS: N = 6, $p \leq 0.0001$; one-way ANOVA with Tukey's test). This indicated the presence of an inflammatory response in the LPS condition, which was not present in controls or *T. crassiceps* homogenate treatment alone. Interestingly, the co-treatment of both LPS and *T. crassiceps* homogenate together suppressed the LPS-induced activation of microglial cells to only 6% activated cells, which was significantly different from the LPS-treated slices (LPS vs LPS and *T. crassiceps* homogenate: N =6, $p \leq$

0.0001, one-way ANOVA with Tukey's test), this constitutes an anti-inflammatory effect being exerted by the *Taenia* homogenate on OBSCs **(Fig 4.2 A & B)**.

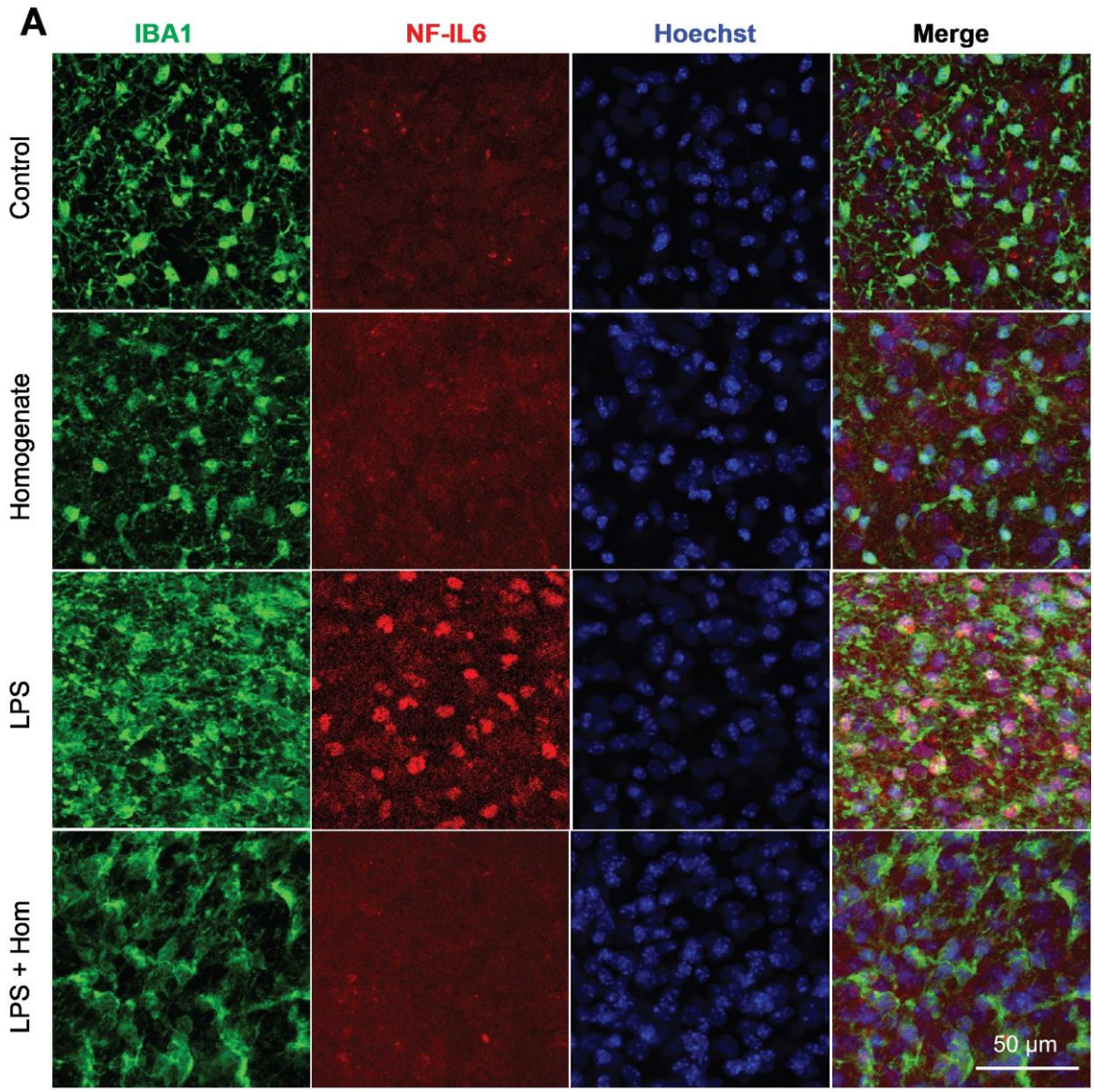
A
IBA1
NF-IL6
Hoechst
Merge
Control
Homogenate
LPS
LPS + Hom
50 µm

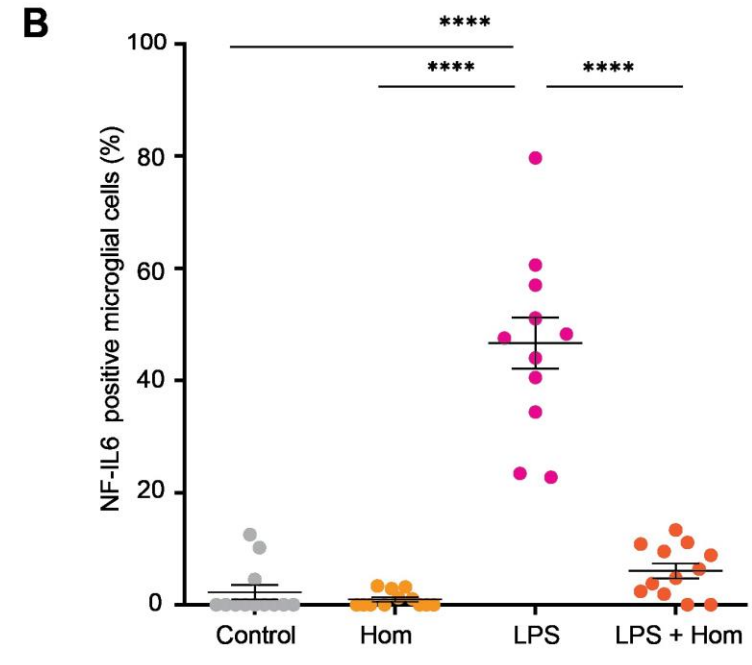
B
****
****
****
100
80
60
40
20
0
NF-IL6 positive microglial cells (%)
Control
Hom
LPS
LPS + Hom

Figure 4.2 *T. crassiceps* whole cyst homogenate suppresses LPS-induced microglial activation in OBSCs. A) Confocal microscope images of OBSCs stained with IBA1 to mark microglial cells, NF-IL6 as an inflammatory readout, and Hoechst nuclear marker. Comparing microglial activation between untreated control slices to *T. crassiceps* homogenate, LPS, and LPS and *T. crassiceps* homogenate treated slices. **B)** population data displaying low microglial activation in controls and *T. crassiceps* homogenate treated slices. LPS treatment increased the proportion of activated microglial cells; however, cotreatment with both LPS and *T. crassiceps* homogenate suppressed that activation almost back to baseline control levels, constituting an anti-inflammatory effect of the *Taenia* larvae on microglial activation. Values are mean ± SEM; each data point represents an imaged z region. N = 6 slices per condition, **** $p \leq 0.0001$, One-way analysis of variance (ANOVA) with Tukey multiple comparisons post-hoc test.

Comparatively, a Tukey multiple comparison test found no significant differences in microglial activation between either controls and *T. crassiceps* homogenate only, to LPS and *T. crassiceps* homogenate treated groups. This highlights the extreme immunosuppressive effects of *Taenia* larvae on microglial activation, as activation almost returns to baseline control levels in the LPS and *T. crassiceps* homogenate co-treatment (Controls vs LPS and *T. crassiceps* homogenate: N = 6, $p = 0.6981$, *T. crassiceps* homogenate vs LPS and *T. crassiceps* homogenate: N = 6, $p = 0.4695$, one-way ANOVA with Tukey's test).

A similar finding was observed for astrocytes. There was also low NF-IL6 immunoreactivity in untreated controls and *T. crassiceps* homogenate-only slices. Additionally, there was low colocalization between NF-IL6 and S100β in both these treatment groups. The proportion of activated astrocytes for controls (2%) was not significantly different to that of *T. crassiceps* homogenate-only (2.3%) **(Fig 4.3 A & B)** (N = 3, $p \geq 0.9999$, one-way ANOVA with Tukey's test). However, treating OBSCs with 10 ng/ml of LPS increased the proportion of activated astrocytes to 64.4%, highlighting an inflammatory response in these slices. There was observably also a significant increase in the NF-IL6 immunoreactivity as well as an increase in the colocalization between NF-IL6 and S100β in this treatment group **(Fig 4.3 A & B)**. Interestingly, the co-treatment of both LPS and *T. crassiceps* homogenate together again significantly suppressed the activation of astrocytes that was observed in the LPS treated group to only 2.3% activated astrocytes (LPS vs LPS and *T. crassiceps* homogenate: N = 3, $p \leq 0.0001$, one-way ANOVA with Tukey's test). This was not significantly different from either control or *T. crassiceps* homogenate-only treated slices. This highlights that the *Taenia* larvae suppressed the activation of cells back to baseline levels where they

were comparatively not different to untreated control slices (Control vs LPS and *T. crassiceps* homogenate: N = 3, $p \geq 0.9999$; *T. crassiceps* homogenate vs LPS and *T. crassiceps* homogenate: N = 3, $p \geq 0.9999$, one-way ANOVA with Tukey's test).

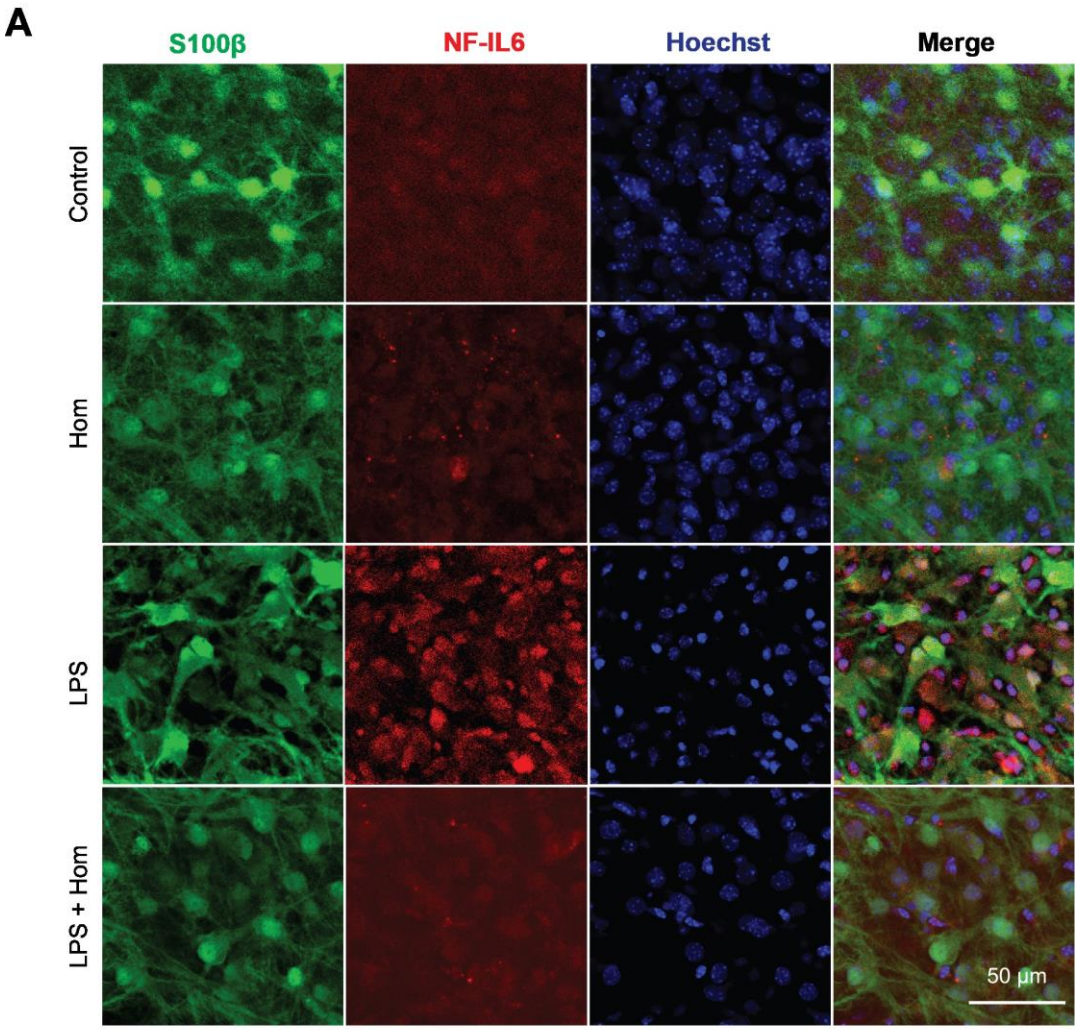
A
S100β
NF-IL6
Hoechst
Merge
Control
Hom
LPS
LPS + Hom
50 µm
B
****
****
****
NF-IL6 positive astrocytic cells (%)
100
80
60
40
20
0
Control
Hom
LPS
LPS + Hom

Figure 4.3 *T. crassiceps* whole cyst homogenate suppresses LPS-induced astrocytic activation in OBSCs. A) Confocal microscope images of OBSCs stained with the astrocytic marker S100β, along with the inflammatory transcription factor NF-IL6 and Hoechst nuclear marker. Images were obtained from a mid-slice (5 µm depth) plane of a z-stack performed on the confocal microscope at 40X magnification **B)** population data displaying low astrocyte activation in both controls and *T. crassiceps* homogenate treated slices. LPS treatment increased the proportion of activated astrocytes; however, cotreatment with both LPS and *T. crassiceps* homogenate significantly suppressed that activation of astrocytes. Values are mean ± SEM; each data point represents an imaged z region. N = 3 slices, **** $p \leq 0.0001$, One-way analysis of variance (ANOVA) with Tukey multiple comparison posthoc test.

4.4 *TAENIA CRASSICEPS* WHOLE CYST HOMOGENATE MODULATES LPS INDUCED CYTOKINE RELEASE IN OBSCS.

Next, I wanted to confirm the findings in **Chapter 4.3** in a different manner by investigating the effects of viable *Taenia* larvae homogenate on releasable pro-inflammatory cytokines IL-6 and TNF-α. To do this, mouse OBSCs were prepared from post-natal day 7 mice and cultured for six days before being exposed to one of the four different treatment conditions (as highlighted in **Chapter 4.3**) for 24 hours via the culture medium, after which the culture medium was collected for ELISAs to determine pro-inflammatory cytokine concentrations.

I found that treating OBSCs with 10 ng/ml of the pro-inflammatory stimulant LPS significantly increased the releasable concentrations of both the pro-inflammatory cytokines IL-6 and TNF-α as compared to controls and *T. crassiceps* homogenate treated slices **(Fig 4.4 A & B).** The average concentration for LPS-treated slices was 2.7 ng/ml for IL-6 and 1.9 ng/ml for TNF-α, as compared to untreated controls, which had an average IL-6 concentration of 0.02 ng/ml and 0.03 ng/ml of TNF-α, and *T. crassiceps* homogenate only group which had an average concentration of 0.04 ng/ml for both IL-6 and TNF-α (LPS vs control: IL-6, N = 36, $p \leq 0.0001$; TNF-α, N = 41, $p \leq 0.0001$; LPS vs *T. crassiceps* homogenate: IL-6, N = 18 - 36, $p \leq 0.0001$; TNF-α, N = 18 - 41, $p \leq 0.0001$, one-way ANOVA with Tukey's test). Interestingly, and in line with what was observed at the protein level, the co-treatment with both LPS and *T. crassiceps* homogenate significantly suppressed the LPS-induced release of both the pro-inflammatory cytokines in question, further highlighting the anti-inflammatory effects of *Taenia* larvae on inflammation **(Fig 4.4 A & B)**. Comparison wise, A one-way ANOVA with a Tukey's test found that the average concentration of both IL-6 (0.2 ng/ml) and TNF-α (0.1 ng/ml) released in the LPS and *T. crassiceps* homogenate

group was not significantly different to that of controls and *T. crassiceps* homogenate alone, highlighting again the strong immunosuppressive effects of *Taenia* larvae on inflammation (LPS and *T. crassiceps* homogenate vs control: IL-6, N = 28 - 36, p = 0.7644; TNF-α, N = 28 - 36, p = 0.9428; LPS and *T. crassiceps* homogenate vs *T. crassiceps* homogenate: IL-6, N = 18 - 26, p = 9059; TNF-α, N = 18 – 26, p = 0.9805, one-way ANOVA with Tukey's test). As compared to the LPS-treated slices, however, there was a significant decrease/suppression in releasable pro-inflammatory cytokines in the combined LPS and *T. crassiceps* homogenate group (LPS and *T. crassiceps* homogenate vs LPS: IL-6, N = 28 – 36, $p \leq 0.0001$; TNF-α, N = 28 -36, $p \leq 0.001$, one-way ANOVA with Tukey's test).

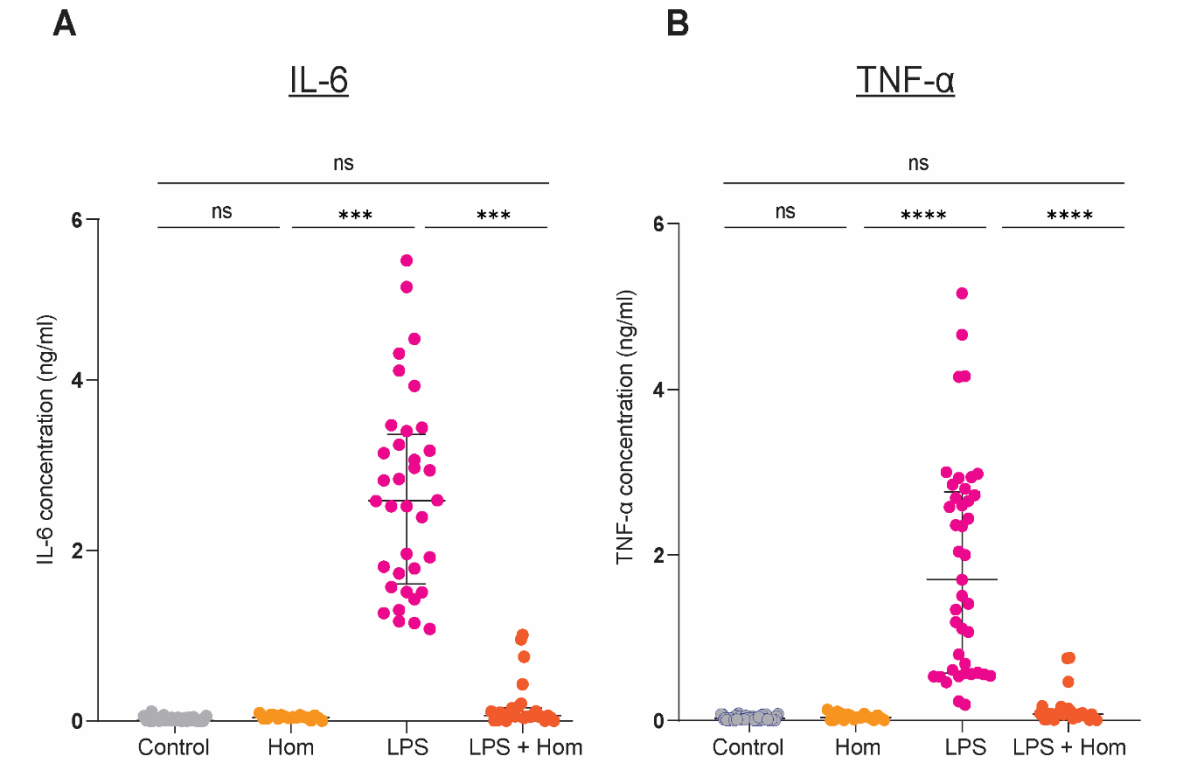

Figure 4.4 *T. crassiceps* whole cyst homogenate modulates LPS-induced pro-inflammatory cytokines IL-6 and TNF -α release. A) Concentration of the pro-inflammatory cytokine IL-6 released by OBSCs in culture media, showing a strong LPS response after 24 hours in treatment as compared to controls and *T. crassiceps* homogenate group. Suppression of LPS-induced IL-6 release is observed in the co-treatment of both LPS and *T. crassiceps* homogenate, highlighting an anti-inflammatory effect the *Taenia* larvae are exerting. **B)** The concentration of the pro-inflammatory cytokine TNF-α released by OBSCs in the culture media also displayed a substantial increase in release in response to LPS

treatment as compared to untreated controls and *T. crassiceps* homogenate only group and an observable suppression of cytokine release in the LPS and *T. crassiceps* homogenate co-treatment. Values with median ± IQR, *** $p \leq 0.0001$; **** $p \leq 0.0001$; ns = not significant; One-way ANOVA with Tukey multiple comparisons test. IL-6 and TNF-α: N = 18 - 41, depending on the condition.

4.5 THE ACTIVE ANTI-INFLAMMATORY AGENT(S) IN *T. CRASSICEPS* WHOLE CYST HOMOGENATE IS A LARGE HYDROPHILIC PROTEIN THAT MODULATES PRO-INFLAMMATORY CYTOKINE RELEASE.

Having established that *T. crassiceps* whole cyst homogenate significantly alters glial activation and pro-inflammatory cytokine release, I wanted to explore further what component of the *Taenia* larvae was mediating this anti-inflammatory effect. This exploration started with Dr Anja de Lange, who, in her PhD studies in the Raimondo lab, used size exclusion fractionation with ammonium sulphate protein precipitation to demonstrate that the active anti-inflammatory agent in *Taenia* homogenate was a hydrophilic protein larger than 100kDa **(Fig 4.5 A & B).** To further home in on the active anti-inflammatory agent, we used size exclusion fractionation and ammonium sulphate (AS) precipitation to make a whole cyst *T. crassiceps* homogenate of proteins larger than 100 kDa with an AS saturation of 50% (50% AS > 100 kDa Hom). We then used size exclusion chromatography to further separate the proteins within this 50% AS >100 kDa Hom by their size. For this, we collaborated with Dr Jeremy Woodward, who ran the 50% AS >100 kDa homogenate through a column suitable for analysing water-soluble linear polymers with molecular weights of up to 1000 kDa, which eventually resulted in 62 different fractions separated by their sizes. We pooled these fractions and used them to treat OBSCs concurrently with 10 ng/ml of LPS so that each treatment consisted of LPS with 6 to 8 different individual fractions pooled together. In the first treatment, 9 pooled fraction groups were used to treat OBSCs. These were compared to OBSCs treated in various experimental controls, mainly **1)** OBSCs treated with 10 ng/ml of LPS; **2)** OBSCs co-treated with LPS (10 ng/ml) and whole cyst *T. crassiceps* homogenate at 200 ug/ml (LPS+Hom); and lastly **3)** a co-treatment of LPS (10ng/ml) and 200 ug/ml of 50% AS >100 kDa Hom (to confirm that this fraction on its own possessed anti-inflammatory properties before we further fractionated it). Slices were treated for 24 hours via the culture medium, after which

the medium was collected to run ELISAs and measure the concentrations of IL-6 and TNF-α.

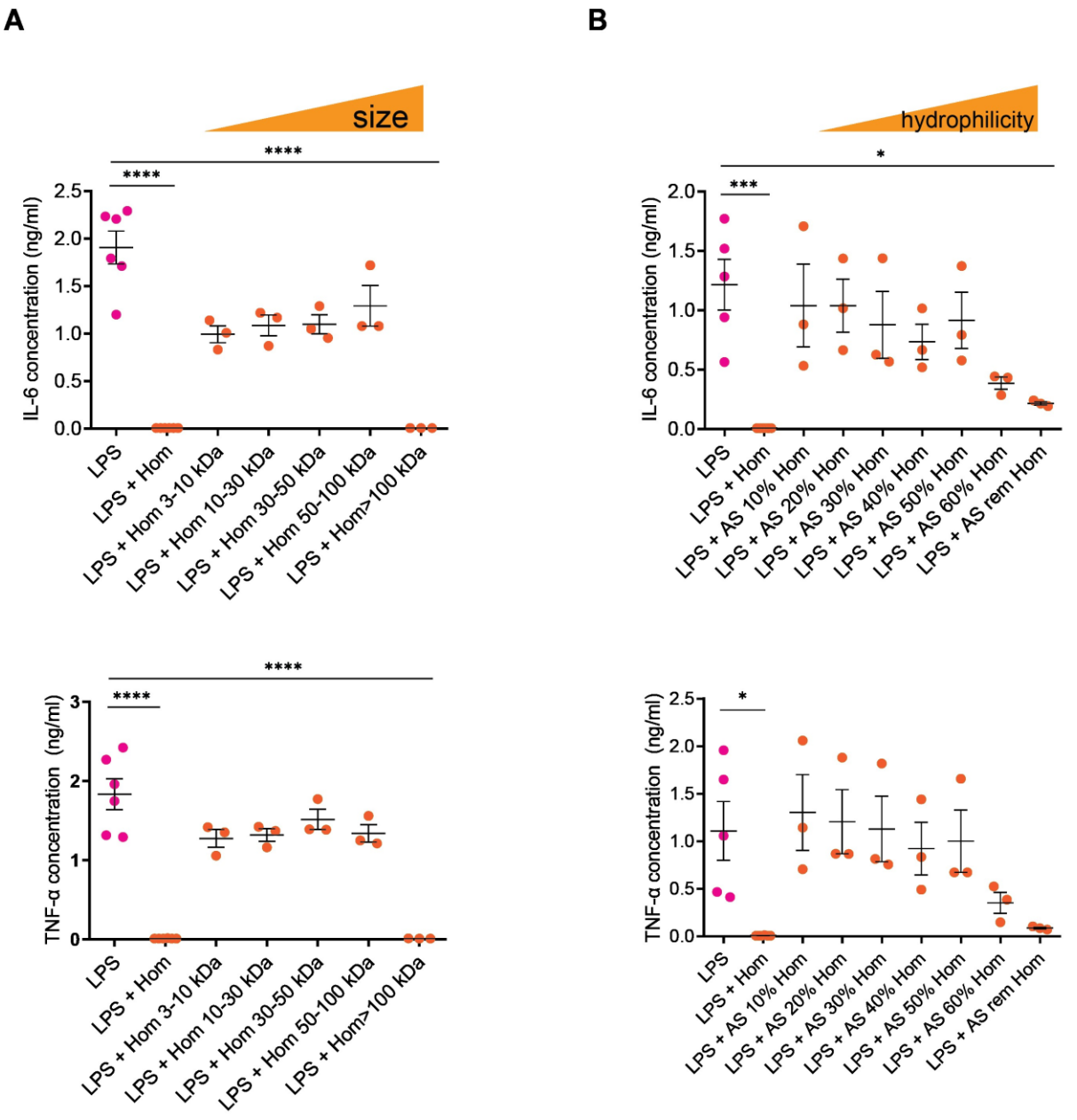

Figure 4.5 The active anti-inflammatory agent in *T. crassiceps* whole cyst homogenate is a large hydrophilic protein. **A)** The pro-inflammatory cytokine release (IL-6 and TNF-α) by mouse OBSCs treated with 10 ng/ml of LPS for 24 hours alone or concurrently with *T. crassiceps* homogenate fractionated by size. Size fractionation of whole cyst *T. crassiceps* homogenate was done by sequentially passing it through Amicon Ultra-15 centrifugal filter units with 3 kDa, 10 kDa, 30 kDa, 50 kDa, and 100 kDa molecular weight cut-offs. The most potent anti-inflammatory effect was only observed on the >100 kDa size fraction, suppressing both IL-6 and TNF-α. **B)** The release of the pro-inflammatory cytokines (IL-6 and TNF-α) in culture media by OBSCs. Slices were treated with LPS concurrently with *T. crassiceps* homogenate, which was separated into fractions of increasing hydrophilicity through ammonium sulphate (AS) protein precipitation. AS saturations ranged from 10% to 60%, with the anti-inflammatory suppression of both IL-6 and TNF-α release only being observed in the

homogenate fractions with the highest hydrophilicity. Values with median ± SEM, * $p \leq 0.01$; *** $p \leq 0.0001$; **** $p \leq 0.0001$; One-way ANOVA with Tukey multiple comparisons test. IL-6 and TNF-α: N = 3-6. This data was collected by Dr Anja de Lange during her PhD in the Raimondo Lab.

As expected, LPS treatment significantly increased the concentrations of both IL-6 and TNF-α released by OBSCs (**Fig 4.6 A & B)**. This release was significantly suppressed in the co-treatments with both LPS+Hom and LPS+50% AS >100 kDa Hom (LPS vs LPS+Hom: IL-6: $p \leq 0.01$; TNF-α: $p \leq 0.0001$; LPS vs LPS+50% AS >100kDa Hom: IL-6: $p \leq 0.0001$; TNF-α: $p \leq 0.0001$, N= 2-3; one-way ANOVA with Tukey's test).

In terms of anti-inflammatory properties, all 9 groups of pooled fractions displayed some degree of pro-inflammatory suppression; however, LPS+Fraction4 and LPS+Fraction5 demonstrated the most significant level of suppression of both IL-6 and TNF-α **(Fig 4.6 A & B)** (LPS vs LPS+Fraction4: IL-6: $p \leq 0.01$; TNF-α: $p \leq 0.001$; LPS vs LPS+Fraction5: IL-6: $p \leq 0.0001$; TNF-α: $p \leq 0.001$, N= 2-3; one-way ANOVA with Tukey's test). The suppression caused by these fractions was not significantly different from either the LPS+Hom or LPS + 50% AS >100 kDa Hom treatments (**LPS+Hom vs LPS+Fraction4**: IL-6: $p \geq 0.9999$; TNF-α: $p \geq 0.9999$; **LPS+50% AS >100 kDa Hom vs LPS+Fraction4**: IL-6: $p \geq 0.9999$; TNF-α: $p \geq 0.9999$; **LPS+Hom vs LPS+Fraction5**: IL-6: $p \geq 0.9999$; TNF-α: $p \geq 0.9999$; **LPS+50% AS >100 kDa Hom vs LPS+Fraction5**: IL-6: $p \geq 0.9999$; TNF-α: $p \geq 0.9999$, N= 2-3; one-way ANOVA with Tukey's test).

From these findings, it was clear that the active anti-inflammatory agent(s) were likely in pooled Fraction 4 and Fraction 5. For our second round of treatments, we decided to home in further on these two groups of pooled fractions, which consisted of 16 individual fractions. Our next step was to treat OBSCs with smaller groups of pooled fractions from Fraction 4 and Fraction 5. In the end, each treatment consisted of only 2 to 3 different individual fractions pooled together instead of the 7-8 we conducted in our first round of treatments. Here, we had 7 smaller groups of pooled fractions applied concurrently with 10 ng/ml of LPS treatment. These were also compared to various experimental controls, namely **1)** LPS at 10 ng/ml; **2)** LPS and *T. crassiceps* whole cyst homogenate (LPS+Hom); **3)** and finally, LPS and a combination of all 16 individual fractions together (LPS+ Comb Fracs). Again, treatment occurred via the culture medium for 24 hours, after which the medium was collected for IL-6 and TNF-α

quantification.

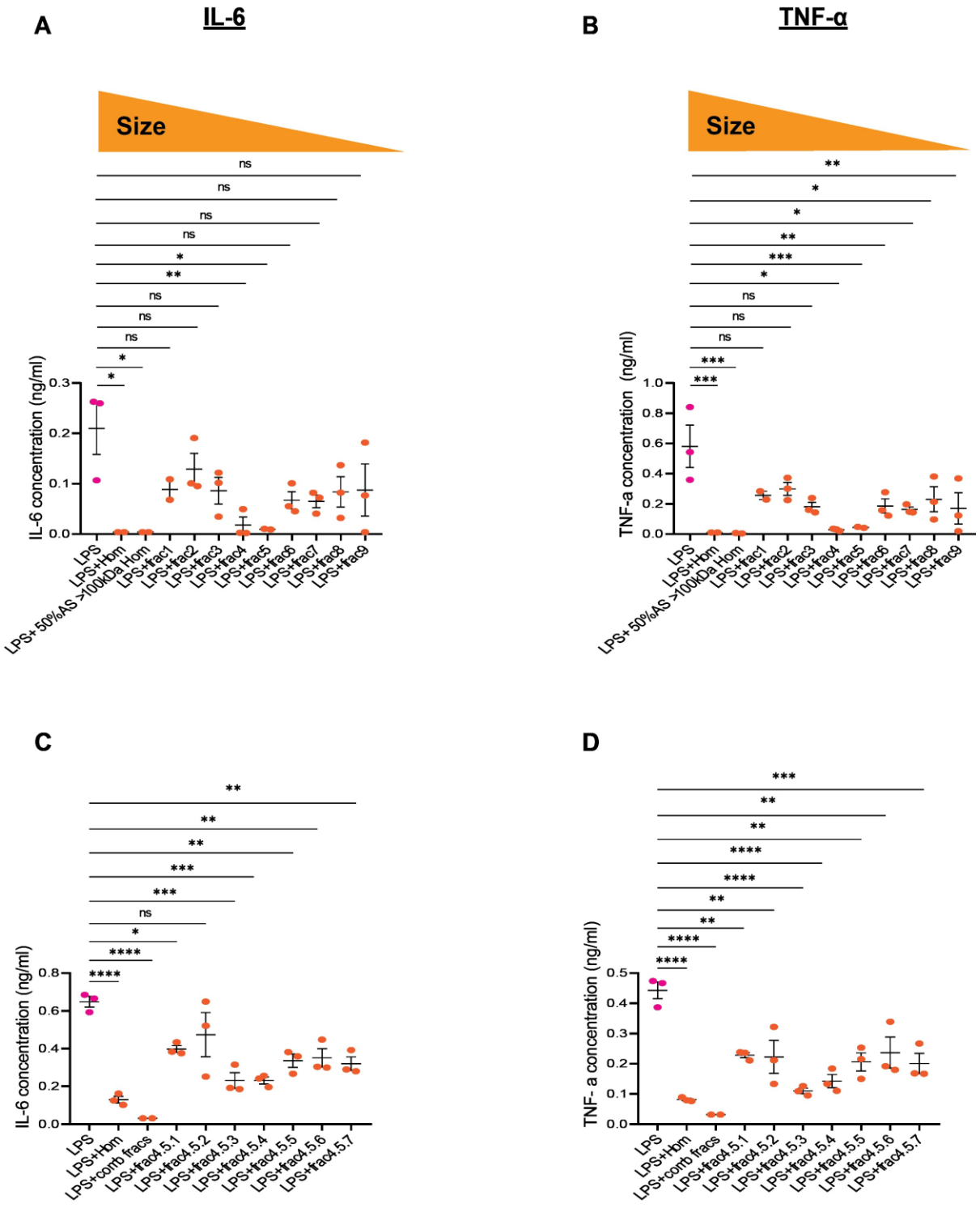

Figure 4.6 The active anti-inflammatory agent(s) in *T. crassiceps* whole cyst homogenate is larger than 100 kDa and modulates pro-inflammatory cytokine release. OBSCs prepared from post-natal day 7 mice were treated with 9 groups of fractions composed of 6 to 8 individual fractions pooled together. Fractions were obtained by running 50% AS > 100 kDa whole cyst *T. crassiceps* homogenate through a 1000 kDa column using size exclusion chromatography. Slices were treated for 24 hours via culture medium, after which medium was collected to quantify the concentrations of IL-6 and TNF-α using ELISAs. **A)**

Concentration of IL-6 released in culture medium by OBSCs showing a strong increase in release in response to LPS treatment; this was immediately suppressed when LPS was co-treated with both standard Homogenate (LPS+Hom) alone and 50% AS >100 kDa Hom. Interestingly, all groups of pooled fractions seemed to display a level of pro-inflammatory suppression; however, LPS+Fraction 4 and LPS+Fraction 5 displayed the most significant level of suppression. **B)** Concentration of TNF-α released by OBSCs in culture medium. Again, a strong LPS response was observed that was most significantly suppressed when co-treated with Fraction 4 and Fraction 5. **C)** The individual fractions that made up Fractions 4 and 5 from **A & B** were pooled into smaller fractions consisting of 2 or 3 individual fractions and used to treat OBSCs together with LPS. As before, treatment was carried out over 24 hours via culture medium, after which the concentrations of IL-6 and TNF-α was quantified. A significant increase in the release of IL-6 was observed in response to LPS treatment, which was suppressed through co-treatment with both *T. crassiceps* homogenate and Comb Fracs (a combination of all individual fractions that made up Fraction 4 and 5 in **A & B**). A degree of suppression was observed from all of the pooled fractions; however, LPS + Frac4.5.3 and LPS + Frac4.5.4 caused the most suppression of IL-6 release. **D)** as in 'C', however, quantifying the release of TNF-α. Again, significant TNF-α suppression is observed in the cotreatment of LPS + Frac4.5.3 and LPS+Frac4.5.4. Values with median ± SEM, * $p \leq 0.01$; ** $p \leq 0.001$; *** $p \leq 0.0001$; **** $p \leq 0.0001$; One-way ANOVA with Tukey multiple comparisons test. IL-6 and TNF-α N = 2 or 3.

A significant increase in the release of both IL-6 and TNF-α was observed when OBSCs were treated with LPS (**Fig 4.6 C & D)**; however, this pro-inflammatory reaction was immediately suppressed in the co-treatments of both LPS+Hom and LPS+Comb Fracs (LPS vs LPS+Hom: IL-6: $p \leq 0.0001$; TNF-α: $p \leq 0.0001$; LPS vs LPS+Comb Fracs: IL-6: $p \leq 0.0001$; TNF-α: $p \leq 0.0001$, N= 2-3; one-way ANOVA with Tukey's test). Interestingly again, all of the groups of pooled fractions also maintained a slight degree of pro-inflammatory cytokine suppression; however, the most significant effect was observed in LPS+Frac4.5.3 and LPS+Frac4.5.4 (LPS vs LPS+Frac4.5.3: IL-6: $p \leq 0.0001$; TNF-α: $p \leq 0.0001$; LPS vs LPS+Frac4.5.4: IL-6: $p \leq 0.0001$; TNF-α: $p \leq 0.0001$, N= 2-3; one-way ANOVA with Tukey's test). Our next goal will be to use SDS-PAGE and mass spectrometry to establish the molecular weights of the proteins in fractions 4.5.3 and 4.5.4 and hopefully identify what these anti-inflammatory proteins are.

4.6 *T. CRASSICEPS* WHOLE CYST HOMOGENATE PREVENTS THE LPS-INDUCED UPREGULATION OF INFLAMMATORY GENES IN BOTH MICROGLIA AND ASTROCYTES.

I further wanted to investigate whether *Taenia* larvae were exerting changes in the expression of key inflammatory genes that were upregulated in response to LPS treatment in microglia and astrocytes using single nucleus RNA-sequencing. To this end, OBSCs from post-natal day 7 mice were prepared, untreated control slices were then compared to slices treated with *T. crassiceps* homogenate, LPS, and finally, LPS and *T. crassiceps* homogenate together. The same snRNA-sequencing pipeline highlighted in **Chapters 2.5 and 3.7** was then performed so that, in the end, nuclei were clustered according to their gene expression profiles. More than 10 different cell types were identified, including microglia, astrocytes, excitatory, and inhibitory neurons **(Fig 4.7 A)**. I was also interested in whether there was a treatment-dependent change in the proportion of cells that were microglia and/or astrocytes between the groups. I thus visualised the proportion of cells and nuclei clustered in both cell types, where I observed no significant differences in cell proportions and cell nuclei numbers between the treatment groups (N = 4, $p \leq 0.5117$, one-way ANOVA with Tukey's test) **(Fig 4.7 A & B)**. While the LPS and *T. crassiceps* homogenate co-treatment group did have fewer nuclei as compared to the rest of the treatment groups, the proportion of cells as a percentage was not significantly different to the rest, and the slight observed differences were attributed to inter-sample variability (LPS and *T. crassiceps* homogenate vs control: N= 4, $p = 0.4630$; LPS and *T. crassiceps* homogenate vs LPS: N = 4, $p = 0.6960$, one-way ANOVA with Tukey's test).

Using DESeq2, I then visualised the average expression of the top 20 differentially expressed inflammatory genes for both microglia and astrocytes in the various treatments; these genes were ranked according to their absolute Log2FoldChange. There was an observable global upregulation of inflammatory genes in response to LPS treatment in both microglia and astrocytes that were expressed in low levels in both controls and the *T. crassiceps* homogenate-only group. Genes such as *Lcn2, Timp1*, and *Ccl5,* all key genes that regulate inflammatory processes in the brain, were upregulated in both cell types in response to LPS. Other genes, such as microglial-specific *Pik3ap1,* which plays a crucial role in microglial motility and proliferation during

inflammation, were also upregulated in response to LPS. Surprisingly, the addition of *T. crassiceps* homogenate to LPS universally suppressed the upregulation of all the inflammatory genes previously upregulated by LPS by itself in both microglia and astrocytes **(Fig 4.7 D&C),** highlighting the broad anti-inflammatory capacity of *Taenia* larvae on inflammation. Genes such as *Msr1* and *Irf7* that were highly upregulated in microglia in response to LPS treatment were not as highly expressed in the co-treatment of both LPS and *T. crassiceps* homogenate together; their average expression was only slightly higher than controls and *T. crassiceps* homogenate only. Interestingly, the *Cebpβ* gene that encodes for the NF-IL6 protein that we used to track inflammation at the protein level followed a similar trend of high upregulation in response to LPS treatment that is not observed in the untreated controls or *T. crassiceps* homogenate group and prevention of that upregulation when we co-treated with both LPS and *T. crassiceps* homogenate together, further substantiating our findings from **Chapter 4.3 – 4.4**.

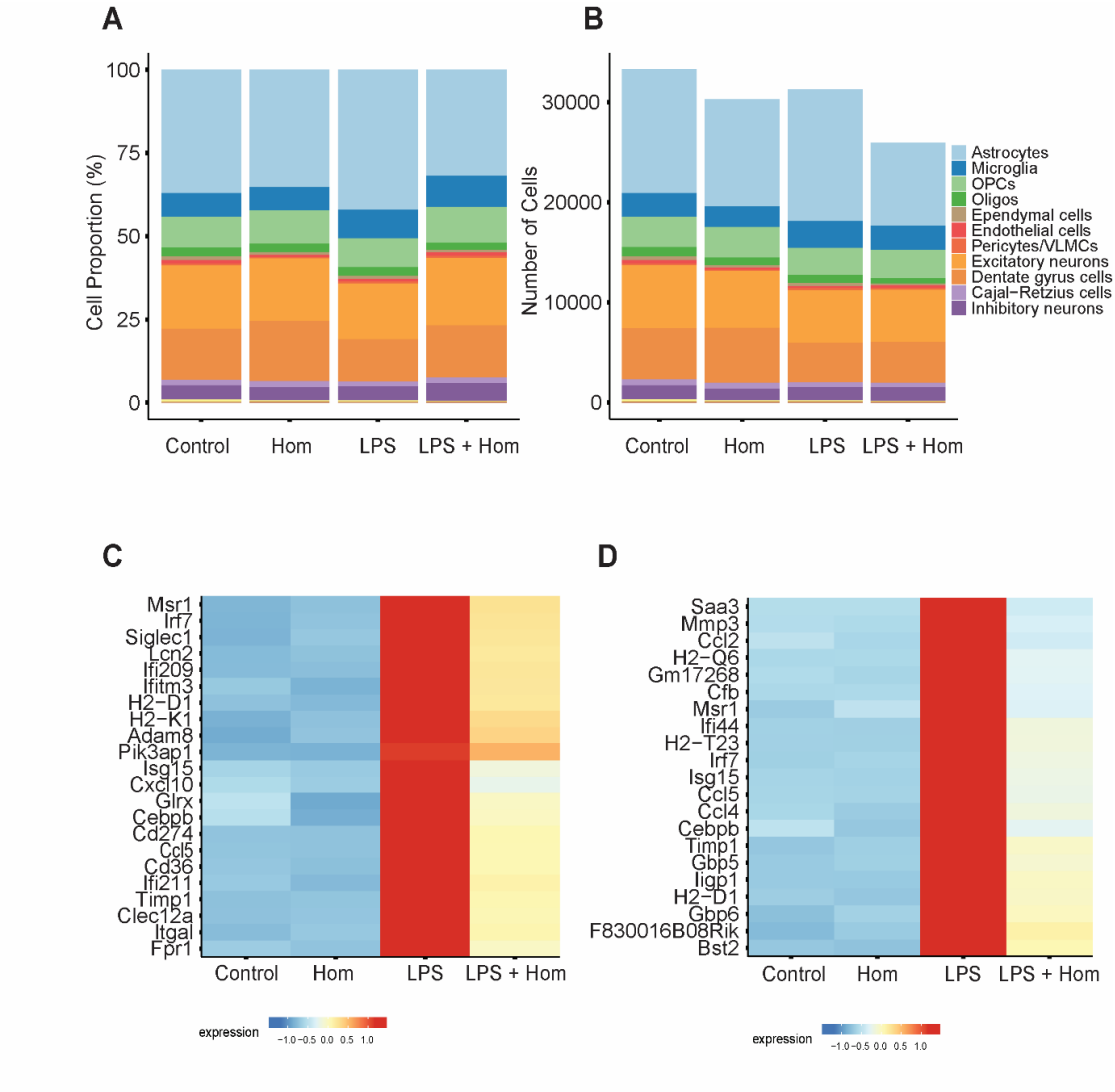

Figure 4.7 *T. crassiceps* whole cyst homogenate prevents the LPS-induced upregulation of inflammatory genes in both microglia and astrocytes. A) Cell proportions in the different cell clusters across the various treatment groups display no significant treatment-dependent changes in the proportion of nuclei belonging to each cell type. **B)** The number of nuclei in the various clusters across the various treatment groups, where there were also no significant differences in nuclei numbers across samples; the slight differences are attributed to intergroup/sample variability. **C)** Heatmap showing the average expression of the top 20 differentially expressed inflammatory genes in microglia in control, *T. crassiceps* homogenate, LPS, and LPS and *T. crassiceps* treated OBSCs. **D)** Heatmap showing the top 20 differentially expressed inflammatory genes in astrocytes across the four treatment groups.

4.7 DISCUSSION

Seizures are the most common presenting symptom in neurocysticercosis, occurring in about 80% of all symptomatic cases (Carpio & Romo, 2014). Seizures are frequently accompanied by neuroinflammation; however, in NCC, both are typically associated with degenerating cysts and are characteristically absent during the viable cyst stage, which occurs immediately post-infection. As a result, there remains a gap in knowledge on how viable *Taenia* larvae can exist in the host for extended periods without eliciting symptoms. Especially unknown is how microglia and astrocytes respond during infection. To this end, in this chapter, I investigated how viable *Taenia* larvae modulate neuroinflammation in the brain using mouse OBSCs by explicitly looking at changes in the activation of microglia and astrocytes, exploring gene expression changes and by measuring the release of pro-inflammatory cytokines.

In the first experiment, I established an *in vitro* model of NCC (reflecting the viable cyst stage) by treating OBSCs with homogenate made from live *T. crassiceps*, a closely related cestode to the human disease-causing *Taenia solium*. This model is characteristically different from previously utilised *in vitro* models to investigate molecular and cellular mechanisms in NCC, such as cultured cell lines (Chile et al., 2016; Palma et al., 2019; Uddin et al., 2005, 2010), in that it allows observation of all major innate cell types without influence from adaptive immune responses. In establishing the model, I first determined that *T. crassiceps* homogenate made from viable larvae does not exert a cytotoxic effect on glia. I explored this by comparing the total proportion of cells that were either microglia or astrocytes in stained OBSCs. I compared untreated controls to slices treated with *T. crassiceps* homogenate at 0 µm, 5 µm and 10 µm slice depths. Here, I observed cell distributions and densities consistent with the findings in **Chapter 3.2**, in that microglial cells formed a sheath at the 0 µm layer, and the total proportion of cells decreased with slice depth. Similarly, the proportion of cells that were astrocytes increased with slice depth, with the highest proportion being recorded at 5 µm. More significantly, I found that for both microglia and astrocytes, there were no significant *T. crassiceps* homogenate treatment-dependent decreases in the total proportion of cells. In fact, the average proportion of cells that were either microglia or astrocytes was almost always slightly higher in the *T. crassiceps* homogenate treatment groups as compared to controls (though these

differences were not significantly different from each other). These findings suggest that the *T. crassiceps* homogenate was not specifically inducing glial cell death in OBSCs.

Next, I investigated the effects of *T. crassiceps* homogenate on inflammation by looking at changes in the activation of microglia and astrocytes. I used dual immunofluorescence to stain for microglia or astrocytes with the inflammatory transcription factor NF-IL6 in OBSCs treated in four comparable conditions **1)** untreated controls, **2)** *T. crassiceps* homogenate (as a model of the viable stage of NCC), **3)** LPS (to elicit an inflammatory response), **4)** LPS and *T. crassiceps* homogenate concurrently (to investigate potential immunomodulatory effects of *Taenia* larvae on inflammation). Here, I found low levels of microglial and astrocytic activation in both control and *T. crassiceps*-treated OBSCs. Treating OBSCs with the TLR4 ligand and pro-inflammatory stimulant LPS significantly increased the proportion of activated microglia and astrocytes, constituting an inflammatory response, as demonstrated in the previous chapter and in line with the findings reported by Delbridge et al. (2020), Huuskonen et al. (2005), and Papageorgiou et al. (2016). Interestingly, the addition of *T. crassiceps* homogenate to LPS suppressed the previously observed LPS-induced activation of both microglia and astrocytes, suggesting that the *Taenia* larvae exert an anti-inflammatory effect on glia by preventing their activation.

To confirm these findings, I ran experiments to measure the concentrations of pro-inflammatory cytokines IL-6 and TNF-α released in culture medium by OBSCs across the various treatment groups. I observed similar results where LPS treatment significantly increased the concentrations of released IL-6 and TNF-α, as compared to controls and *T. crassiceps* homogenate-treated OBSCs. Furthermore, in line with the findings I observed at the protein level using immunofluorescence staining, the co-treatment of both LPS and *T. crassiceps* homogenate suppressed the release of both of these pro-inflammatory cytokines returning them almost back to baseline control levels, again highlighting a robust anti-inflammatory effect of the *T. crassiceps* homogenate. In support of these findings, the capacity of *T. crassiceps* to attenuate the release of inflammatory cytokines has been previously reported in literature. For example, Landa et al. (2019) found that *T. crassiceps* microRNAs strongly decreased

the expression of IL-6, TNF-α, and IL-12 in a murine culture of macrophages. Likewise, another study also reported *T. crassiceps* excretory/secretory products down-regulating the release of LPS-induced pro-inflammatory cytokines such as IL-6 and TNF-α in murine dendritic cells (Terrazas et al., 2011).

I was curious whether *T. crassiceps* homogenate was exerting transcriptomic changes in OBSCs; we thus explored gene expression changes in microglia and astrocytes in response to *T. crassiceps* treatment using snRNA-sequencing. To this end, we visualised the average expression of the top 20 differentially expressed inflammatory genes in both microglia and astrocytes across the aforementioned treatments. Here, we observed a global upregulation of inflammatory genes in response to LPS treatment that were expressed in low levels in controls and *T. crassiceps* homogenate-treated slices in both microglia and astrocytes. Microglial upregulated genes included the chemokine *Cxcl10,* whose expression has been found to be essential in LPS-induced microglial activation (Chen et al., 2023), *Adam8*, an MMP involved in leukocyte recruitment during inflammation (Dreymueller et al., 2017) and *Msr1* which has been shown to interact with TLR on the cell surface of microglia to activate pro-inflammatory signalling pathways such as NF-κB (Gudgeon et al., 2022). Similarly, there was an LPS-induced upregulation of inflammatory genes in astrocytic cells, such as the chemokine *Ccl2,* which plays a role in glial activation; in fact, astrocytic-derived *Ccl2* has been shown to induce M1 activation in microglial cells during inflammation (He et al., 2016). Interestingly, the co-treatment of both LPS and *T. crassiceps* homogenate prevented the strong LPS-induced upregulation of all of these inflammatory genes so that their expression was only slightly higher than that of controls and *T. crassiceps* homogenate by itself, further highlighting the anti-inflammatory effect that the *Taenia* larvae seem to be exerting in OBSCs. This effect was also observed in the *Cebpβ* gene that encodes for NF-IL6 which is the protein that we targeted as a marker for tracking activation and inflammation at the protein level in both microglia and astrocytes.

Taken together, the suppression of glial activation and pro-inflammatory cytokine release, as well as the prevention of LPS-induced upregulation of inflammatory genes by *Taenia* larvae homogenate, leads me to hypothesise that *Taenia* may be exerting its effect on TLR4 directly. If *Taenia* homogenate is acting by blocking TLR4 from

recognising PAMPs such as LPS, it means it will also prevent the initiation of a myriad of inflammatory signalling pathways such as the JAK/STAT, NF-κB, and NF-IL6 signalling pathways, which are critical in upregulating the transcription of a wide array of inflammatory genes and molecules. If this is, in fact, the case, as highlighted by our findings, it may result in the following effects: **1)** preventing the activation of microglia and astrocytes by preventing the translocation of important inflammatory transcription factors (such as NF-IL6) into the nucleus, **2)** this, in turn, prevents the transcription of inflammatory genes that are regulated by the nuclear translocation of these transcription factors such as that of the pro-inflammatory cytokine IL-6 **3)** and as a result, we will observe low production of these inflammatory molecules in the LPS and homogenate co-treatment. Given that we did not observe significant changes in glial activation, cytokine release, and gene expression changes exerted by *T. crassiceps* homogenate on its own (and as compared to controls), it suggests that on their own viable *Taenia* larvae have no pro-inflammatory capacity, which means in the co-treatment of both LPS and *T. crassiceps* homogenate, the homogenate may be acting by preventing LPS binding to receptors that recognise it and initiate classical pro-inflammatory signalling cascades. TLR4 seems to be the most plausible target.

Interestingly, previous literature has suggested that the viable asymptomatic phase of NCC is predominantly mediated by T lymphocytes skewing the Th1/Th2 axis towards a Th2 anti-inflammatory phenotype (De Lange et al., 2018; Peón et al., 2016; Verma et al., 2011). However, my findings demonstrate that even in the complete absence of all T cells and adaptive immunity, *Taenia* larvae can still exert a powerful anti-inflammatory effect on resident immune cells, most likely by blocking TLR activation. These findings address some gaps in the literature about the role of innate microglia and astrocytes in the neuroimmune response to viable *Taenia* infection. Additionally, they highlight the usefulness of OBSCs in investigating inflammatory changes in the brain.

From my findings, it is clear that there is an anti-inflammatory component in *Taenia* larvae that is eliciting these stark suppressive effects on inflammation. Working collaboratively with Dr Anja de Lange and Dr Jeremy Woodward, I explored what this may be. Dr de Lange has previously reported that the active anti-inflammatory agent in *Taenia* larvae is a hydrophilic protein larger than 100 kDa. Using size exclusion

chromatography, we fractionated *Taenia* homogenate as described in **Chapter 4.5** and **Figs 4.5-4.6**. Thus far, we have observed stark suppressive effects in more than one fraction. This leads me to hypothesise that the active anti-inflammatory component in *Taenia* larvae may be a complex of proteins or a single large protein present in multiple fractions. This is supported by the fact that none of the fractions individually elicited as robust a suppression as when whole cyst homogenate was used; however, the fact that a subset of fractions elicited a significantly larger anti-inflammatory effect as compared to the others has given us reason to believe that we are gradually homing in on the active component.

While size exclusion chromatography separates water-soluble proteins by their size, it does not give information on the exact molecular weights of individual proteins (Gaborieau et al., 2008; Gruendling et al., 2008). As such, in order to precisely identify the molecular weights of the proteins contained within each fraction with high resolution and potentially identify the protein(s) itself, we would need to separate the proteins in each fraction further using techniques such as Sodium dodecyl-sulphate polyacrylamide gel electrophoresis (SDS-PAGE), or by more advanced protein identification techniques such as mass spectrometry. Ultimately, identifying this active anti-inflammatory protein will be crucial in aiding the overall understanding of the pathogenesis of NCC and potentially revealing important aspects of host-pathogen interaction that can be exploited for new therapeutic strategies. It could also aid in developing diagnostic tools, especially those that can be utilised in the viable stage of disease where patients may remain asymptomatic.

There are several limitations of my experiments that should be noted. First, I used *T. crassiceps* which is a different species from the disease-causing *Taenia solium*, and though they present with very similar antigenic similarities and *T. crassiceps* has been demonstrated to cause cysticerci in rodents (Ordoñez et al., 2003; Willms & Zurabian, 2010), there are lifecycle differences between the two species which may mean *T. crassiceps* may not fully recapitulate what is truly occurring in the human infection. This is, however, the driving motivation for the next chapter, where I establish a human model of neuroinflammation to help better characterise this disease in human tissue. In addition, I used viable whole cyst homogenate made from frozen *T. crassiceps* larvae; as a result, I only characterised inflammatory changes at one time point during

infection; treating OBSCs with degenerating cysts may help better understand and characterise inflammatory changes throughout the whole span of infection. In line with that, we were unable to measure levels of anti-inflammatory cytokines across treatments, which may have been significantly altered. However, this is unlikely as in other experiments performed in the Raimondo Lab using snRNAseq, *T. crassiceps* homogenate alone was not observed to drive any significant changes in any genes, at least not those that mediate anti-inflammatory processes. Lastly, even though investigating these innate inflammatory changes in isolation from the adaptive immune responses has provided insight into how resident immune brain cells respond in this infection, the lack of critical adaptive elements means that specific inflammatory changes occurring *in situ,* such as cell-cell communication between innate and adaptive immune cells, which may affect inflammation, were not captured in our *in vitro* model.

In summary, in this chapter, I showed that *Taenia* larvae suppress the brain's pro-inflammatory responses by specifically preventing the activation of innate immune microglia and astrocytes, suppressing the release of pro-inflammatory cytokines, and preventing the upregulation of key inflammatory genes. This may help explain why the parasite is able to persist and develop in the brain with no symptoms in the host.

CHAPTER 5

ESTABLISHING AN *IN-VITRO* HUMAN MODEL OF NEUROINFLAMMATION

5.1 INTRODUCTION

Neuroinflammation is a significant factor in numerous neurological disorders, including those caused by parasitic infections, such as neurocysticercosis (Steyn et al., 2022; White, 2000). However, despite the high global incidence and burden of these diseases, the understanding of the mechanisms underlying neuroinflammatory responses remains limited, mainly due to a lack of physiologically relevant human *in vitro* models.

Traditional animal models have been instrumental in providing valuable insights into the pathogenesis of neuroinflammatory diseases; however, they often fail to accurately recapitulate human-specific aspects of pathophysiology with critical differences observed in gene regulation, cellular signalling pathways, and immune system components that are often not conserved, leading to discrepancies in the translation of findings to clinical applications (Hartung, 2008; Pamies et al., 2017).

Several studies have reported significant differences in gene regulation and cellular signalling pathways between animal and human models. Hodge et al. (2019), for example, reported species-specific differences in astrocyte reactivity and signalling in response to neuroinflammatory stimuli, with human astrocytes displaying unique gene expression profiles and functional responses compared to their rodent counterparts. Likewise, Junhee Seok et al. (2013) demonstrated disparities in gene expression patterns between mice and humans in response to acute inflammatory stress, such as burns and endotoxemia. In addition, they found that the genomic response to these stressors was conserved among humans but poorly correlated with the corresponding mouse models, highlighting the limited translatability of animal models in human inflammatory conditions. Together, these studies underscore the importance of establishing and employing human-specific models to better understand the complex molecular and cellular mechanisms underlying neuroinflammation.

Human organotypic brain slice cultures (hOBSCs) present an attractive alternative to traditional animal models and animal-derived cell cultures, as they provide a conserved *in vitro* environment that retains human-specific cellular organisation, cell-cell interactions, and molecular profiles (Cho et al., 2007; Humpel, 2015). For this reason, this chapter aimed to establish and elucidate a translational *in vitro* model of neuroinflammation using human organotypic brain slice cultures (hOBSCs).

To this end, we used human cortical organotypic brain slice cultures (hOBSCs), which we compared to human acute slices from the same patient for baseline comparison of glial cell morphology and neuroinflammation. I confirmed the presence and intact morphology of microglia, astrocytes, and neurons in both human acute slices and hOBSCs using immunofluorescence staining. Using double immunofluorescence of cell-type specific neuroglial markers with the inflammatory transcription factor NF-IL6, I reported that untreated control hOBSCs displayed high levels of glial activation and inflammation compared to acute slices. I also observed high levels of glial activation in both untreated controls and hOBSCs treated with the neuroimmune activator LPS. Nonetheless, LPS-treated slices released higher concentrations of pro-inflammatory cytokine than control hOBSCs. Taken together, these findings demonstrated that hOBSCs do represent a platform for studying neuroinflammatory mechanisms in human tissue, which creates an opportunity for investigating the pathophysiology of a myriad of infections of an inflammatory nature, including NCC.

5.2 ALL MAJOR NEURAL CELL TYPES ARE PRESENT IN HUMAN OBSCS BUT DIFFER IN THEIR PROPORTIONS AS COMPARED TO HUMAN ACUTE BRAIN SLICES.

In a unique collaboration with various neurosurgical centres around Cape Town, we are able to gain access to human cortical tissue resected during epilepsy surgeries. As the patients in question have epilepsy, it is important to note that the tissue we receive cannot be classified as entirely normal. However, we are supplied with what can be considered the "least abnormal" cortical tissue. This could encompass "excess tissue," which is relatively normal tissue that is removed to reach the underlying epileptic foci. Alternatively, as the procedure dictates, broad resection margins are required; we receive tissue from these margins, which again include the least

abnormal tissue. Fresh cortical tissue was obtained from two donor patients aged 5 and 15 years; both tissue sections were from the temporal cortex **(Table 2).** From this tissue, we were able to culture some for use as hOBSCs, as highlighted in **Chapter 2.10**; more importantly, we were able to immediately fix and store slices from the same patients for use as human acute slices, which allowed for comparison with the cultured hOBSCs.

My first goal was to confirm the presence of all major neuroglial cells in both human acute slices and hOBSCs. To achieve this, I used immunofluorescence staining to target cell-type specific markers for microglia (IBA1), astrocytes (GFAP), and neurons (NeuN). I found that all these major cell types are present and have a preserved morphology that is comparable to what is observed *in vivo* in both human acute slices and hOBSCSs **(Fig 5.1 A).** While not observing major phenotypic differences in cell morphology between the two types of slice preparation, astrocytes in hOBSCs appeared to have a predominantly reactive phenotype, with thick and extended processes compared to human acute slices **(Fig 5.1 A)**.

Table 5.1 Patient-specific clinical information for tissue used for human acute and human organotypic brain slice culture preparation

Patient Serial Number	Gender	Age (years)	Country	Brain Region	Disease type
P0025	Female	5	South Africa	Temporal cortex	Focal cortical dysplasia
P0032	Female	15	South Africa	Temporal cortex	Focal epilepsy

In addition, I was curious whether there were differences in the total proportions of these cell types between human acute slices and untreated control hOBSCs. To assess this, I used our cell counter macro in ImageJ to quantify the total proportion of cells that were microglia, astrocytes, and neurons in the two slice preparation conditions. This was done by taking detailed 2-layer z-stacks with a 3 x 3 tile scan at 40X on the confocal microscope. Because of how significantly larger these human sections were as compared to mouse OBSCs, on average, each 3 x 3 tile scan had

an average of about 900 cells. In contrast, mouse OBSCs had only about 300 cells per imaging plane (based on Hoechst positive cell counts).

I found that the proportion of cells that were microglia was significantly higher in cultured hOBSCs as compared to human acute slices, with 39% and 7.9% of cells being identified as microglia, respectively (N = 6, p = 0.0012, Mann- Whitney U test) **(Fig 5.1 B).** Likewise, A Mann- Whitney U test revealed that there was a significant increase in the proportion of cells that were astrocytes between human acutes (0.9%) and untreated hOBSCs (7.8%) **(Fig 5.1 C)** (N = 6, p = 0.0022, Mann- Whitney U test). There were, however, no significant differences in the proportion of cells that were neurons between the two slice preparation conditions. Human acutes had a proportion of 11.5% neuronal cells, which was not significantly different to the 22.4% observed in hOBSCs **(Fig 5.1 D)** (N = 6-7, p = 0.0513, Mann – Whitney U test). These findings highlighted that there was a significant increase in the proportions of microglia and astrocytes from initial acute conditions to when they were incubated in culture for 7 days without any treatment.

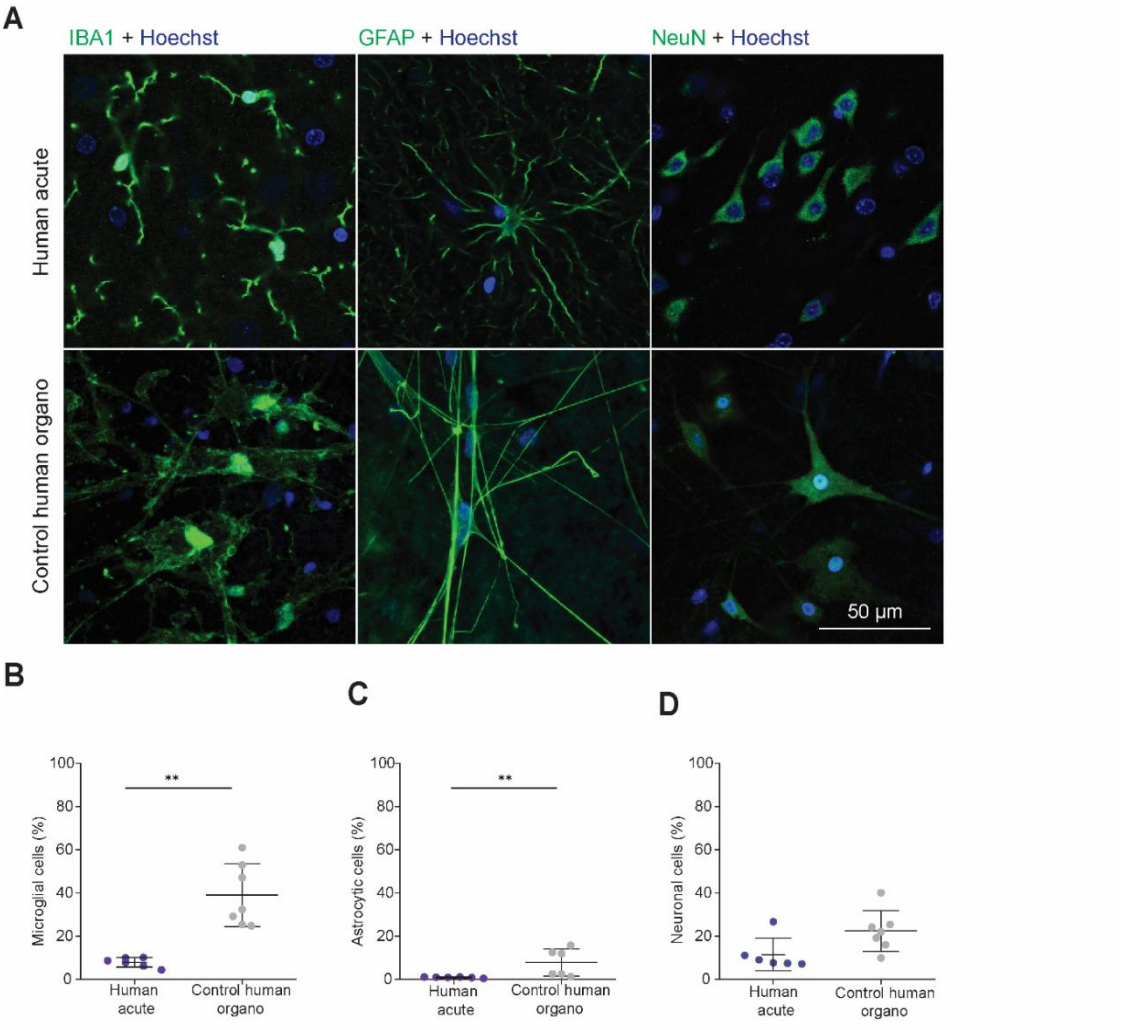

Figure 5.1 All major neural cell types are present in human organotypic brain slice cultures but differ in their proportions as compared to human acute brain slices. A) Confocal microscope images of cortical human acute and human organotypic cultures from the same patient, allowing for meaningful comparison. Slices were stained with IBA1 to label microglial cells, GFAP for astrocytes, and NeuN for neuronal cells. In addition, all cell-type specific markers were co-stained with the Hoechst nuclear marker. **B)** Quantification of the total proportion of microglial cells between human acute and hOBSCs, displaying a significant increase in the proportion of microglia in hOBSCs compared to human acute slices. **C)** Population data of the total proportion of astrocytes between human acute slices and hOBSCs (untreated controls), with hOBSCs displaying higher levels of astrocytes. **D)** Total proportion of neuronal cells showing no significant differences in the total proportion of neurons between the two slice preparations. Values are mean ± SEM; N= 6 to 7; ** $p \leq 0.001$; Mann- Whitney U test. Each data point represents an imaged z region with a 3 x 3 tile scan at 40X magnification.

5.3 HUMAN OBSCS DISPLAY ELEVATED LEVELS OF NF-IL6 EXPRESSION AS COMPARED TO HUMAN ACUTE SLICES.

Microglia have proliferative capacity when activated in response to injury or an inflammatory challenge (Shankaran et al., 2007; Torii et al., 2022). To investigate whether the proliferation of glial cells that I observed in cultured hOBSCs **(Fig. 5.1)** was the result of an inflammatory response resulting from slice injury or culture conditions, I co-stained microglia, astrocytes, and neurons with the inflammatory biomarker NF-IL6. I further compared NF-IL6 activation in human acute slices vs hOBSCs, which had been in culture for 7 days and received no other treatment.

I found low levels of NF-IL6 immunoreactivity and low colocalization between NF-IL6 and IBA1 in human acute slices (13.2%) in comparison to control hOBSCs, which showed a significantly greater proportion of activated microglial cells (90.3%) **(Fig. 5.2 A & B)** (N = 6, p = 0.0022, Mann- Whitney U test).

A similar finding was observed in astrocytes, with low NF-IL6 immunoreactivity and low activation of astrocytes in human acute slices (3.3%) compared to hOBSCs, which had 92.3% of activated astrocytes **(Fig. 5.2 C & D)** (N = 6, p = 0.0022, Mann- Whitney U test).

Neuronal activation remained quite similar between the two slice preparation conditions, and no significant differences in activation observed between human acute slices (11%) and hOBSCs (9.5%) **(Fig. 5.2 E & F)** (N = 6, p = 0.1320, Mann-Whitney U test).

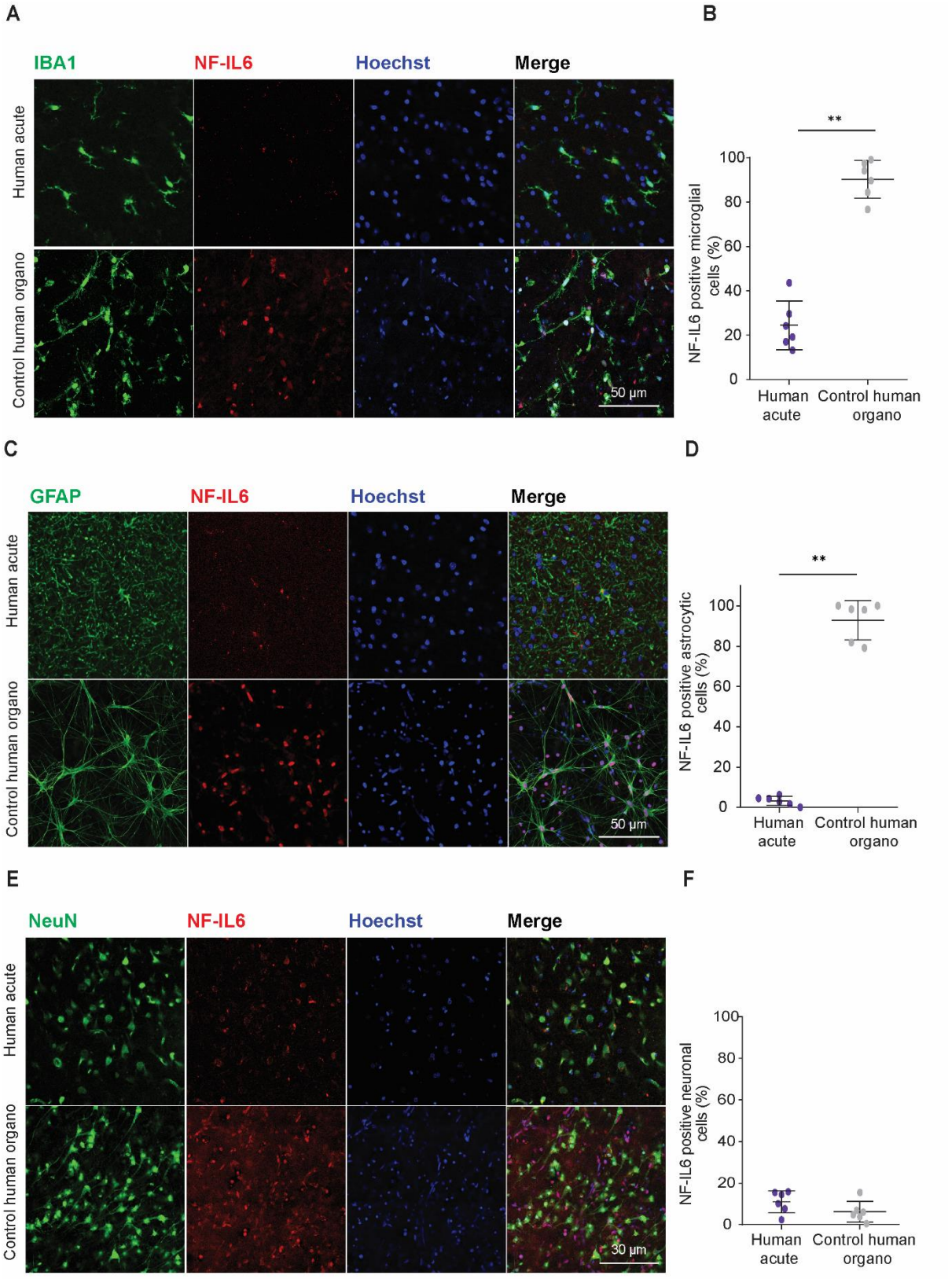

Figure 5.2 Human OBSCs display elevated levels of NF-IL6 expression as compared to human acute slices. A) Human acute slices and hOBSCs (untreated controls) were stained with the IBA1 antibody to target microglial cells; slices were also co-stained with the inflammatory transcription factor NF-IL6 and Hoechst nuclear marker. Images were obtained from z-stacks with a 5x 5 tile scan taken on the confocal microscope at 40X magnification. **B)**

Population data of the proportion of activated microglia as quantified by the IBA1 and NF-IL6 colocalization between the two slice preparation conditions displaying high activation in hOBSCs as compared to human acute slices. **C)** Confocal microscope image of cells stained with GFAP for astrocytes, NF-IL6 as a functional readout for astrocytic activation and Hoechst nuclear marker. **D)** Population data of the proportion of activated astrocytic cells. **E)** Confocal microscope images of slices stained with the neuronal marker NueN and co-stained with NF-IL6 and Hoechst nuclear marker. **F)** Population data of the proportion of activated neuronal cells. Although high NF-IL6 immunoreactivity was observed in hOBSCs, there was low colocalization with NeuN. Values are mean ± SEM; N= 6 to 7; ** $p \leq 0.001$; Mann- Whitney U test. Each data point represents an imaged z region with a 3 x 3 tile scan.

5.4 HUMAN ORGANOTYPIC BRAIN SLICE CULTURES DISPLAY A GRADUAL DECLINE IN THE RELEASE OF THE PRO-INFLAMMATORY CYTOKINE IL-6 OVER 7 DAYS IN CULTURE.

One well-established and typical response to an inflammatory challenge such as that brought upon by injury or infection is the release of pro-inflammatory cytokines by resident immune cells of the CNS (Lu et al., 2008; Sofroniew, 2014; Wang et al., 2015). I thus investigated the concentrations of the pro-inflammatory cytokine IL-6 released in culture medium by hOBSCs in response to surgical resection and slicing injury during culture preparation. To do this, hOBSCs were prepared from cortical human brain tissue resected during epilepsy surgeries; tissue was sectioned into 250 µm slices and plated on Millicell membrane inserts with access to 1.2 ml of culture medium. The medium was changed every second day over a period of 6 days and collected to run ELISAs to quantify IL-6 release. Data for day 7, where slices were treated with fresh culture medium for 24 hours to serve as controls for subsequent experiments, was also plotted and analysed. This data was collected with Dr Anja de Lange, a post-doctoral fellow in the Raimondo lab.

We observed a significant time-dependent decline in the release of IL-6 over the 7 days. Day 2 had the highest release of IL-6 with an average of 3.2 ng/ml; this declined significantly that on day 7, only 0.2 ng/ml was recorded in the culture medium **(Fig 5.3).** Comparatively, a Kruskal-Wallis test with a Dunn's multiple comparisons test showed that from day 6 onwards, the difference in IL-6 release was significantly different to that initially released 2 days post culturing (Day 2 vs Day 6: N = 30, $p \leq 0.001$, Kruskal-Wallis test with a Dunn's multiple comparisons test), this was also the case when Day 2 was compared to Day 7 (Day 2 vs Day 7: N = 19 - 30, $p \leq 0.001$,

Kruskal-Wallis test with a Dunn's multiple comparisons test). These findings suggest that 6 days post-culture is sufficient time for hOBSCs to recover from the initial inflammatory flare-up caused by the injury and trauma elicited by tissue resection and sectioning.

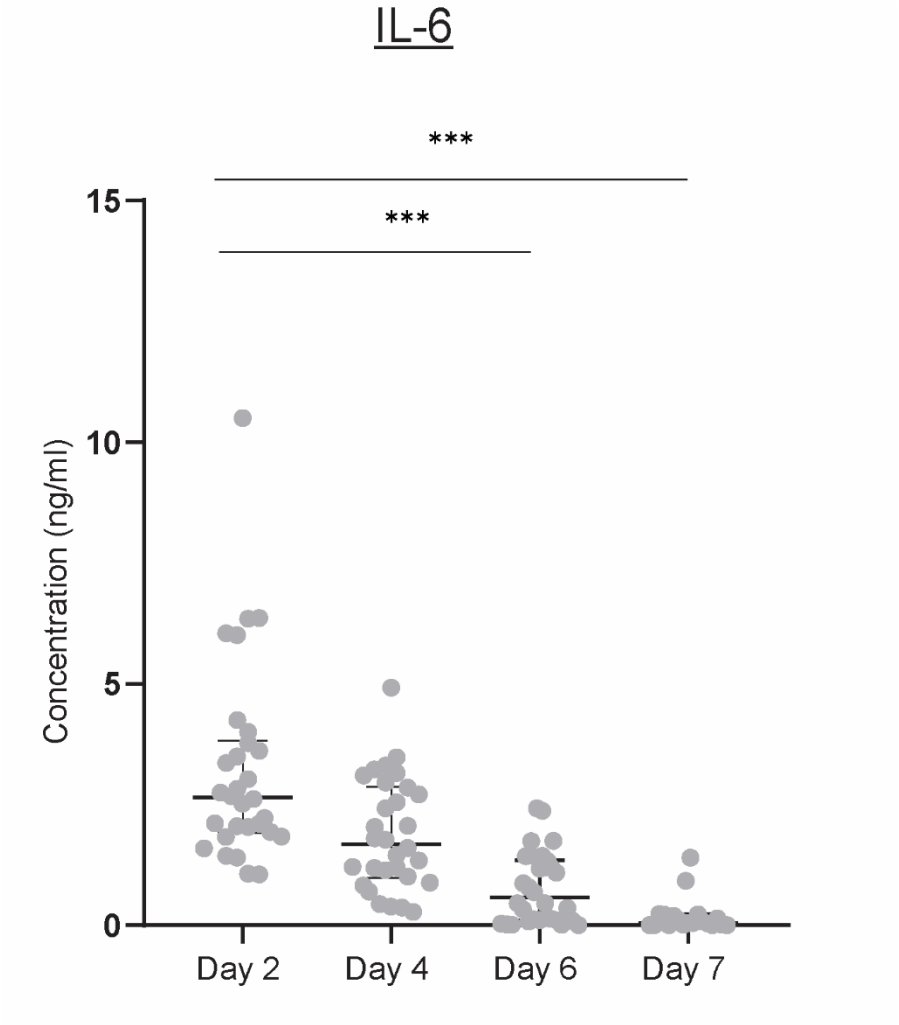

Figure 5.3 Human organotypic brain slice cultures display a gradual decline in the release of the pro-inflammatory cytokine IL-6 over 7 days in culture. The concentration of the pro-inflammatory cytokine IL-6 released by hOBSCs prepared from cortical human brain tissue resected during epilepsy surgery. Tissue was cultured on Millicell culture inserts over a period of 7 days. There was an observable decline in the concentration of IL-6 over the 7 days. Values with median ± IQR, N = 19 – 30, ***$p \leq 0.0001$, Kruskal- Wallis test with Dunn's multiple comparison posthoc test

5.5 THE EFFECT OF LPS TREATMENT ON GLIAL CELL PROPORTIONS AND NF-IL6 EXPRESSION.

My results thus far have demonstrated that inflammatory signalling is activated 7 days post-culture (as indicated by increased NF-IL6 expression). However, pro-inflammatory cytokine release had gone back to baseline levels. I thus wanted to investigate whether I could observe a significant difference in inflammatory activation if the slices were treated with an immunogen such as LPS. To investigate this, I utilized double immunofluorescence staining to **1)** investigate whether there was an LPS-dependent change in the total proportion of microglia, astrocytes, and neurons as compared to untreated control hOBSCS **(Fig 5.4)** and **2)** to investigate differences in the activation of these cell types between untreated control hOBSCs and hOBSCs treated with 10 ng/ml of LPS **(Fig 5.5)**.

Overall, there were no significant LPS-dependent changes in the total proportion of cells that were microglia, astrocytes, or neurons between untreated controls and LPS-treated hOBSCs **(Fig. 5.4 A & B)**. For example, we observed no significant differences in the proportion of microglial cells between control (39%) and LPS-treated (45.3%) hOBSCs (N = 6-7, $p = 0.5350$, Mann-Whitney U test).

A similar finding was observed for astrocytes, with 7.8% of cells being identified as astrocytes in control slices as compared to the 4.7% observed in LPS-treated hOBSCs, which was also not significantly different **(Fig. 5.4 A & C)** (N = 6, $p \geq 0.9999$, Mann- Whitney U test). Likewise, there did not appear to be an LPS-dependent change in the total proportion of cells that were neurons, with control slices having an average of 22.4% of cells that were neurons and LPS-treated hOBSCs 25.7% **(Fig 5.4 A & D)** (N = 6-7, $p = 0.3176$, Mann- Whitney U test).

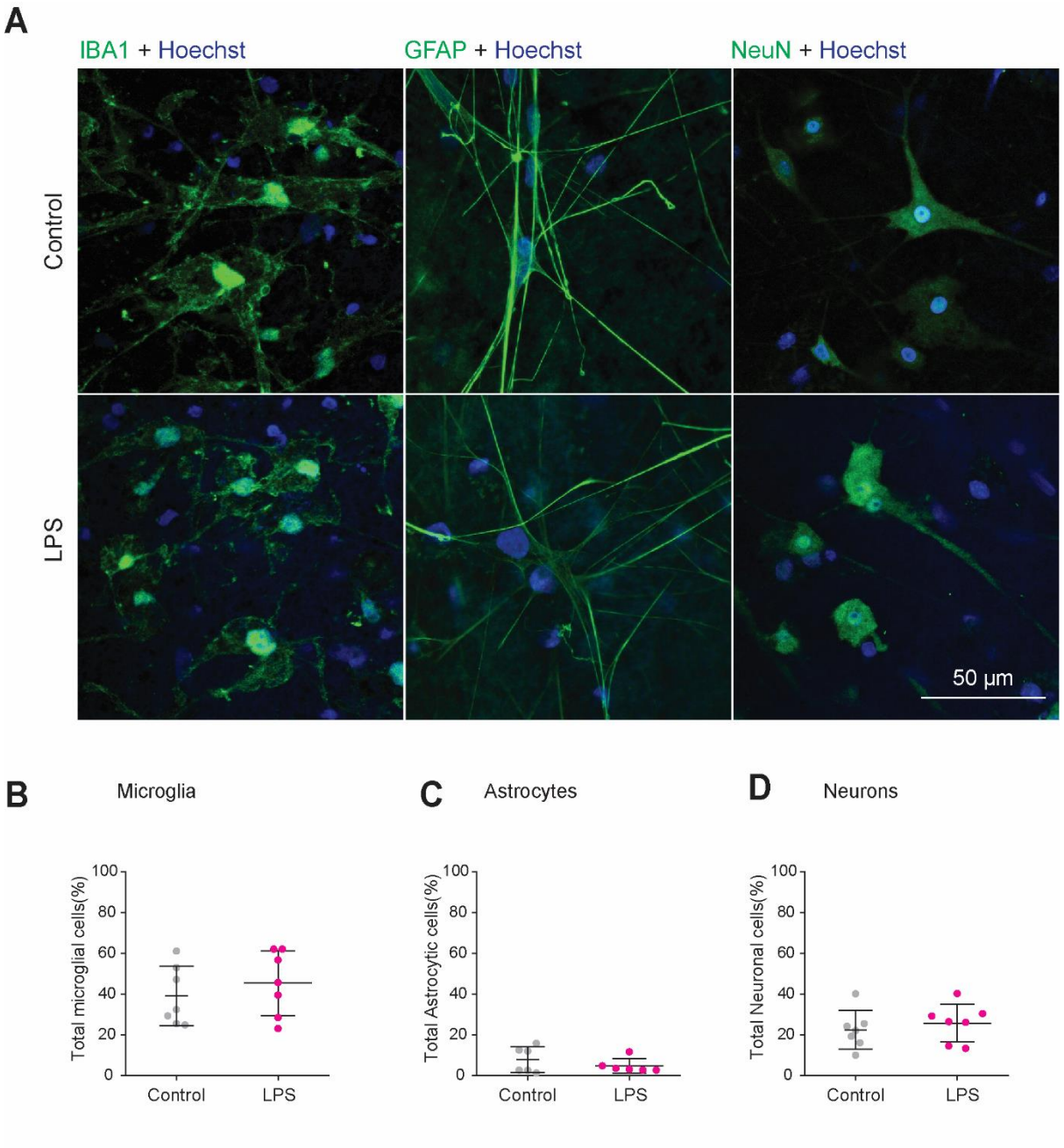

Figure 5.4 All major neural cell types are present in human organotypic brain slice cultures, and their total proportion is unaffected by LPS treatment. A) Confocal microscope images taken at 63X magnification of untreated control and LPS-treated hOBCS stained with cell-type specific markers for microglia (IBA1), astrocytes (GFAP), and neurons (NeuN), displaying phenotypically accurate and preserved morphology of all cell types. All slices were co-stained with Hoechst nuclear marker. **B)** Population data displaying the total proportion of microglial cells between control and LPS-treated hOBSCs with no significant differences in the proportion of microglia between the two treatment groups. **C)** The total proportion of cells that were astrocytes in untreated controls and LPS-treated hOBSCs, again displaying no LPS-dependent change. **D)** The total proportion of cells that were neurons in untreated controls and LPS-treated hOBSCs, with no observable LPS-dependent change in proportions. Values are mean ± SEM; N= 6 to 7; Mann- Whitney U test. Each data point represents an imaged z region with a 3 x 3 tile scan. *In A, figures for control hOBSCs of microglia, astrocytes, and neurons that were previously presented in* ***Fig 5.1*** *are shown for comparison with LPS-treated hOBSCs.*

In terms of inflammatory activation, I observed high levels of NF-IL6 immunoreactivity and high colocalization between NF-IL6 and IBA1 (microglia) in both controls (90.3%) and LPS-treated (91.4%) hOBSCs **(Fig. 5.5 A & B)** (N = 6 -7, *p* = 0.9079, Mann-Whitney U test). This indicated that there were high levels of inflammation in both conditions, even when slices were not treated with an immunogen.

In astrocytes, a similar finding was observed; there were high levels of NF-IL6 and GFAP colocalization between untreated controls (92.3%) and LPS-treated hOBSCs (94%) **(Fig. 5.5 C & D)**, which indicated high levels of activated astrocytic cells and a robust inflammatory response (N = 6, *p* = 0.8139, Mann- Whitney U test).

I also investigated activation in neurons, where even though I observed high NF-IL6 immunoreactivity in both controls and LPS-treated slices, very few of these NF-IL6 positive cells colocalized with NeuN. Only about 9.5% of neuronal cells were activated in controls and were not significantly different from LPS-treated slices where 9.3% of neurons were activated **(Fig. 5.5 E & F)** (N = 5-7, *p* = 0.9079, Mann- Whitney U test). This highlighted that although there was quite a robust inflammatory response in both conditions, it was mediated more by microglia and astrocytes.

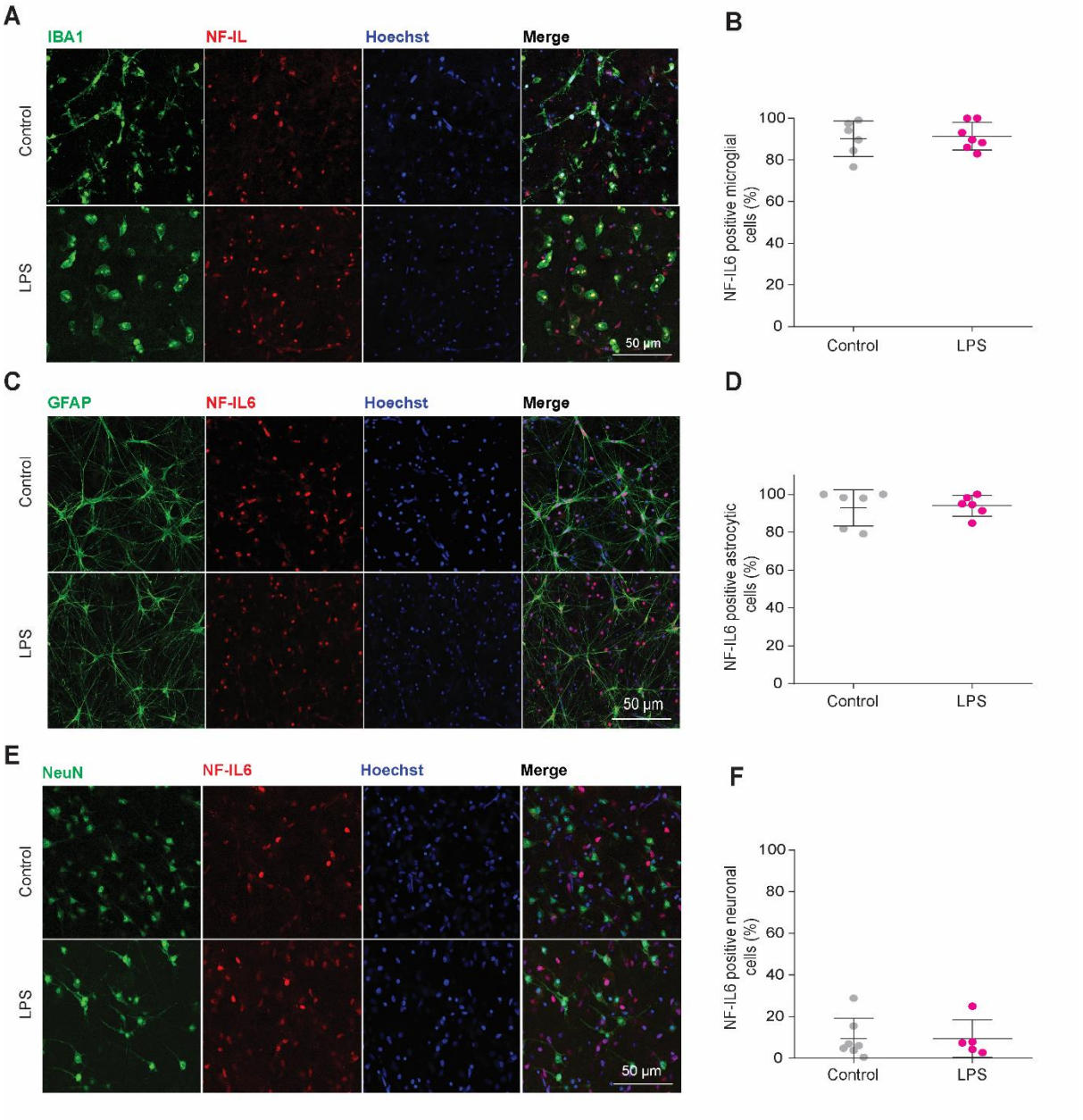

Figure 5.5 Untreated control and LPS-treated human OBSCs both display elevated levels of glial cell activation. After being cultured for six days, hOBSCs were either maintained in their standard culture medium (serving as the control group) or treated with 10 ng/ml of LPS for an additional 24 hours. **A)** Human OBSCs stained with the microglial marker IBA1, the inflammatory transcription factor NF-IL6, and Hoechst nuclear marker. **B)** Population data of the total proportion of activated microglia in control and LPS-treated hOBSCs displaying high levels of activation in both conditions. **C)** Confocal microscope images of hOBSCs stained with GFAP for astrocytes, NF-IL6 as a readout for cell activation, and Hoechst nuclear marker. **D)** Population data of the total proportion of activated astrocytes in control and LPS-treated hOBSCs **E)** Confocal microscope images of hOBSCs stained with NeuN to mark neuronal cells and NF-IL6 to track cellular activation with Hoechst nuclear marker. Very low colocalization between NF-IL6 and NeuN was observed in both conditions. **F)** Population data displaying the proportion of activated neuronal cells with low levels of activation in both conditions. Values are mean ± SEM; each data point represents an imaged z region with a 3 x 3 tile scan. *In A, C, and E figures for control hOBSCs of microglia,*

*astrocytes, and neurons that were previously presented in **Fig 5.2** are shown for comparison with LPS-treated hOBSCs.*

5.6 LPS INDUCES AN INCREASE IN PRO-INFLAMMATORY CYTOKINE RELEASE IN HUMAN OBSCS.

Given the observations in **Fig 5.3** that pro-inflammatory cytokine release is significantly lowered 7 days post-culture and given that glial cells in hOBSCs already showed NF-IL6 expression at baseline, I wanted to determine whether LPS application would still elicit the release of pro-inflammatory cytokines. After 6 days in culture, slices were either maintained in their regular culture medium to serve as control or treated with 10 ng/ml of LPS via culture medium for 24 hours. Culture medium was then collected, and the concentrations of pro-inflammatory cytokines IL-6 and TNF-α were quantified using ELISAs.

I surprisingly observed low concentrations of IL-6 and TNF-α in untreated control hOBSCs with an average concentration of 0.2 ng/ml and 0.08 ng/ml, respectively **(Fig 5.6 A & B)**. This differed from what was observed at the protein level, where I found high levels of NF-IL6 staining in microglia and astrocytes in control hOBSCs. However, treating hOBSCs with the LPS significantly increased the concentration of IL-6 and TNF-α to 4.4 ng/ml and 1.2 ng/ml, respectively (IL-6: N = 9 – 19; $p \leq 0.0001$, Mann-Whitney U test) (TNF-α: N = 9 – 20; $p \leq 0.0001$, Mann- Whitney U test).

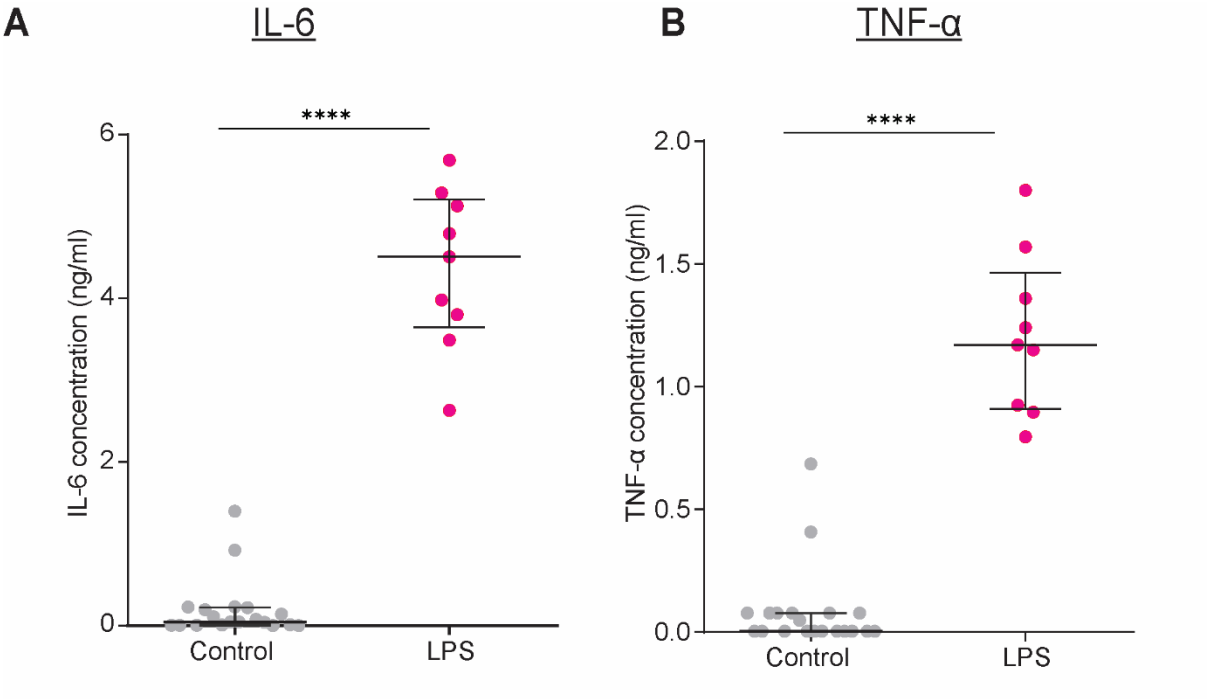

Figure 5.6 LPS induces an increase in pro-inflammatory cytokine release in human OBSCS. A) Quantified concentrations of IL-6 released in the medium by untreated control and LPS-treated hOBSCs. There were observably low levels of released IL-6 in the culture medium in control slices. Treating hOBSCs with LPS, however, significantly increased the levels of released IL-6. **B)** Quantified concentrations of TNF-α released in culture medium by untreated control and LPS-treated hOBSCs. Values with median ± IQR, N = 9 – 20, **** $p \leq 0.0001$, Mann- Whitney U test.

5.7 DISCUSSION

Historically, the neuroimmune responses to infections by parasites have been particularly difficult to study because of a lack of experimental models that accurately recapitulate the host-parasite interactions whilst allowing adequate experimental access to mechanistic processes at cellular and molecular resolution. While animal models have provided an important avenue for studying a lot of these infections, there have been numerous studies that have demonstrated human-specific aspects of neuro infections, drawing into question the transferability of findings based on studies using animal models (Hartung, 2008; Hodge et al., 2019; Junhee Seok et al., 2013; Pamies et al., 2017). As such, there remains a need to develop more representative human-specific models for appropriately studying inflammation in the human brain. Thus, the aim of this chapter was to establish and characterize a human model of neuroinflammation using human organotypic brain slice cultures for use in investigating neuroinflammatory mechanisms in brain pathologies.

In the first experiment, I used immunofluorescence staining to demonstrate that populations of resident cell types such as microglia, astrocytes, and neurons are preserved in both human acute slices and hOBSCs from the same donor patient. I, however, observed changes in glial cell proportions between human acute slices and their cultured counterparts, with a significant increase in both microglia and astrocytic populations in hOBSCs. This is in agreement with studies that have demonstrated an increase in immune-competent glial cells as a result of their activation due to the trauma incurred during surgical resection and post-culture sectioning (Eisemann et al., 2018; Ravi et al., 2019). In contrast to the microglial and astrocytic populations, it has been suggested that it is more difficult to preserve neuronal populations in cultured OBSCs because axotomy during tissue sectioning affects their continued viability (Humpel, 2015). The current study did not observe a relative decline in neuronal populations in hOBSCs; in fact, I observed a slight increase in the total proportion of cells that were neurons in hOBSCs, yet this was not significantly different to human acute slices. However, this finding may not be broadly representative because of how small my sample size was. Interestingly, Ravi et al. (2019) observed a time-dependent decline in neuronal populations over the 14 days human OBSCs were in culture as compared to human acutes. However, the rate of decrease remained steady over the

culture period. It is, however, important to note that the average donor patient age in their study was 24 years old as compared to the current study, where the oldest patient was only 15 years old. This is potentially significant because the neuronal loss reported in hOBSCs has been found to be more profound in cultures from older patients (Humpel, 2015). Additionally, they used cultures made with tissue from all over the neocortex, which cumulatively may have different neuronal distributions, proportions, and overall neuronal rate of loss to what we observed in tissue solely from the temporal cortex.

Given that the tissue used for the results in this chapter was obtained from donor patients who had undergone surgery for epilepsy, it was an important consideration to determine what baseline levels of inflammation may be present in the tissue due to potential underlying disease-associated inflammatory processes. On this note, using NF-IL6 as a readout, I observed that baseline inflammatory activation was relatively low in the acute slices, confirming that tissue received post-surgical resection and used in these experiments was relatively normal and not in an inflammatory state.

The next important question to consider was what the baseline inflammatory state of hOBSCs might be and whether the initial inflammatory response to tissue resection and slicing injury would change over time. Several lines of evidence point to the fact that there is likely some level of underlying or baseline inflammatory activation in the hOBSCs. Firstly, as described previously, I observed an increase in the proportions of glia in hOBSCs as compared to human acute slices. Secondly, after characterising pro-inflammatory cytokine concentrations in the culture media, it was clear that post-sectioning IL-6 release by cultured human brain slices reduced substantially over time. The high concentration of IL-6 on day 2 post-sectioning could be attributed to an inflammatory response to the trauma caused by tissue resection and sectioning during culture preparation. Notably, after 6 days in culture, the release of IL-6 by cultured slices was negligible. This agrees with findings from rodent OBSCs where Chong et al. (2018) and Huuskonen et al. (2005) found that 4 -5 days post-culture was enough time for rodent OBSCs to recover from trauma elicited by tissue sectioning as demonstrated by the significant decline in IL-6 and TNF-α release during this period. The observed decline in pro-inflammatory cytokine release in hOBSCs suggested that perhaps by day 6, slices had dealt with the initial inflammatory flareup elicited post

tissue resection. With that, however, a third line of evidence suggests that some underlying level of pro-inflammatory response was still maintained at these later time points in the hOBSCs. This is because using the pro-inflammatory transcription factor NF-IL6 as a functional readout for pro-inflammatory activation, it was clear that unlike in the acute slices, the majority of microglia and astrocytes were positive for NF-IL6 in untreated hOBSCs.

The most parsimonious explanation for the high NF-IL6 expression in microglia and astrocytes is that the trauma of slicing and ongoing cell death induces a prolonged inflammatory response in untreated hOBSCs. Nonetheless, it is worth considering whether NF-IL6 is a good marker for tracking activation and inflammation in hOBSCs. While the role of NF-IL6 in inflammation and its capacity for use as a functional readout for tracking inflammation in various culture preparations has been reported in literature (Ramji & Foka, 2002; Rummel, 2016; Tanaka et al., 1995), it has not been actively demonstrated in hOBSCs. Furthermore, NF-IL6 has been implicated in other non-inflammatory functions in the body, including homeostasis, cell growth, and cell proliferation (Greenbaum et al., 1998; Ramji & Foka, 2002; Zahnow, 2009). For example, Greenbaum et al. (1998) demonstrated that NF-IL6 plays a critical function in hepatocyte proliferation and liver regeneration following partial hepatectomy in mice, highlighting the role of NF-IL6 in maintaining liver homeostasis following injury. Though not conducted in neural tissue, it does highlight the diverse functions of NF-IL6 in the body. Because of this, in hOBSCs, NF-IL6 may take on another function that is not inflammatory, potentially explaining its high constitutive expression in untreated controls in glia. That said, the low NF-IL6 expression in neurons in hOBSCs suggests that, in all likelihood, it is reflecting a pro-inflammatory response in immune-competent cells. Given this, I explored other avenues that could have led to high NF-IL6 expression in control hOBSCs. For example, it is possible that components/antigens present in the culture medium could be eliciting an inflammatory response in untreated hOBSCs. We used 25% heat-inactivated horse serum in our medium, as per Kim et al. (2020), which could potentially contribute to eliciting an inflammatory response in untreated hOBSCs. To prevent the activation of glia into inflammatory phenotypes, some studies have suggested the use of serum-free medium to eliminate this potential confound (Conti et al., 2005; Ravi et al., 2019). That said, it is worth noting the longstanding use of medium containing horse serum in multiple rodent OBSC studies

investigating inflammatory responses (Papageorgiou et al., 2016). Typically, horse serum has been shown to improve rodent OBSC viability without inflammatory effects, as is evidenced by my own data presented in the previous results chapters.

The high levels of inflammatory activation observed in microglia and astrocytes in untreated hOBSCs prompted the question of whether any further observable signs of an increased pro-inflammatory response would be observable if cultured slices were further exposed to a pro-inflammatory stimulant. To this effect, hOBSCs were treated with the pro-inflammatory stimulant LPS and cytokine release was measured with ELISAs, and direct activation of microglia and astrocytes quantified at a protein level with NF-IL6 signalling.

In response to LPS, I observed a substantial and significant increase in the release of IL-6 and TNF-α by hOBSCs. This is in agreement with my own data from rodent OBSCs and what has been demonstrated in the rodent OBSC literature (Huuskonen et al., 2005; Papageorgiou et al., 2016). This finding was exciting because it highlighted that we could use a neuroimmune activator such as LPS to elicit an inflammatory response in hOBSCs. To the best of my knowledge, we are the first lab to have demonstrated this. This was interesting, given my immunofluorescence data showed that the vast majority of both microglia and astrocytes already expressed NF-IL6 in control slices, meaning that I was unable to demonstrate a further increase in the activation of cells which expressed NF-IL6 following LPS treatment. Nonetheless, it is likely that although NF-IL6 was already somewhat upregulated in control slices, further scope must have existed for the upregulation and release of IL-6 in response to LPS. This could be detected by ELISAs but not by the more sensitive immunofluorescence staining, where the inflammatory signal may already have been saturated.

Ultimately, this again prompts whether NF-IL6 is a good functional read-out for tracking inflammatory changes in hOBSCs at the protein level. NF-IL6 is a cytoplasmic transcription factor whose activation is mediated via the TLR4/MyD88/NF-IL6 inflammatory signalling pathway, resulting in its nuclear translocation (Damm et al., 2011; Rummel, 2016; Uematsu et al., 2002; Zimmermann et al., 2015) and as such it should be a good candidate for tracking activation and inflammation in the brain. However, because of its high constitutive expression in untreated control hOBSCs,

perhaps other inflammatory transcription factors such as STAT-3 (mediated via the JAK/STAT inflammatory pathway) or NF-κB (mediated by the MyD88 and NF-κB inflammatory signalling pathways), whose activation also occurs via TLRs may be additional or alternative options for tracking cell type-specific inflammatory changes in hOBSCs (Hu et al., 2021; Małek et al., 2007; Nadeau & Rivest, 2000; Rummel et al., 2005).

It is worth recognising that further characterization is needed to fully understand the hOBSC model. Such characterization could include investigating gene expression changes between human acute slices and untreated hOBSCs, as well as between control and LPS-treated hOBSCs. Single nucleus RNA-sequencing could be used for this. Looking at transcriptomic changes of inflammatory genes at a single-cell resolution could also be used as a means for confirming inflammatory changes in hOBSCs. Delbridge et al. (2020), for example, found that there were transcriptomic changes in rodent OBSCs when treated with LPS, where they observed an upregulation of inflammatory genes such as *Cd14* and *Cxlc19* in microglia. This observation is in line with the findings made in **Chapter 3**, where we observed an upregulation of inflammatory genes such as *Timp1* and *Lcn2* in our rodent model of neuroinflammation using OBSCs. These experiments will be important to replicate in hOBSCs as they may reveal crucial transcriptomic differences. With that, as we continue to characterize this model, using a serum-free medium may be useful in potentially reducing confounding inflammatory reactions that may be elicited by antigens present in the serum. These experiments also need to be replicated on a larger sample size. It is worth considering, however, that the tissue used in this study is from donor patients undergoing neurosurgical procedures and is not always readily available.

In summary, this chapter highlights the large capacity that hOBSCs have as a model for investigating innate inflammatory responses in the human brain in isolation from adaptive immune responses. This presents a powerful platform for studying neuroimmune responses in human diseases such as NCC in actual human tissue.

CHAPTER 6

OVERALL DISCUSSION AND CONCLUSIONS

The neuroinflammatory mechanisms in the viable stage of NCC infection remain grossly understudied. Especially unknown are the cell-type specific responses of microglia and astrocytes during this stage of infection, with one of the main challenges being a lack of relevant *in vitro* models of neuroinflammation that allow for this exploration. Thus, in this thesis, I utilised two *in vitro* models of neuroinflammation, namely rodent and human OBSCs. These allowed for the tracking of LPS-induced inflammation and activation of microglia and astrocytes at the protein level using immunofluorescence staining by colocalizing the signalling of the inflammatory transcription factor NF-IL6 with cell-type specific glial markers **(Chapters 3 and 5)**. Additionally, I illustrate that OBSCs also allow for the investigation of these inflammatory responses at a transcriptomic level using snRNA-sequencing, as well as the quantification of downstream releasable pro-inflammatory cytokines using ELISAs. Furthermore, using the rodent model, I demonstrated that the co-application of both LPS and viable *T. crassiceps* homogenate resulted in the suppression of LPS-induced glial activation and pro-inflammatory cytokine release and prevented the LPS-induced upregulation of inflammatory genes in both these cell types **(Chapter 4)**. Below, I discuss the utility and limitations of rodent and human OBSCs in investigating neuroinflammatory processes in NCC and how the findings of my thesis may be used to inform future work in the field.

6.1 ORGANOTYPIC BRAIN SLICE CULTURES PRESENT A RELIABLE PLATFORM TO MODEL NEUROINFLAMMATORY PROCESSES IN NEUROCYSTICERCOSIS.

One of the significant strengths of OBSCs, as demonstrated by my findings from **Chapters 3 and 5**, is that they allow for the application of immunogenic agents to elicit inflammation. Additionally, they permit the systematic tracking of inflammatory responses in various ways, for example, by measuring the concentrations of pro-inflammatory cytokines released in culture medium by OBSCs. The quantification of cytokine release in response to a pro-inflammatory stimulant or tissue sectioning has

previously been characterised in rodent OBSCs (Delbridge et al., 2020; Huuskonen et al., 2005; Papageorgiou et al., 2016; Ravi et al., 2019). However, in human OBSCs, reported cytokine data only focuses on characterising release in response to injury of tissue resection and sectioning during culture preparation (Ravi et al., 2019). In **Chapter 5**, it was demonstrated that human OBSCs, much like their rodent counterparts, are reactive to LPS treatment and significantly increase the release of pro-inflammatory cytokines after a 24-hour treatment period, a finding that has not been reported before in literature. The capacity to elicit an inflammatory response in human OBSCs underscores the model's utility for investigating the pathogenesis of infections and diseases characterised by inflammation, such as NCC and neurodegenerative diseases, such as Alzheimer's disease.

Findings from this thesis have demonstrated that OBSCs allow for the tracking of microglia and astrocytic activation using immunofluorescence staining of cell type-specific markers with inflammatory transcription factors. This creates an opportunity to not only visualise glial morphologies and relative distribution within slices but also to track changes in their activation status in an inflammatory milieu. Given these capabilities, the model also holds potential for studying cell-to-cell interactions and communication among immune cells in inflammatory conditions. Moreover, since this model retains neuronal populations, it opens avenues to probe the interaction between neurons and glia in NCC, an area that is currently underexplored. Many researchers have leveraged OBSCs' ability to preserve synaptic connections between different cell types to explore electrophysiological processes in various diseases. This has proven especially beneficial in deciphering mechanisms linked to seizures and epileptogenesis, as evidenced by multiple studies (Andersson et al., 2016; Chong et al., 2018; De Simoni & My Yu, 2006; Papageorgiou et al., 2016; Raimondo et al., 2013; Ravi et al., 2019; Stoppini et al., 1991).

Another strength of this model is demonstrated by the findings from **Chapter 4**, where viable *T. crassiceps* larvae caused a suppression of LPS-induced microglial and astrocytic activation in rodent OBSCs. Previous research has suggested that the immunomodulatory effects of viable *Taenia* larvae result from *Taenia* releasing excretory/secretory antigens that skew the Th1/Th2 axis towards a Th2 phenotype (Peón et al., 2016). As such, the asymptomatic viable stage of NCC is accompanied

by a predominantly Th2 response that is characterised by an anti-inflammatory environment and the release of anti-inflammatory cytokines (De Lange et al., 2018; Peón et al., 2016; Verma et al., 2011). A study that investigated the host-cysticerci relationship in a *T. crassiceps* model of NCC, for example, found that viable *T. crassiceps* larvae secreted factors that induced anergy in T cells located close to the cysticerci by downregulating CD4+ cells of Th1 phenotype and upregulating CD4+ cells of Th2 phenotype (Villa & Kuhn, 1996). Correspondingly, Avechavaleta et al. (1998) found that during early infection, *Taenia solium* metacestodes release a factor that depressed both T cell proliferative responses and pro-inflammatory cytokine production. The findings of this thesis, however, show that even in the absence of these peripheral immune cells (T cells) and the complete absence of adaptive immune responses, *T. crassiceps* homogenate still exerts a powerful anti-inflammatory effect in OBSCs, likely by preventing the activation of TLR-mediated inflammatory signalling pathways. My thesis, therefore, highlights that OBSCs present a platform for studying innate immune responses in isolation from confounding adaptive immune factors. This could be instrumental in studying brain diseases where the responses of innate cells are yet to be fully elucidated.

In **Chapters 3 and 4**, I demonstrated that OBSCs could also be used to investigate transcriptomic changes in response to LPS and viable *Taenia* homogenate using snRNA-sequencing. This not only serves as confirmation of inflammation but also provides insight into gene expression changes occurring in response to this infection. Though others have previously utilised OBSCs to investigate transcriptomic changes in microglia in response to LPS treatment (Delbridge et al., 2020), to the best of my knowledge, we are the first to explore inflammatory responses in both astrocytes and microglia in a viable model of NCC using OBSCs. Additionally, though not actively investigated in this thesis, human OBSCs also provide immense capacity to measure gene expression changes in response to various stimuli. Ravi et al. (2019), for example, used bulk RNA sequencing to investigate whether there were differences in the bulk gene expression profiles between human acute and human OBSCs. They then looked at the expression profiles of “signature genes” representing the different cell types as a proxy for the abundance of these cell types in the acute versus cultured slices. This experiment could be significantly improved by performing actual single-cell methods such as snRNA-sequencing in the tissue. Nonetheless, their results do

correlate with mine in some respects; for example, the microglial signature was increased in the cultured slices as compared to the acutes. Similarly, in my results, the relative abundance of microglia was higher in the hOBSCs as compared to acutes, again likely resulting from an inflammatory response to the tissue sectioning. Replicating my rodent OBSC transcriptomic experiments with human OBSCs treated with *T. solium* in the future could provide the first dataset to inform how *Taenia* modulates gene expression in a human model of viable NCC.

Unlike *in vivo* models, the versatility of this model system allows unrestricted access to brain tissue, allowing large sample sizes without utilising a lot of experimental animals. This is highlighted in **Chapters 3 and 4,** where inflammation and NCC are modelled *in vitro*. This not only saves on costs but also minimises the suffering and discomfort of animals whilst still providing high throughput and high-quality datasets.

6.2 SOME LIMITATIONS OF ORGANOTYPIC BRAIN SLICE CULTURES AND THE FINDINGS FROM THIS THESIS.

The findings from this thesis using OBSCs have filled some significant gaps on the neuroinflammatory mechanisms of NCC; however, they have also highlighted some limitations and considerations that should be kept in mind when this model system is utilised. While one of the biggest strengths of this model is the ability to investigate NCC disease processes on innate resident cells in isolation of adaptive immune responses, it does not fully recapitulate what actually happens in the human disease. Certain aspects of the human infection, such as BBB disruptions that play a crucial role in peripheral immune cell trafficking as well as invasion of the brain environment by *Taenia* via vascular structures, are not modelled (Alroy et al., 2018; Prodjinotho et al., 2020). Thus, essential components of the neuroimmune axis may not be fully replicated in the model, limiting the transferability of findings. However, this could be improved by introducing peripheral immune cells to OBSCs. As Ling et al. (2008) demonstrated, T cells can be introduced and activated within this model system, much like *in vivo* environments. Achieving this with other peripheral immune cells may add complexity to the model, allowing investigation of both innate and adaptive responses in a systematic and controlled manner.

Another limitation of the models used in this thesis emerges from **Chapter 4**. Here, *T. crassiceps* was chosen to model the human disease-causing parasite *T. solium*.

Additionally, rodent OBSCs were employed to model the human hosts. In this layered approach, both the parasite and the host models are one step removed from the actual human context, highlighting the challenge with modelling NCC. While *T. crassiceps* produces cysticerci in rodent tissues and shares similarities with *T. solium*, the inflammatory responses they trigger may differ. With that, however, human OBSCs present a unique avenue to use *T. solium* in a viable human model of NCC, with the potential to significantly strengthen and improve the current findings.

While the most significant limitation from **Chapter 5** was the scarce availability of human slices, in terms of characterising inflammatory responses, findings from this chapter also demonstrated that human OBSCs displayed high expression of NF-IL6 in microglia and astrocytes even prior to LPS stimulation. As such, it was challenging to conclusively ascertain the specific responses of microglia and astrocytes to LPS treatment on top of the inflammation already present. However, it was clear that there were significant changes in response to LPS treatment, as demonstrated by the measurable increase in pro-inflammatory cytokine concentrations in this treatment group compared to controls. I attributed the high level of constitutive NF-IL6 expression in these cell types as a response to the initial tissue resection, axotomy and ongoing cell death. Because the activation of both of these cell types occurs on a continuum rather than in an all or none manner, even low levels of NF-IL6 expression will likely be picked up by the highly sensitive immunofluorescence antibody I utilised, 'saturating' the inflammatory signal. It may thus be worth exploring the use of other pro-inflammatory activators and transcription factors as possible functional read-outs for inflammation. For example, the JAK/STAT signalling pathway that mediates the activation of the transcription factor STAT3 can become activated by the synthetic analogue of double-stranded RNA poly I: C, a TLR3 agonist that has been shown to elicit an inflammatory response in rodent cell cultures and OBSCs (He et al., 2021; Pan et al., 2012; Yousif et al., 2018). Using STAT3 as a readout for cell activation could contribute to the characterisation of glial responses in human OBSCs, including in a human model of NCC.

6.3 A COMPREHENSIVE COMPARISON BETWEEN RODENT-DERIVED ORGANOTYPIC BRAIN SLICE CULTURES AND HUMAN-DERIVED ORGANOTYPIC BRAIN SLICE CULTURES.

Rodent models have long been used to study neuroinflammatory mechanisms in human diseases (Delbridge et al., 2020; Huuskonen et al., 2005; Papageorgiou et al., 2016). However, there is growing consensus that certain cellular and molecular aspects of human neuroinflammation cannot be recapitulated using animal models. Here, I present in table form the major similarities and differences in investigating inflammatory processes between the rodent OBSCs utilised in **Chapters 3 and 4** and the human OBSCs used in **Chapter 5**.

One of the key similarities between these two models is that both retain glial and neuronal populations, a phenomenon that has been well-documented in the literature (Awala et al., 2023; Delbridge et al., 2020; Papageorgiou et al., 2016; Ravi et al., 2019). However, due to the considerably larger size of hOBSCs, they allow for imaging of more extensive regions. As a result, more cells (~900 cells) can be recorded per imaging plane as compared to rodent tissue, where approximately 300 cells can be documented per region. I also observed noticeable differences in the morphology and density of astrocytes between the two models. In rodent OBSCs stained with the astrocytic marker GFAP, astrocytes showed a dense aggregation of processes, making it challenging to identify the soma. In contrast, human astrocytes were more sparsely distributed, allowing for easier identification of individual cells. Due to these differences, I used the S100β marker, which has more nuclear localization, for rodent OBSCs and retained GFAP for human OBSCs.

Additionally, there were observable differences in the distribution of glia and neurons between rodent and human OBSCs. In **Chapters 3 and 4**, I observed that microglia in rodent OBSCs formed a sheath at the top of the slice 6 days post-culturing, which I hypothesised was a response to the trauma of tissue sectioning (Matejuk & Ransohoff, 2020). Comparatively, the distribution of cells in human OBSCs was more even, with no apparent sheath formation, as observed in **Chapter 5**. This suggests that the inflammatory response in rodent tissue is likely associated with significant microglial migration and proliferation, which may not occur to the same extent in human tissue, although this would need to be confirmed with a cell migration/ proliferation assay. Paradoxically, however, untreated human OBSCs displayed high constitutive expression of NF-IL6 in microglia and astrocytes, whereas in rodent OBSCs, NF-IL6 was interestingly only constitutively expressed in neurons. It is also worth considering

that NF-IL6 has been shown to also play a role in non-inflammatory homeostatic functions in humans (Rummel, 2016; Uematsu et al., 2002; Zimmermann et al., 2015). This could provide an additional reason for the observed high levels of NF-IL6 in untreated control hOBSCs, especially when cytokine data showed low concentrations of pro-inflammatory cytokines in this group. This further underscores the differences in immune responses between the two models.

An important similarity observed between rodent and human OBSCs is the increase in the release of pro-inflammatory cytokines in response to LPS treatment, in agreement with what has been demonstrated by other researchers in rodent models (Delbridge et al., 2020; Huuskonen et al., 2005; Papageorgiou et al., 2016), this thesis shows that the same findings can also be observed and replicated in human OBSCs. The observed upregulation in the release of the same pro-inflammatory cytokines between these two models highlights that the same or similar inflammatory signalling pathway, genes and even receptors are being activated in response to LPS treatment, an observation that supports the utility of the rodent model.

Table 6.1 A comprehensive analysis of murine and human OBSC models comparing cellular, morphological, and inflammatory responses.

Feature	Rodent OBSC Model	Human OBSC Model
Cell populations	Both glial and neuronal populations are retained, allowing for comprehensive morphology and neuroinflammatory studies.	Similar to murine, retains both glial and neuronal populations, providing a detailed view of brain slice physiology.
Imaging capability	Limited imaging capacity (~300 cells/plane) due to smaller slice size, restricting the extent of regional analysis.	Enhanced imaging capacity (~900 cells/plane) due to larger slice size, allowing for more extensive regional analysis.
Microglial response to tissue sectioning	Microglial sheath formation observed, indicative of a robust inflammatory response to slice preparation trauma.	Lack of microglial sheath, suggesting a different inflammatory reaction to slicing in human tissue.
Astrocyte density and distribution	Astrocytes are densely aggregated, making it difficult to distinguish individual cell bodies.	Astrocytes are more evenly distributed, facilitating easier identification and analysis of individual cells.
Astrocytic marker preference	Preference for S100β marker due to its nuclear localization, aiding in dense astrocyte areas.	GFAP marker preferred for its effectiveness in sparsely distributed astrocytes, enabling

		clear delineation of cell structures.
Baseline NF-IL6 expression patterns	Low NF-IL6 expression in microglia and astrocytes from untreated slices however, high constitutive expression in neurons.	High NF-IL6 expression in microglia and astrocytes from untreated slices, attributed to inflammatory response to tissue sectioning. Low NF-IL6 expression in neurons.
NF-IL6 expression in response to LPS treatment	NF-IL6 expression increased in both microglia and astrocytes indicative of inflammatory activation.	NF-IL6 expression also slightly further increases in microglia and astrocytes from what is observed in untreated slices. Low NF-IL6 expression in neurons.
Pro-inflammatory cytokine release (baseline vs LPS)	Increase in IL-6 and TNF-α released in medium following LPS treatment, confirming the model's responsiveness to induced inflammation.	A similar increase in IL-6 and TNF-α release post-LPS treatment, also supporting the model's applicability to study inflammatory responses in human tissue.
Model representation and relevance	While valuable for preliminary studies, differences in cell behaviour and immune responses may limit direct applicability to human pathology.	Provides a closer approximation of human brain responses, offering more directly translatable insights into human neuroinflammation.

While some important neuroimmune mechanisms seem to parallel each other between rodent and human OBSCs, it is clear that these two models are not exactly the same or totally homologous. Key differences observed in inflammatory processes could limit the ease of transferring rodent findings to humans. The human system is, by definition, more representative of the human brain and thus presents a more attractive avenue to investigate cellular and molecular disease processes with more relevant clinical applications.

6.4 BUILDING ON THE FOUNDATION: POSSIBLE CLINICAL IMPLICATIONS AND FUTURE EXPLORATIONS STEMMING FROM THE FINDINGS OF THIS THESIS.

In **Chapter 4**, I demonstrated that viable whole cyst *Taenia* larvae modulate central aspects of the inflammatory response; namely, they suppress LPS-induced glial activation and the release of pro-inflammatory cytokines, and further, they prevent the upregulation of inflammatory genes in rodent OBSCs. Aspects of cytokine release in response to *Taenia* infection have been demonstrated in the literature before (Amit et al., 2011; Verma et al., 2011); however, to the best of my knowledge, I am the first to demonstrate a suppression of glial activation, and gene expression changes in an *in vitro* model of viable NCC. These findings add to the greater body of literature on NCC immunology, highlighting that the effect of *Taenia* infection also significantly attenuates the responses of innate immune cells.

In **Chapter 4**, we attempted to isolate the active anti-inflammatory agent in *Taenia larvae*, using size exclusion fractionation and chromatography, finding that the active anti-inflammatory agent is a hydrophilic protein larger than 100 kDa. Identifying this protein is of considerable importance. Firstly, it could represent a powerful anti-inflammatory substance in its own right, with the potential for use in treating brain inflammation in a host of disorders. Secondly, its identification could create avenues to selectively inhibit its anti-inflammatory properties in the early stage of the disease, facilitating clearance of the larvae before more severe clinical symptoms develop. Thirdly, it could help identify involved signalling pathways that could then be targeted for treatment. Finally, there is potential for its use as a biomarker to help diagnose the disease, especially in the early viable stages of the disease, where serology does not always detect the presence of the larvae (Nash & Garcia, 2011). More notably, this would benefit rural communities where access to neuroimaging facilities is not readily available. Taken together, this all warrants further thorough investigation because it could have important clinical implications in the diagnosis, management, and treatment of this infection.

The *in-vitro* model of viable neurocysticercosis that we developed in **Chapter 4** provides an invaluable framework for dissecting the mechanisms of neuroinflammation and its role in NCC, advancing our fundamental understanding of the pathophysiological mechanisms of the disease. This model's utility in basic and

translational research is underscored by studies such as those by Amit et al (2011) who explored the immunological aspects of neurocysticercosis and their potential implications for epilepsy. By using our model to delve into the cellular and molecular dynamics of *Taenia*-induced inflammation, we can build on this existing knowledge base, identifying key pathways and mediators that drive the neuroinflammatory response. Such research not only advances our understanding of mechanistic workings in neurocysticercosis but also contributes to the broader field of neuroimmunology. Ultimately setting the groundwork for future translational research that could, in time, lead to therapeutic innovations.

In **Chapters 3 and 5**, I established and elucidated *in vitro* models of neuroinflammation using rodent and human OBSCs, highlighting their capacity for tracking inflammatory responses at the protein and gene expression levels. These models could also prove helpful in investigating disease processes in other illnesses characterised by neuroinflammation, such as Alzheimer's disease, traumatic brain injury, and ischemia (Mercurio et al., 2022; Nazem et al., 2015; Sanchis et al., 2019; Venneti et al., 2009; Wang et al., 2014; Wang et al., 2015). Human OBSCs have already been utilised to demonstrate important aspects of neurodegenerative disorders. Sebollela et al. (2012), for example, used human OBSCs to demonstrate that doses of amyloid-β peptide can result in the differential expression of genes that regulate pathways essential for neuronal physiology and that are reportedly dysregulated in Alzheimer's disease. Likewise, another study that exposed human OBSCs to Alzheimer's-associated amyloid-β oligomers to investigate their neurotoxic effect found that it resulted in hyperphosphorylation of Tau protein, another well-established Alzheimer's marker (Sebollela et al., 2012). There is, therefore, capacity for OBSCs to investigate inflammatory mechanisms in these diseases. For example, in **Chapter 5**, I observed an increased release of the pro-inflammatory cytokine TNF-α in human OBSCs in response to LPS treatment. TNF-α has been implicated in excitotoxicity in various neurodegenerative disorders (Olmos & Lladó, 2014), highlighting various ways these models could be utilised in investigating mechanisms in such diseases.

Moreover, the relevance of the models characterized in this thesis also extends to experimental pharmacology, not primarily for drug discovery but for understanding how various ligands can influence the neuroinflammatory response to brain infection.

This enables a more nuanced assessment of the inflammatory and anti-inflammatory pathways and their modulators with the primary goal of dissecting the complex interactions within the neuroinflammatory cascade, thereby providing a detailed map of potential intervention points that could be explored and exploited in subsequent translational research. Such systematic explorations can bridge the gap between basic research and potential clinical applications.

With that, other avenues warrant future exploration based on the findings from this thesis. One of these could be the use of a transgenic microglial CX3CR1-Cre reporter mouse line and live imaging with two-photon microscopy to investigate microglia *in vivo* and *in vitro* without having to stain them using immunohistochemistry. Drawing from the work of Dailey et al. (2013), two-photon microscopy can be utilised to investigate microglial behaviour, including motility, migration, and phagocytosis in response to various stimuli. This means that in the future, we could potentially investigate these processes in response to both LPS treatment and *Taenia* larvae, giving real-time data on how these cells respond during infection.

6.5 CONCLUSION

In this doctoral thesis, I utilised two *in vitro* models to study neuroinflammatory responses, particularly in the context of NCC. I demonstrated that these models present a robust platform that allows for the successful tracking of cell-type specific inflammatory responses of microglia and astrocytes at the protein level using immunofluorescence staining and at a transcriptomic level using snRNA-sequencing. I further show that this inflammatory response can also be confirmed by quantifying the release of inflammatory cytokines. In a model of NCC using rodent OBSCs mimicking CNS infection with viable larvae, I reported the novel findings that *Taenia* larvae suppress the LPS-induced activation of microglia and astrocytes, modulate the release of pro-inflammatory cytokines, and prevent the upregulation of key inflammatory genes, which may explain how the parasite is able to invade the CNS with minimal host responses. Further, considerable progress was made in identifying that the protein which mediates this effect is large and hydrophilic.

While the specific inflammatory mechanisms and active anti-inflammatory agent(s) within *Taenia* larvae remain areas of uncertainty, findings from this thesis have provided new insight into neuroimmune modulation occurring in this infection, which

informs our collective understanding of the pathogenesis of NCC. Additionally, models elucidated in this thesis can be utilised in investigating neuroinflammatory mechanisms more broadly. It is, therefore, my hope that this thesis will encourage and stimulate continued exploration into the neuroinflammatory mechanisms underlying not only NCC but a host of other potential disorders.

REFERENCES

Abdel Ghaffar, N. F., Asiri, R. N., AL-Eitan, L. N., Alamri, R. S., Alshyarba, R. M., Alrefeidi, F. A., Asiri, A., & Alghamdi, M. A. (2021). Improving public stigma, sociocultural beliefs, and social identity for people with epilepsy in the Aseer region of Saudi Arabia. *Epilepsy & Behavior Reports*, *16*. https://doi.org/10.1016/J.EBR.2021.100442

Acaz-Fonseca, E., Ortiz-Rodriguez, A., Azcoitia, I., Garcia-Segura, L. M., & Arevalo, M. A. (2019). Notch signaling in astrocytes mediates their morphological response to an inflammatory challenge. *Cell Death Discovery 2019 5:1*, *5*(1), 1–14. https://doi.org/10.1038/s41420-019-0166-6

Akira, S., Isshiki, H., Sugita, T., Tanabe, O., Kinoshita, S., Nishio, Y., Nakajima, T., Hirano, T., & Kishimoto, T. (1990). A nuclear factor for IL-6 expression (NF-IL6) is a member of a C/EBP family. *The EMBO Journal*, *9*(6), 1897–1906. http://www.ncbi.nlm.nih.gov/pubmed/2112087

Ali, A. E., Mahdy, H. M., Elsherbiny, D. M., & Azab, S. S. (2018). Rifampicin ameliorates lithium-pilocarpine-induced seizures, consequent hippocampal damage and memory deficit in rats: Impact on oxidative, inflammatory and apoptotic machineries. *Biochemical Pharmacology*, *156*, 431–443. https://doi.org/10.1016/J.BCP.2018.09.004

Alroy, K. A., Arroyo, G., Gilman, R. H., Gonzales-Gustavson, E., Gallegos, L., Gavidia, C. M., Verastegui, M., Rodriguez, S., Lopez, T., Gomez-Puerta, L. A., Alroy, J., Garcia, H. H., & Gonzalez, A. E. (2018). Carotid Taenia solium Oncosphere Infection: A Novel Porcine Neurocysticercosis Model. *The American Journal of Tropical Medicine and Hygiene*, *99*(2), 380. https://doi.org/10.4269/AJTMH.17-0912

Alvarez, J. I., Mishra, B. B., Gundra, U. M., Mishra, P. K., & Teale, J. M. (2010). Mesocestoides corti intracranial infection as a murine model for neurocysticercosis. *Parasitology*, *137*(3), 359–372. https://doi.org/10.1017/S0031182009991971

Amit, P., Prasad, K. N., Kumar, G. R., Shweta, T., Sanjeev, J., Kumar, P. V., & Mukesh, T. (2011). Immune response to different fractions of Taenia solium cyst fluid antigens in patients with neurocysticercosis. *Experimental Parasitology*, *127*(3), 687–692. https://doi.org/10.1016/J.EXPPARA.2010.11.006

Awala, A. N., Kauchali, M., de Lange, A., Higgitt, E. R., Mbangiwa, T., Raimondo, J. V., & Dangarembizi, R. (2023). Mouse Organotypic Brain Slice Cultures: A Novel Model for Studying Neuroimmune Responses to Cryptococcal Brain Infections. *Methods in Molecular Biology (Clifton, N.J.)*, *2667*, 31–45. https://doi.org/10.1007/978-1-0716-3199-7_3

Baram, T. Z., Gerth, A., & Schultz, L. (1997). Febrile seizures: an appropriate-aged model suitable for long-term studies. *Developmental Brain Research*, *98*(2), 265–270. https://doi.org/10.1016/S0165-3806(96)00190-3

Barbarosie, M., & Avoli, M. (1997). CA3-Driven Hippocampal-Entorhinal Loop Controls Rather than Sustains *In Vitro* Limbic Seizures. *The Journal of Neuroscience*, *17*(23), 9308–9314. https://doi.org/10.1523/JNEUROSCI.17-23-09308.1997

Barker, C. F., & Billingham, R. E. (1978). Immunologically Privileged Sites. *Advances in Immunology*, *25*(C), 1–54. https://doi.org/10.1016/S0065-2776(08)60930-X

Bartfai, T., & Schultzberg, M. (1993). Cytokines in neuronal cell types. *Neurochemistry International*, *22*(5), 435–444. https://doi.org/10.1016/0197-0186(93)90038-7

Bern, C., Garcia, H. H., Evans, C., Gonzalez, A. E., Verastegui, M., Tsang, V. C. W., & Gilman, R. H. (1999). Magnitude of the disease burden from neurocysticercosis in a developing country. *Clinical Infectious Diseases*, *29*(5), 1203–1209. https://doi.org/10.1086/313470/2/29-5-1203-TBL003.GIF

Bernardino, L., Balosso, S., Ravizza, T., Marchi, N., Ku, G., Randle, J. C., Malva, J. O., & Vezzani, A. (2008). Inflammatory events in hippocampal slice cultures prime neuronal susceptibility to excitotoxic injury: A crucial role of P2X7 receptor-mediated IL-1β release. *Journal of Neurochemistry*, *106*(1), 271–280. https://doi.org/10.1111/J.1471-4159.2008.05387.X

Bommarito, A., Richiusa, P., Carissimi, E., Pizzolanti, G., Rodolico, V., Zito, G., Criscimanna, A., Di Blasi, F., Pitrone, M., Zerilli, M., Amato, M. C., Spinelli, G.,

Carina, V., Modica, G., Latteri, A., Galluzzo, A., & Giordano, C. (2011). BRAFV600E mutation, TIMP-1 upregulation, and NF-κB activation: closing the loop on the papillary thyroid cancer trilogy. *Endocrine-Related Cancer*, *18*(6), 669–685. https://doi.org/10.1530/ERC-11-0076

Brenner, M. (2014). Role of GFAP in CNS injuries. *Neuroscience Letters*, *565*, 7. https://doi.org/10.1016/J.NEULET.2014.01.055

Bromberg, J., & Wang, T. C. (2009). Inflammation and Cancer: IL-6 and STAT3 Complete the Link. *Cancer Cell*, *15*(2), 79–80. https://doi.org/10.1016/j.ccr.2009.01.009

Buckmaster, P. S., Abrams, E., & Wen, X. (2017). Seizure frequency correlates with loss of dentate gyrus GABAergic neurons in a mouse model of temporal lobe epilepsy. *Journal of Comparative Neurology*, *525*(11), 2592–2610. https://doi.org/10.1002/CNE.24226

Burneo, J. G., & Cavazos, J. E. (2014). Neurocysticercosis and Epilepsy. *Epilepsy Currents*, *14*(1 Supplement), 23–28.

Butala, C., Brook, T. M., Majekodunmi, A. O., & Welburn, S. C. (2021). Neurocysticercosis: Current Perspectives on Diagnosis and Management. *Frontiers in Veterinary Science*, *8*, 615703. https://doi.org/10.3389/FVETS.2021.615703

Cabral-Pacheco, G. A., Garza-Veloz, I., Castruita-De la Rosa, C., Ramirez-Acuña, J. M., Perez-Romero, B. A., Guerrero-Rodriguez, J. F., Martinez-Avila, N., & Martinez-Fierro, M. L. (2020). The Roles of Matrix Metalloproteinases and Their Inhibitors in Human Diseases. *International Journal of Molecular Sciences*, *21*(24), 9739. https://doi.org/10.3390/ijms21249739

Cangalaya, C., Bustos, J. A., Calcina, J., Vargas-Calla, A., Suarez, D., Gonzalez, A. E., Chacaltana, J., Guerra-Giraldez, C., Mahanty, S., Nash, T. E., & García, H. H. (2016). Perilesional Inflammation in Neurocysticercosis - Relationship Between Contrast-Enhanced Magnetic Resonance Imaging, Evans Blue Staining and Histopathology in the Pig Model. *PLOS Neglected Tropical Diseases*, *10*(7), e0004869. https://doi.org/10.1371/journal.pntd.0004869

Carabin, H., Krecek, R. C., Cowan, L. D., Michael, L., Foyaca-Sibat, H., Nash, T., & Willingham, A. L. (2006). Estimation of the cost of Taenia solium cysticercosis in Eastern Cape Province, South Africa. *Tropical Medicine & International Health : TM & IH*, *11*(6), 906–916. https://doi.org/10.1111/J.1365-3156.2006.01627.X

Carabin, H., Ndimubanzi, P. C., Budke, C. M., Nguyen, H., Qian, Y., Cowan, L. D., Stoner, J. A., Rainwater, E., & Dickey, M. (2011). Clinical Manifestations Associated with Neurocysticercosis: A Systematic Review. *PLoS Neglected Tropical Diseases*, *5*(5). https://doi.org/10.1371/JOURNAL.PNTD.0001152

Cardona, A. E., Restrepo, B. I., Jaramillo, J. M., & Teale, J. M. (1999). Development of an Animal Model for Neurocysticercosis: Immune Response in the Central Nervous System Is Characterized by a Predominance of γδ T Cells. *The Journal of Immunology*, *162*(2), 995–1002. https://doi.org/10.4049/jimmunol.162.2.995

Carpio, A. (2002). Neurocysticercosis: an update. *The Lancet Infectious Diseases*, *2*(12), 751–762. https://doi.org/10.1016/S1473-3099(02)00454-1

Carpio, A., & Carpio, A. (2013). Neurocysticercosis and Epilepsy. *Novel Aspects on Cysticercosis and Neurocysticercosis*. https://doi.org/10.5772/52389

Carpio, A., Escobar, A., & Hauser, W. A. (1998). Cysticercosis and epilepsy: a critical review. *Epilepsia*, *39*(10), 1025–1040. https://doi.org/10.1111/J.1528-1157.1998.TB01287.X

Carpio, A., & Romo, M. L. (2014). The relationship between neurocysticercosis and epilepsy: An endless debate. *Arquivos de Neuro-Psiquiatria*, *72*(5), 383–390. https://doi.org/10.1590/0004-282X20140024

Carpio, A., Romo, M. L., Hauser, W. A., & Kelvin, E. A. (2021). New understanding about the relationship among neurocysticercosis, seizures, and epilepsy. *Seizure*, *90*, 123–129. https://doi.org/10.1016/j.seizure.2021.02.019

Chen, Y. C., Zhu, G. Y., Wang, X., Shi, L., Du, T. T., Liu, D. F., Liu, Y. Y., Jiang, Y., Zhang, X., & Zhang, J. G. (2017). Anterior thalamic nuclei deep brain stimulation reduces disruption of the blood–brain barrier, albumin extravasation, inflammation and apoptosis in kainic acid-induced epileptic rats. *39*(12), 1103–1113. https://doi.org/10.1080/01616412.2017.1379241

Chen, Z., Hu, W., Mendez, M. J., Gossman, Z. C., Chomyk, A., Boylan, B. T., Kidd, G. J., Phares, T. W., Bergmann, C. C., & Trapp, B. D. (2023). Neuroprotection by Preconditioning in Mice is Dependent on MyD88-Mediated CXCL10 Expression in Endothelial Cells. *ASN NEURO*, *15(24)*. https://doi.org/10.1177/17590914221146365

Chile, N., Clark, T., Arana, Y., Ortega, Y. R., Palma, S., Mejia, A., Angulo, N., Kosek, J. C., Kosek, M., Gomez-Puerta, L. A., Garcia, H. H., Gavidia, C. M., Gilman, R. H., Verastegui, M., Gilman, R. H., Gonzalez, A. E., Tsang, V. C. W., Rodriguez, S., Gonzalez, I., … Friedland, J. (2016). In Vitro Study of Taenia solium Postoncospheral Form. *PLOS Neglected Tropical Diseases*, *10*(2), e0004396. https://doi.org/10.1371/JOURNAL.PNTD.0004396

Cho, S., Wood, A., & Bowlby, M. (2007). Brain slices as models for neurodegenerative disease and screening platforms to identify novel therapeutics. *Current Neuropharmacology*, *5*(1), 19–33. https://doi.org/10.2174/157015907780077105

Chong, S. A., Balosso, S., Vandenplas, C., Szczesny, G., Hanon, E., Claes, K., Van Damme, X., Danis, B., Van Eyll, J., Wolff, C., Vezzani, A., Kaminski, R. M., & Niespodziany, I. (2018). Intrinsic Inflammation Is a Potential Anti-Epileptogenic Target in the Organotypic Hippocampal Slice Model. *Neurotherapeutics*, *15*(2), 470. https://doi.org/10.1007/S13311-018-0607-6

Chromium Next GEM Single Cell V(D)J Reagent Kits v1.1 with Feature Barcode technology for Cell Surface Protein. (2021). www.10xgenomics.com/trademarks.

Clinton White, A. (2019). Controlling the host response in neurocysticercosis. *American Journal of Tropical Medicine and Hygiene*, *100*(3), 483–484. https://doi.org/10.4269/ajtmh.18-0908

Coleman, L. G., Zou, J., & Crews, F. T. (2020). Microglial depletion and repopulation in brain slice culture normalizes sensitized proinflammatory signaling. *Journal of Neuroinflammation*, *17*(1), 1–20. https://doi.org/10.1186/S12974-019-1678-Y/FIGURES/12

Conti, L., Pollard, S. M., Gorba, T., Reitano, E., Toselli, M., Biella, G., Sun, Y., Sanzone, S., Ying, Q. L., Cattaneo, E., & Smith, A. (2005). Niche-Independent

Symmetrical Self-Renewal of a Mammalian Tissue Stem Cell. *PLOS Biology*, *3*(9), e283. https://doi.org/10.1371/JOURNAL.PBIO.0030283

Crespel, A., Coubes, P., Rousset, M. C., Brana, C., Rougier, A., Rondouin, G., ... & Lerner-Natoli, M. (2002). Inflammatory reactions in human medial temporal lobe epilepsy with hippocampal sclerosis. Brain research, 952(2), 159-169. https://doi.org/10.1016/S0006-8993(02)03050-0

Croft, C. L., Futch, H. S., Moore, B. D., & Golde, T. E. (2019). Organotypic brain slice cultures to model neurodegenerative proteinopathies. *Molecular Neurodegeneration 2019 14:1*, *14*(1), 1–11. https://doi.org/10.1186/S13024-019-0346-0

Dailey, M. E., Eyo, U., Fuller, L., Hass, J., & Kurpius, D. (2013). Imaging microglia in brain slices and slice cultures. *Cold Spring Harbor Protocols*, *2013*(12), 1142–1148. https://doi.org/10.1101/pdb.prot079483

Damm, J., Luheshi, G. N., Gerstberger, R., Roth, J., & Rummel, C. (2011). Spatiotemporal nuclear factor interleukin-6 expression in the rat brain during lipopolysaccharide-induced fever is linked to sustained hypothalamic inflammatory target gene induction. *The Journal of Comparative Neurology*, *519*(3), 480–505. https://doi.org/10.1002/cne.22529

Damm, J., Wiegand, F., Harden, L. M., Gerstberger, R., Rummel, C., & Roth, J. (2012). Fever, sickness behavior, and expression of inflammatory genes in the hypothalamus after systemic and localized subcutaneous stimulation of rats with the Toll-like receptor 7 agonist imiquimod. *Neuroscience*, *201*, 166–183. https://doi.org/10.1016/J.NEUROSCIENCE.2011.11.013

De Aluja, A. S., Villalobos, A. N. M., Plancarte, A., Rodarte, L. F., Hernández, M., & Sciutto, E. (1996). Experimental Taenia solium cysticercosis in pigs: characteristics of the infection and antibody response. *Veterinary Parasitology*, *61*(1–2), 49–59. https://doi.org/10.1016/0304-4017(95)00817-9

De Lange, A., Mahanty, S., & Raimondo, J. V. (2018). Model systems for investigating disease processes in neurocysticercosis. *Parasitology*, *May*, 1–10. https://doi.org/10.1017/s0031182018001932

De Lange, A. ’Walters A. ’Hsu N.-J. ’Jacobs M. 2, ’Raimondo J. V. (2020). Enzyme linked immunosorbent assays (ELISAs) for mouse IL-10, IL-6, IL-1β and TNF-α. *Protocols.Io*.

Deckers, N., Kanobana, K., Silva, M., Gonzalez, A. E., Garcia, H. H., Gilman, R. H., & Dorny, P. (2008). Serological responses in porcine cysticercosis: A link with the parasitological outcome of infection. *International Journal for Parasitology*, *38*(10), 1191–1198. https://doi.org/10.1016/J.IJPARA.2008.01.005

Del Brutto, O. H. (2012). Neurocysticercosis: A review. *TheScientificWorldJournal*, *2012*. https://doi.org/10.1100/2012/159821

Delbridge, A. R. D., Huh, D., Brickelmaier, M., Burns, J. C., Roberts, C., Challa, R., Raymond, N., Cullen, P., Carlile, T. M., Ennis, K. A., Liu, M., Sun, C., Allaire, N. E., Foos, M., Tsai, H. H., Franchimont, N., Ransohoff, R. M., Butts, C., & Mingueneau, M. (2020). Organotypic Brain Slice Culture Microglia Exhibit Molecular Similarity to Acutely-Isolated Adult Microglia and Provide a Platform to Study Neuroinflammation. *Frontiers in Cellular Neuroscience*, *14*. https://doi.org/10.3389/fncel.2020.592005

Dreymueller, D., Pruessmeyer, J., Schumacher, J., Fellendorf, S., Hess, F. M., Seifert, A., Babendreyer, A., Bartsch, J. W., & Ludwig, A. (2017). The metalloproteinase ADAM8 promotes leukocyte recruitment in vitro and in acute lung inflammation. *American Journal of Physiology - Lung Cellular and Molecular Physiology*, *313*(3), L602–L614. https://doi.org/10.1152/AJPLUNG.00444.2016/ASSET/IMAGES/LARGE/ZH500081772900008.JPEG

Du, L., Zhang, Y., Chen, Y., Zhu, J., Yang, Y., & Zhang, H. L. (2016). Role of Microglia in Neurological Disorders and Their Potentials as a Therapeutic Target. *Molecular Neurobiology 2016 54:10*, *54*(10), 7567–7584. https://doi.org/10.1007/S12035-016-0245-0

Du, L., Zhang, Y., Chen, Y., Zhu, J., Yang, Y., & Zhang, H.-L. (2017). Role of Microglia in Neurological Disorders and Their Potentials as a Therapeutic Target. *Molecular Neurobiology*, *54*(10), 7567–7584. https://doi.org/10.1007/s12035-016-0245-0

Dubé, C. M., Ravizza, T., Hamamura, M., Zha, Q., Keebaugh, A., Fok, K., Andres, A. L., Nalcioglu, O., Obenaus, A., Vezzani, A., & Baram, T. Z. (2010). Epileptogenesis Provoked by Prolonged Experimental Febrile Seizures: Mechanisms and Biomarkers. *The Journal of Neuroscience*, *30*(22), 7484–7494. https://doi.org/10.1523/JNEUROSCI.0551-10.2010

Eisemann, T., Costa, B., Strelau, J., Mittelbronn, M., Angel, P., & Peterziel, H. (2018). An advanced glioma cell invasion assay based on organotypic brain slice cultures. *BMC Cancer*, *18*(1), 1–10. https://doi.org/10.1186/S12885-018-4007-4/FIGURES/6

Eme-Scolan, E., & Dando, S. J. (2020). Tools and Approaches for Studying Microglia In vivo. *Frontiers in Immunology*, *11*, 2301. https://doi.org/10.3389/FIMMU.2020.583647/BIBTEX

Dametto, E. (2016). Histopathology of the human brain in neurocysticercosis. J Mol Histol Med Physiol, 1(1), 106.

Eyo, U. B., Peng, J., Murugan, M., Mo, M., Lalani, A., Xie, P., Xu, P., Margolis, D. J., & Wu, L. J. (2016). Regulation of Physical Microglia–Neuron Interactions by Fractalkine Signaling after Status Epilepticus. *ENeuro*, *3*(6). https://doi.org/10.1523/ENEURO.0209-16.2016

Field, R., Campion, S., Warren, C., Murray, C., & Cunningham, C. (2010). Systemic challenge with the TLR3 agonist poly I:C induces amplified IFNα/β and IL-1β responses in the diseased brain and exacerbates chronic neurodegeneration. *Brain, Behavior, and Immunity*, *24*(6), 996. https://doi.org/10.1016/J.BBI.2010.04.004

Fisher, R. S., Van Emde Boas, W., Blume, W., Elger, C., Genton, P., Lee, P., & Engel, J. (2005). Epileptic Seizures and Epilepsy: Definitions Proposed by the International League Against Epilepsy (ILAE) and the International Bureau for Epilepsy (IBE). *Epilepsia*, *46*(4), 470–472. https://doi.org/10.1111/J.0013-9580.2005.66104.X

Fleury, A., Cardenas, G., Adalid-Peralta, L., Fragoso, G., & Sciutto, E. (2016). Immunopathology in Taenia solium neurocysticercosis. *Parasite Immunology*, *38*(3), 147–157. https://doi.org/10.1111/PIM.12299

Fleury, A., Gomez, T., Alvarez, I., Meza, D., Huerta, M., Chavarria, A., Carrillo Mezo, R. A., Lloyd, C., Dessein, A., Preux, P. M., Dumas, M., Larralde, C., Sciutto, E., & Fragoso, G. (2003). High Prevalence of Calcified Silent Neurocysticercosis in a Rural Village of Mexico. *Neuroepidemiology*, *22*(2), 139–145. https://doi.org/10.1159/000068748

Fleury, A., Trejo, A., Cisneros, H., García-Navarrete, R., Villalobos, N., Hernández, M., Hernández, J. V., Hernández, B., Rosas, G., Bobes, R. J., de Aluja, A. S., Sciutto, E., & Fragoso, G. (2015). Taenia solium: Development of an Experimental Model of Porcine Neurocysticercosis. *PLOS Neglected Tropical Diseases*, *9*(8), e0003980. https://doi.org/10.1371/JOURNAL.PNTD.0003980

Flisser, A., Espinoza, B., Tovar, A., Plancarte, A., & Correa, D. (1986). Host-parasite relationship in cysticercosis: Immunologic study in different compartments of the host. *Veterinary Parasitology*, *20*(1–3), 95–102. https://doi.org/10.1016/0304-4017(86)90094-4

Forrester, J. V., Xu, H., Lambe, T., & Cornall, R. (2008). Immune privilege or privileged immunity? *Mucosal Immunology 2008 1:5*, *1*(5), 372–381. https://doi.org/10.1038/mi.2008.27

Frasnelli, M. E., Tarussio, D., Chobaz-Péclat, V., Busso, N., & So, A. (2005). TLR2 modulates inflammation in zymosan-induced arthritis in mice. *Arthritis Research & Therapy*, *7*(2), R370. https://doi.org/10.1186/AR1494

Frenger, M. J., Hecker, C., Sindi, M., Issberner, A., Hartung, H. P., Meuth, S. G., Dietrich, M., & Albrecht, P. (2021). Semi-Automated Live Tracking of Microglial Activation in CX3CR1GFP Mice During Experimental Autoimmune Encephalomyelitis by Confocal Scanning Laser Ophthalmoscopy. *Frontiers in Immunology*, *12*. https://doi.org/10.3389/FIMMU.2021.761776

Frigerio, F., Frasca, A., Weissberg, I., Parrella, S., Friedman, A., Vezzani, A., & Noe', F. M. (2012). Long-lasting pro-ictogenic effects induced in vivo by rat brain

exposure to serum albumin in the absence of concomitant pathology. *Epilepsia*, *53*(11), 1887–1897. https://doi.org/10.1111/J.1528-1167.2012.03666.X

Fuchs, F., Damm, J., Gerstberger, R., Roth, J., & Rummel, C. (2013). Activation of the inflammatory transcription factor nuclear factor interleukin-6 during inflammatory and psychological stress in the brain. *Journal of Neuroinflammation*, *10*(1), 905. https://doi.org/10.1186/1742-2094-10-140

Gaborieau, M., Nicolas, J., Save, M., Charleux, B., Vairon, J.-P., Gilbert, R. G., & Castignolles, P. (2008). Separation of complex branched polymers by size-exclusion chromatography probed with multiple detection. *Journal of Chromatography A*, *1190*(1–2), 215–223. https://doi.org/10.1016/j.chroma.2008.03.031

Garcia, H. H., & Del Brutto, O. H. (2017). Antiparasitic treatment of neurocysticercosis - the effect of cyst destruction in seizure evolution. *Epilepsy & Behavior : E&B*, *76*, 158. https://doi.org/10.1016/J.YEBEH.2017.03.013

García, H. H., Evans, C. A. W., Nash, T. E., Takayanagui, O. M., White, A. C., Botero, D., Rajshekhar, V., Tsang, V. C. W., Schantz, P. M., Allan, J. C., Flisser, A., Correa, D., Sarti, E., Friedland, J. S., Manuel Martinez, S., Gonzalez, A. E., Gilman, R. H., & Del Brutto, O. H. (2002). Current Consensus Guidelines for Treatment of Neurocysticercosis. *CLINICAL MICROBIOLOGY REVIEWS*, *15*(4), 747–756. https://doi.org/10.1128/CMR.15.4.747-756.2002

García, H. H., Gonzalez, A. E., Evans, C. A. W., & Gilman, R. H. (2003). Taenia solium cysticercosis. *Lancet*, *362*(9383), 547–556. https://doi.org/10.1016/S0140-6736(03)14117-7

Garcia, H. H., Nash, T. E., & Del Brutto, O. H. (2014). Clinical symptoms, diagnosis, and treatment of neurocysticercosis. *The Lancet. Neurology*, *13*(12), 1202. https://doi.org/10.1016/S1474-4422(14)70094-8

Garza, A., Tweardy, D. J., Weinstock, J., Viswanathan, B., & Robinson, P. (2010). Substance P signaling contributes to granuloma formation in taenia crassiceps infection, a murine model of cysticercosis. *Journal of Biomedicine and Biotechnology*, *2010*. https://doi.org/10.1155/2010/597086

Gilmore, T. D. (2006). Introduction to NF-κB: players, pathways, perspectives. *Oncogene 2006 25:51*, *25*(51), 6680–6684. https://doi.org/10.1038/sj.onc.1209954

Giovannoni, F., & Quintana, F. J. (2020). The Role of Astrocytes in CNS Inflammation. *Trends in Immunology*, *41*(9), 805. https://doi.org/10.1016/J.IT.2020.07.007

Greenbaum, L. E., Li, W., Cressman, D. E., Peng, Y., Ciliberto, G., Poli, V., & Taub, R. (1998). CCAAT enhancer- binding protein beta is required for normal hepatocyte proliferation in mice after partial hepatectomy. *The Journal of Clinical Investigation*, *102*(5), 996–1007. https://doi.org/10.1172/JCI3135

Gripper, L. B., & Welburn, S. C. (2017). The causal relationship between neurocysticercosis infection and the development of epilepsy - a systematic review. *Infectious Diseases of Poverty*, *6*(1), 31. https://doi.org/10.1186/S40249-017-0245-Y)

Gruendling, T., Guilhaus, M., & Barner-Kowollik, C. (2008). Quantitative LC-MS of polymers: Determining accurate molecular weight distributions by combined size exclusion chromatography and electrospray mass spectrometry with maximum entropy data processing. *Analytical Chemistry*, *80*(18), 6915–6927. https://doi.org/10.1021/AC800591J/SUPPL_FILE/AC800591J-FILE002.PDF

Gruol, D. L. (2015). IL-6 regulation of synaptic function in the CNS. *Neuropharmacology*, *96*(0 0), 42. https://doi.org/10.1016/J.NEUROPHARM.2014.10.023

Gudgeon, J., Marín-Rubio, J. L., & Trost, M. (2022). The role of macrophage scavenger receptor 1 (MSR1) in inflammatory disorders and cancer. *Frontiers in Immunology*, *13*, 6173. https://doi.org/10.3389/FIMMU.2022.1012002/BIBTEX

Guo, L., Li, X., & Tang, Q.-Q. (2015). Transcriptional Regulation of Adipocyte Differentiation: A Central Role for CCAAT/Enhancer-binding Protein (C/EBP) β. *Journal of Biological Chemistry*, *290*(2), 755–761. https://doi.org/10.1074/jbc.R114.619957

Guo, S., Wang, H., & Yin, Y. (2022). Microglia Polarization From M1 to M2 in Neurodegenerative Diseases. *Frontiers in Aging Neuroscience*, *14*. https://doi.org/10.3389/fnagi.2022.815347

Hamerman, J. A., Pottle, J., Ni, M., He, Y., Zhang, Z.-Y., & Buckner, J. H. (2016). Negative regulation of TLR signaling in myeloid cells-implications for autoimmune diseases. *Immunological Reviews*, *269*(1), 212–227. https://doi.org/10.1111/imr.12381

Hartung, T. (2008). Thoughts on limitations of animal models. *Parkinsonism & Related Disorders*, *14 Suppl 2*(SUPPL.2). https://doi.org/10.1016/J.PARKRELDIS.2008.04.003

Hayden, M. S., & Ghosh, S. (2004). Signaling to NF-kappaB. *Genes & Development*, *18*(18), 2195–2224. https://doi.org/10.1101/GAD.1228704

He, M., Dong, H., Huang, Y., Lu, S., Zhang, S., Qian, Y., & Jin, W. (2016). Astrocyte-Derived CCL2 is Associated with M1 Activation and Recruitment of Cultured Microglial Cells. *Cellular Physiology and Biochemistry*, *38*(3), 859–870. https://doi.org/10.1159/000443040

He, Y., Taylor, N., Yao, X., & Bhattacharya, A. (2021). Mouse primary microglia respond differently to LPS and poly(I:C) in vitro. *Scientific Reports 2021 11:1*, *11*(1), 1–14. https://doi.org/10.1038/s41598-021-89777-1

Herden, C., Gerstberger, R., Soares, D. M., Schneiders, J., Fuchs, F., Damm, J., Gerstberger, R., Roth, J., & Rummel, C. (n.d.). *The transcription factor nuclear factor interleukin 6 mediates pro-and anti-inflammatory responses during LPS-induced systemic inflammation in mice*. https://doi.org/10.1016/j.bbi.2015.03.008

Hodge, R. D., Bakken, T. E., Miller, J. A., Smith, K. A., Barkan, E. R., Graybuck, L. T., Close, J. L., Long, B., Johansen, N., Penn, O., Yao, Z., Eggermont, J., Höllt, T., Levi, B. P., Shehata, S. I., Aevermann, B., Beller, A., Bertagnolli, D., Brouner, K., … Lein, E. S. (2019). Conserved cell types with divergent features in human versus mouse cortex. *Nature*, *573*(7772), 61–68. https://doi.org/10.1038/s41586-019-1506-7

Hovens, I., Nyakas, C., & Schoemaker, R. (2014). A novel method for evaluating microglial activation using ionized calcium-binding adaptor protein-1 staining: cell body to cell size ratio. *Neuroimmunology and Neuroinflammation*, *1*(2), 82. https://doi.org/10.4103/2347-8659.139719

Hu, A., Yuan, H., Qin, Y., Zhu, Y., Zhang, L., Chen, Q., & Wu, L. (2022). Lipopolysaccharide (LPS) increases susceptibility to epilepsy via interleukin-1 type 1 receptor signaling. *Brain Research*, *1793*, 148052. https://doi.org/10.1016/J.BRAINRES.2022.148052

Hu, X., li, J., Fu, M., Zhao, X., & Wang, W. (2021). The JAK/STAT signaling pathway: from bench to clinic. *Signal Transduction and Targeted Therapy 2021 6:1*, *6*(1), 1–33. https://doi.org/10.1038/s41392-021-00791-1

Huang, L.-K., & Wang, M.-J. J. (1995). Image thresholding by minimizing the measures of fuzziness. *Pattern Recognition*, *28*(1), 41–51. https://doi.org/10.1016/0031-3203(94)E0043-K

Hubbard, J. A., & Binder, D. K. (2016). Inflammation. *Astrocytes and Epilepsy*, 313–342. https://doi.org/10.1016/B978-0-12-802401-0.00013-2

Humpel, C. (2015). Organotypic brain slice cultures: A review. *Neuroscience*, *305*, 86–98. https://doi.org/10.1016/J.NEUROSCIENCE.2015.07.086

Huuskonen, J., Suuronen, T., Miettinen, R., van Groen, T., & Salminen, A. (2005). A refined in vitro model to study inflammatory responses in organotypic membrane culture of postnatal rat hippocampal slices. *Journal of Neuroinflammation*, *2*. https://doi.org/10.1186/1742-2094-2-25

Jessen, N. A., Munk, A. S. F., Lundgaard, I., & Nedergaard, M. (2015). The Glymphatic System: A Beginner's Guide. *Neurochemical Research*, *40*(12), 2583–2599. https://doi.org/10.1007/s11064-015-1581-6

Junhee Seok, H. Shaw Warren, Alex, G. C., Michael, N. M., Henry, V. B., Xu, W., Richards, D. R., McDonald-Smith, G. P., Gao, H., Hennessy, L., Finnerty, C. C., López, C. M., Honari, S., Moore, E. E., Minei, J. P., Cuschieri, J., Bankey, P. E., Johnson, J. L., Sperry, J., … Tompkins, R. G. (2013). Genomic responses in mouse models poorly mimic human inflammatory diseases. *Proceedings of the*

National Academy of Sciences of the United States of America, *110*(9), 3507–3512. https://doi.org/10.1073/PNAS.1222878110/SUPPL_FILE/SAPP.PDF

Jurga, A. M., Paleczna, M., & Kuter, K. Z. (2020). Overview of General and Discriminating Markers of Differential Microglia Phenotypes. *Frontiers in Cellular Neuroscience*, *14*. https://doi.org/10.3389/fncel.2020.00198

Jüttler, E., Tarabin, V., & Schwaninger, M. (2002). Interleukin-6 (IL-6): A possible neuromodulator induced by neuronal activity. *Neuroscientist*, *8*(3), 268–275. https://doi.org/10.1177/1073858402008003012

Kaur, G., & Dufour, J. M. (2012). Cell lines: Valuable tools or useless artifacts. *Spermatogenesis*, *2*(1), 1. https://doi.org/10.4161/SPMG.19885

Keshet, Y., & Seger, R. (2010). *The MAP Kinase Signaling Cascades: A System of Hundreds of Components Regulates a Diverse Array of Physiological Functions* (pp. 3–38). https://doi.org/10.1007/978-1-60761-795-2_1

Kim, M.-H., Radaelli, C., Thomsen, E. R., Mahoney, J. T., Long, B., Taormina, M. J., Kebede, S., Gamlin, C., Sorensen, S. A., Campagnola, L., Dee, N., D'Orazi, F., Ko, A. L., Ojemann, J. G., Silbergeld, D. L., Gwinn, R. P., Cobbs, C., Keene, C. D., Jarsky, T., … Lein, E. S. (2020). Molecular and genetic approaches for assaying human cell type synaptic connectivity. *BioRxiv*, 2020.10.16.343343. https://doi.org/10.1101/2020.10.16.343343

Kokona, D., Jovanovic, J., Ebneter, A., & Zinkernagel, M. S. (2017). In Vivo Imaging of Cx3cr1gfp/gfp Reporter Mice with Spectral-domain Optical Coherence Tomography and Scanning Laser Ophthalmoscopy. *Journal of Visualized Experiments : JoVE*, *2017*(129). https://doi.org/10.3791/55984

Krasovska, V., & Doering, L. C. (2018). Regulation of IL-6 secretion by astrocytes via TLR4 in the fragile X mouse model. *Frontiers in Molecular Neuroscience*, *11*, 272. https://doi.org/10.3389/FNMOL.2018.00272/BIBTEX

Lafon, M., Megret, F., Lafage, M., & Prehaud, C. (2006). The innate immune facet of brain: Human neurons express TLR-3 and sense viral dsRNA. *Journal of Molecular Neuroscience*, *29*(3), 185–194. https://doi.org/10.1385/JMN:29:3:185/METRICS

Lama, J., Zambrano, M., García, H. H., Del Brutto, V. J., Campos, X., Del Brutto, O. H., & Salgado, P. (2015). Calcified Neurocysticercosis Associates with Hippocampal Atrophy: A Population-Based Study. *The American Journal of Tropical Medicine and Hygiene*, *92*(1), 64–68. https://doi.org/10.4269/ajtmh.14-0453

Lee, V. L. L., Shaikh, Mohd. F., Lee, V. L. L., & Shaikh, Mohd. F. (2019). Inflammation: Cause or Consequence of Epilepsy? *Epilepsy - Advances in Diagnosis and Therapy*. https://doi.org/10.5772/INTECHOPEN.83428

Levy, D. E., & Darnell, J. E. (2002). STATs: transcriptional control and biological impact. *Nature Reviews Molecular Cell Biology*, *3*(9), 651–662. https://doi.org/10.1038/nrm909

Liddelow, S. A., Guttenplan, K. A., Clarke, L. E., Bennett, F. C., Bohlen, C. J., Schirmer, L., Bennett, M. L., Münch, A. E., Chung, W.-S., Peterson, T. C., Wilton, D. K., Frouin, A., Napier, B. A., Panicker, N., Kumar, M., Buckwalter, M. S., Rowitch, D. H., Dawson, V. L., Dawson, T. M., … Barres, B. A. (2017). Neurotoxic reactive astrocytes are induced by activated microglia. *Nature*, *541*(7638), 481–487. https://doi.org/10.1038/nature21029

Lier, J., Streit, W. J., & Bechmann, I. (2021). Beyond Activation: Characterizing Microglial Functional Phenotypes. *Cells*, *10*(9). https://doi.org/10.3390/CELLS10092236

Linnerbauer, M., Wheeler, M. A., & Quintana, F. J. (2020). Astrocyte Crosstalk in CNS Inflammation. *Neuron*, *108*(4), 608–622. https://doi.org/10.1016/J.NEURON.2020.08.012

L'Ollivier, C., González, L. M., Gárate, T., Martin, L., Martha, B., Duong, M., Huerre, M., Cuisenier, B., Harrison, L. J. S., Dalle, F., & Bonnin, A. (2012). Histological and molecular biology diagnosis of neurocysticercosis in a patient without history of travel to endemic areas – Case report. *Parasite*, *19*(4), 441. https://doi.org/10.1051/PARASITE/2012194441

Losi, G., Cammarota, M., & Carmignoto, G. (2012). The role of astroglia in the epileptic brain. *Frontiers in Pharmacology*, *3 JUL*, 132. https://doi.org/10.3389/FPHAR.2012.00132/BIBTEX

Louveau, A., Harris, T. H., & Kipnis, J. (2015). Revisiting the Mechanisms of CNS Immune Privilege. *Trends in Immunology*, *36*(10), 569–577. https://doi.org/10.1016/j.it.2015.08.006

Love, M. I., Huber, W., & Anders, S. (2014). Moderated estimation of fold change and dispersion for RNA-seq data with DESeq2. *Genome Biology*, *15*(12), 550. https://doi.org/10.1186/s13059-014-0550-8

Lu, Y. C., Yeh, W. C., & Ohashi, P. S. (2008). LPS/TLR4 signal transduction pathway. *Cytokine*, *42*(2), 145–151. https://doi.org/10.1016/J.CYTO.2008.01.006

Lyman, M., Lloyd, D. G., Ji, X., Vizcaychipi, M. P., & Ma, D. (2014). Neuroinflammation: The role and consequences. *Neuroscience Research*, *79*(1), 1–12. https://doi.org/10.1016/J.NEURES.2013.10.004

Ma, Y., Li, J., Chiu, I., Wang, Y., Sloane, J. A., Lü, J., Kosaras, B., Sidman, R. L., Volpe, J. J., & Vartanian, T. (2006). Toll-like receptor 8 functions as a negative regulator of neurite outgrowth and inducer of neuronal apoptosis. *Journal of Cell Biology*, *175*(2), 209–215. https://doi.org/10.1083/JCB.200606016

Mafojane, N. A., Appleton, C. C., Krecek, R. C., Michael, L. M., & Willingham, A. L. (2003). The current status of neurocysticercosis in Eastern and Southern Africa. *Acta Tropica*, *87*(1), 25–33. https://doi.org/10.1016/S0001-706X(03)00052-4

Małek, R., Borowicz, K. K., Jargiełło, M., & Czuczwar, S. J. (2007). Role of nuclear factor kappaB in the central nervous system. *Pharmacological Reports : PR*, *59*(1), 25–33.

Mao, L., Wang, K., Zhang, Q., Wang, J., Zhao, Y., Peng, W., & Ding, J. (2022). Felt Stigma and Its Underlying Contributors in Epilepsy Patients. *Frontiers in Public Health*, *10*, 991. https://doi.org/10.3389/FPUBH.2022.879895/BIBTEX

Matejuk, A., & Ransohoff, R. M. (2020). Crosstalk Between Astrocytes and Microglia: An Overview. *Frontiers in Immunology*, *11*, 1416. https://doi.org/10.3389/FIMMU.2020.01416/BIBTEX

Matos-Silva, H., Reciputti, B. P., de Paula, É. C., Oliveira, A. L., Moura, V. B. L., Vinaud, M. C., Oliveira, M. A. P., & de Souza Lino, R. (2012). Experimental encephalitis caused by Taenia crassiceps cysticerci in mice. *Arquivos de Neuro-Psiquiatria*, *70*(4), 287–292. https://doi.org/10.1590/S0004-282X2012005000010

Mattson, M. P., & Meffert, M. K. (2006). Roles for NF-κB in nerve cell survival, plasticity, and disease. *Cell Death & Differentiation 2006 13:5*, *13*(5), 852–860. https://doi.org/10.1038/sj.cdd.4401837

McGinnis, C. S., Murrow, L. M., & Gartner, Z. J. (2019). DoubletFinder: Doublet Detection in Single-Cell RNA Sequencing Data Using Artificial Nearest Neighbors. *Cell Systems*, *8*(4), 329-337.e4. https://doi.org/10.1016/j.cels.2019.03.003

Mercurio, D., Fumagalli, S., Schafer, M. K., Pedragosa, J., Ngassam, L. D. C., Wilhelmi, V., ... & De Simoni, M. G. (2022). Protein expression of the microglial marker Tmem119 decreases in association with morphological changes and location in a mouse model of traumatic brain injury. Frontiers in Cellular Neuroscience, 16, 820127. https://doi.org/10.3389/fncel.2022.820127

Merle, N. S., Church, S. E., Fremeaux-Bacchi, V., & Roumenina, L. T. (2015). Complement System Part I Molecular Mechanisms of Activation and Regulation. *Frontiers in Immunology*, *6*. https://doi.org/10.3389/fimmu.2015.00262

Messing, A., & Brenner, M. (2020). GFAP at 50. *ASN NEURO*, *12*. https://doi.org/10.1177/1759091420949680

Mewes, A., Franke, H., & Singer, D. (2012). Organotypic Brain Slice Cultures of Adult Transgenic P301S Mice—A Model for Tauopathy Studies. *PLOS ONE*, *7*(9), e45017. https://doi.org/10.1371/JOURNAL.PONE.0045017

Moguel, B., Moreno-Mendoza, N., Bobes, R. J., Carrero, J. C., Chimal-Monroy, J., Díaz-Hernández, M. E., Herrera-Estrella, L., & Laclette, J. P. (2015). Transient transgenesis of the tapeworm Taenia crassiceps. *SpringerPlus*, *4*(1), 1–9. https://doi.org/10.1186/S40064-015-1278-Y/FIGURES/4

Nachtergaele, S., & He, C. (2017). The emerging biology of RNA post-transcriptional modifications. *RNA Biology*, *14*(2), 156–163. https://doi.org/10.1080/15476286.2016.1267096

Nadeau, S., & Rivest, S. (2000). Role of Microglial-Derived Tumor Necrosis Factor in Mediating CD14 Transcription and Nuclear Factor κ B Activity in the Brain during Endotoxemia. *Journal of Neuroscience*, *20*(9), 3456–3468. https://doi.org/10.1523/JNEUROSCI.20-09-03456.2000

Nash, T. E., Del Brutto, O. H., Butman, J. A., Corona, T., Delgado-Escueta, A., Duron, R. M., ... & Garcia, H. H. (2004). Calcific neurocysticercosis and epileptogenesis. Neurology, 62(11), 1934-1938. https://doi.org/10.1212/01.WNL.0000129481.12067.06

Nash, T. E., & Garcia, H. H. (2011). Diagnosis and Treatment of Neurocysticercosis. *Nature Reviews. Neurology*, *7*(10), 584. https://doi.org/10.1038/NRNEUROL.2011.135

Nash, T. E., Pretell, E. J., Lescano, A. G., Bustos, J. A., Gilman, R. H., Gonzalez, A. E., & Garcia, H. H. (2008). Perilesional brain oedema and seizure activity in patients with calcified neurocysticercosis: a prospective cohort and nested case-control study. *The Lancet Neurology*, *7*(12), 1099–1105. https://doi.org/10.1016/S1474-4422(08)70243-6

Nazem, A., Sankowski, R., Bacher, M., & Al-Abed, Y. (2015). Rodent models of neuroinflammation for Alzheimer's disease. *Journal of Neuroinflammation*, *12*(1), 1–15. https://doi.org/10.1186/S12974-015-0291-Y/FIGURES/1

Ndimubanzi, P. C., Carabin, H., Budke, C. M., Nguyen, H., Qian, Y., Rainwater, E., Dickey, M., Reynolds, S., & Stoner, J. A. (2010). A Systematic Review of the Frequency of Neurocyticercosis with a Focus on People with Epilepsy. *PLoS Neglected Tropical Diseases*, *4*(11), e870 1-17. https://doi.org/10.1371/journal.pntd.0000870

Olmos, G., & Lladó, J. (2014). Tumor Necrosis Factor Alpha: A Link between Neuroinflammation and Excitotoxicity. *Mediators of Inflammation*, *2014*, 1–12. https://doi.org/10.1155/2014/861231

Oprica, M., … C. E.-J. of C. and, & 2003, undefined. (2003). Inflammatory mechanisms associated with brain damage induced by kainic acid with special reference to the interleukin-1 system. *Wiley Online Library*, *7*(2), 127–140. https://doi.org/10.1111/j.1582-4934.2003.tb00211.x

Ordoñez, G., Rembao, D., & Sotelo, J. (2003). Taenia crassiceps cysticercosis in mice does not increase the carcinogenic effect of methyl-nitrosourea. *Experimental Parasitology*, *103*(3–4), 169–170. https://doi.org/10.1016/S0014-4894(03)00088-2

Ortinski, P. I., Dong, J., Mungenast, A., Yue, C., Takano, H., Watson, D. J., Haydon, P. G., & Coulter, D. A. (2010). Selective induction of astrocytic gliosis generates deficits in neuronal inhibition. *Nature Neuroscience 2010 13:5*, *13*(5), 584–591. https://doi.org/10.1038/nn.2535

O'Shea, J. J., & Plenge, R. (2012). JAK and STAT Signaling Molecules in Immunoregulation and Immune-Mediated Disease. *Immunity*, *36*(4), 542–550. https://doi.org/10.1016/j.immuni.2012.03.014

Palma, S., Chile, N., Carmen-Orozco, R. P., Trompeter, G., Fishbeck, K., Cooper, V., Rapoport, L., Bernal-Teran, E. G., Condori, B. J., Gilman, R. H., & Verastegui, M. R. (2019). In vitro model of postoncosphere development, and in vivo infection abilities of Taenia solium and Taenia saginata. *PLOS Neglected Tropical Diseases*, *13*(3), e0007261. https://doi.org/10.1371/JOURNAL.PNTD.0007261

Pamies, D., Barreras, P., Block, K., Makri, G., Kumar, A., Wiersma, D., Smirnova, L., Zhang, C., Bressler, J., Christian, K. M., Harris, G., Ming, G. L., Berlinicke, C. J., Kyro, K., Song, H., Pardo, C. A., Hartung, T., & Hogberg, H. T. (2017). A human brain microphysiological system derived from induced pluripotent stem cells to study neurological diseases and toxicity. *ALTEX*, *34*(3), 362–376. https://doi.org/10.14573/ALTEX.1609122

Pan, L. N., Zhu, W., Li, C., Xu, X. L., Guo, L. J., & Lu, Q. (2012). Toll-like receptor 3 agonist Poly I:C protects against simulated cerebral ischemia in vitro and in vivo. *Acta Pharmacologica Sinica 2012 33:10*, *33*(10), 1246–1253. https://doi.org/10.1038/aps.2012.122

Papageorgiou, I. E., Lewen, A., Galow, L. V., Cesetti, T., Scheffel, J., Regen, T., Hanisch, U.-K., & Kann, O. (2016). TLR4-activated microglia require IFN-γ to induce severe neuronal dysfunction and death in situ. *Proceedings of the National Academy of Sciences*, *113*(1), 212–217. https://doi.org/10.1073/pnas.1513853113

Pardo, A., Vining, P. G., Guo, L., Skolasky, R. L., Carson, S., & Freeman, M. (2004). The pathology of Rasmussen syndrome: stages of cortical involvement and neuropathological studies in 45 hemispherectomies. *Wiley Online Library*, *45*(5), 516–526. https://doi.org/10.1111/j.0013-9580.2004.33103.x

Park, B. S., & Lee, J. O. (2013). Recognition of lipopolysaccharide pattern by TLR4 complexes. *Experimental & Molecular Medicine 2013 45:12*, *45*(12), e66–e66. https://doi.org/10.1038/emm.2013.97

Park, M. H., & Hong, J. T. (2016). Roles of NF-κB in Cancer and Inflammatory Diseases and Their Therapeutic Approaches. *Cells*, *5*(2). https://doi.org/10.3390/CELLS5020015

Patel, D. C., Tewari, B. P., Chaunsali, L., & Sontheimer, H. (2019). Neuron–glia interactions in the pathophysiology of epilepsy. *Nature Reviews. Neuroscience*, *20*(5), 282. https://doi.org/10.1038/S41583-019-0126-4

Patsalos, P. N., & Perucca, E. (2003). Clinically important drug interactions in epilepsy: general features and interactions between antiepileptic drugs. *The Lancet Neurology*, *2*(6), 347–356. https://doi.org/10.1016/S1474-4422(03)00409-5

Peón, A. N., Ledesma-Soto, Y., & Terrazas, L. I. (2016). Regulation of immunity by Taeniids: lessons from animal models and in vitro studies. *Parasite Immunology*, *38*(3), 124–135. https://doi.org/10.1111/PIM.12289

Poli, V. (1998). The Role of C/EBP Isoforms in the Control of Inflammatory and Native Immunity Functions. *Journal of Biological Chemistry*, *273*(45), 29279–29282. https://doi.org/10.1074/jbc.273.45.29279

Poltorak, A., He, X., Smirnova, I., Liu, M. Y., Van Huffel, C., Du, X., Birdwell, D., Alejos, E., Silva, M., Galanos, C., Freudenberg, M., Ricciardi-Castagnoli, P., Layton, B., & Beutler, B. (1998). Defective LPS signaling in C3H/HeJ and C57BL/10ScCr

mice: Mutations in Tlr4 gene. *Science*, *282*(5396), 2085–2088. https://doi.org/10.1126/SCIENCE.282.5396.2085

Prasad, A., Gupta, R. K., Pradhan, S., Tripathi, M., Pandey, C. M., & Prasad, K. N. (2008). What triggers seizures in neurocysticercosis? A MRI-based study in pig farming community from a district of North India. *Parasitology International*, *57*(2), 166–171. https://doi.org/10.1016/j.parint.2007.12.001

Prasad, A., Prasad, K. N., Gupta, R. K., & Pradhan, S. (2009). Increased expression of ICAM-1 among symptomatic neurocysticercosis. *Journal of Neuroimmunology*, *206*(1–2), 118–120. https://doi.org/10.1016/j.jneuroim.2008.09.015

Preux, P. M., & Druet-Cabanac, M. (2005). Epidemiology and aetiology of epilepsy in sub-Saharan Africa. *Lancet Neurology*, *4*(1), 21–31. https://doi.org/10.1016/S1474-4422(04)00963-9

Prodjinotho, U. F., Lema, J., Lacorcia, M., Schmidt, V., Vejzagic, N., Sikasunge, C., Ngowi, B., Winkler, A. S., & da Costa, C. P. (2020). Host immune responses during Taenia solium Neurocysticercosis infection and treatment. *PLOS Neglected Tropical Diseases*, *14*(4), e0008005. https://doi.org/10.1371/JOURNAL.PNTD.0008005

Quinzo, M. J., Perteguer, M. J., Brindley, P. J., Loukas, A., & Sotillo, J. (2022). Transgenesis in parasitic helminths: a brief history and prospects for the future. *Parasites and Vectors*, *15*(1), 1–16. https://doi.org/10.1186/S13071-022-05211-Z/TABLES/1

Qureshi, S. T., Larivière, L., Leveque, G., Clermont, S., Moore, K. J., Gros, P., & Malo, D. (1999). Endotoxin-tolerant mice have mutations in toll-like receptor 4 (Tlr4). *Journal of Experimental Medicine*, *189*(4), 615–625. https://doi.org/10.1084/JEM.189.4.615

Ramji, D. P., & Foka, P. (2002). CCAAT/enhancer-binding proteins: structure, function and regulation. *The Biochemical Journal*, *365*(Pt 3), 561–575. https://doi.org/10.1042/BJ20020508

Ravi, V. M., Joseph, K., Wurm, J., Behringer, S., Garrelfs, N., d'Errico, P., Naseri, Y., Franco, P., Meyer-Luehmann, M., Sankowski, R., Shah, M. J., Mader, I., Delev,

D., Follo, M., Beck, J., Schnell, O., Hofmann, U. G., & Heiland, D. H. (2019). Human organotypic brain slice culture: a novel framework for environmental research in neuro-oncology. *Life Science Alliance*, *2*(4). https://doi.org/10.26508/LSA.201900305

Reid, J. K., & Kuipers, H. F. (2021). She Doesn't Even Go Here: The Role of Inflammatory Astrocytes in CNS Disorders. *Frontiers in Cellular Neuroscience*, *15*, 332. https://doi.org/10.3389/FNCEL.2021.704884/BIBTEX

Restrepo, B. I., Alvarez, J. I., Castaño, J. A., Arias, L. F., Restrepo, M., Trujillo, J., Colegial, C. H., & Teale, J. M. (2001). Brain Granulomas in Neurocysticercosis Patients Are Associated with a Th1 and Th2 Profile. *Infection and Immunity*, *69*(7), 4554–4560. https://doi.org/10.1128/IAI.69.7.4554-4560.2001

Ries, C. (2014). Cytokine functions of TIMP-1. *Cellular and Molecular Life Sciences*, *71*(4), 659–672. https://doi.org/10.1007/s00018-013-1457-3

Ringheim, G. E., Burgher, K. L., & Heroux, J. A. (1995). Interleukin-6 mRNA expression by cortical neurons in culture: Evidence for neuronal sources of interleukin-6 production in the brain. *Journal of Neuroimmunology*, *63*(2), 113–123. https://doi.org/10.1016/0165-5728(95)00134-4

Robel, S., Buckingham, S. C., Boni, J. L., Campbell, S. L., Danbolt, N. C., Riedemann, T., Sutor, B., & Sontheimer, H. (2015). Reactive astrogliosis causes the development of spontaneous seizures. *The Journal of Neuroscience : The Official Journal of the Society for Neuroscience*, *35*(8), 3330–3345. https://doi.org/10.1523/JNEUROSCI.1574-14.2015

Robertson, F. C., Lepard, J. R., Mekary, R. A., Davis, M. C., Yunusa, I., Gormley, W. B., Baticulon, R. E., Mahmud, M. R., Misra, B. K., Rattani, A., Dewan, M. C., & Park, K. B. (2019). Epidemiology of central nervous system infectious diseases: a meta-analysis and systematic review with implications for neurosurgeons worldwide. *Journal of Neurosurgery*, *130*(4), 1107–1126. https://doi.org/10.3171/2017.10.JNS17359

Robinson, P., Garza, A., Weinstock, J., Serpa, J. A., Goodman, J. C., Eckols, K. T., Firozgary, B., & Tweardy, D. J. (2012). Substance P Causes Seizures in

Neurocysticercosis. *PLOS Pathogens*, *8*(2), e1002489. https://doi.org/10.1371/JOURNAL.PPAT.1002489

Roman, G., Sotelo, J., Del Brutto, O., Flisser, A., Dumas, M., Wadia, N., Botero, D., Cruz, M., Garcia, H., de Bittencourt, P. R. M., Trelles, L., Arriagada, C., Lorenzana, P., Nash, T. E., & Spina-Franca, A. (2000). A proposal to declare neurocysticercosis an international reportable disease. *Bulletin of the World Health Organization*, *78*(3), 399–406.

Rostami, J., Mothes, T., Kolahdouzan, M., Eriksson, O., Moslem, M., Bergström, J., Ingelsson, M., O'Callaghan, P., Healy, L. M., Falk, A., & Erlandsson, A. (2021). Crosstalk between astrocytes and microglia results in increased degradation of α-synuclein and amyloid-β aggregates. *Journal of Neuroinflammation*, *18*(1), 1–20. https://doi.org/10.1186/S12974-021-02158-3/FIGURES/9

Ruan, C., & Elyaman, W. (2022). A New Understanding of TMEM119 as a Marker of Microglia. *Frontiers in Cellular Neuroscience*, *16*, 233. https://doi.org/10.3389/FNCEL.2022.902372/BIBTEX

Rummel, C. (2016). Inflammatory transcription factors as activation markers and functional readouts in immune-to-brain communication. *Brain, Behavior, and Immunity*, *54*, 1–14. https://doi.org/10.1016/j.bbi.2015.09.003

Rummel, C., Voss, T., Matsumura, K., Korte, S., Gerstberger, R., Roth, J., & Hübschle, T. (2005). Nuclear STAT3 translocation in guinea pig and rat brain endothelium during systemic challenge with lipopolysaccharide and interleukin-6. *Journal of Comparative Neurology*, *491*(1), 1–14. https://doi.org/10.1002/CNE.20653

Saijo, K., & Glass, C. K. (2011). Microglial cell origin and phenotypes in health and disease. *Nature Reviews Immunology 2011 11:11*, *11*(11), 775–787. https://doi.org/10.1038/nri3086

Sanchis, P., Fernández-Gayol, O., Vizueta, J., Comes, G., Canal, C., Escrig, A., Molinero, A., Giralt, M., & Hidalgo, J. (2019). Microglial cell-derived interleukin-6 influences behavior and inflammatory response in the brain following traumatic brain injury. *Glia*, glia.23758. https://doi.org/10.1002/glia.23758

Sato, A., Kamio, N., Yokota, A., Hayashi, Y., Tamura, A., Miura, Y., Maekawa, T., & Hirai, H. (2020). C/EBPβ isoforms sequentially regulate regenerating mouse hematopoietic stem/progenitor cells. *Blood Advances*, *4*(14), 3343–3356. https://doi.org/10.1182/bloodadvances.2018022913

Schiweck, J., Eickholt, B. J., & Murk, K. (2018). Important shapeshifter: Mechanisms allowing astrocytes to respond to the changing nervous system during development, injury and disease. *Frontiers in Cellular Neuroscience*, *12*, 261. https://doi.org/10.3389/FNCEL.2018.00261/BIBTEX

Schoeps, B., Frädrich, J., & Krüger, A. (2023). Cut loose TIMP-1: an emerging cytokine in inflammation. *Trends in Cell Biology*, *33*(5), 413–426. https://doi.org/10.1016/j.tcb.2022.08.005

Sebollela, A., Freitas-Correa, L., Oliveira, F. F., Paula-Lima, A. C., Saraiva, L. M., Martins, S. M., Mota, L. D., Torres, C., Alves-Leon, S., de Souza, J. M., Carraro, D. M., Brentani, H., De Felice, F. G., & Ferreira, S. T. (2012). Amyloid-β Oligomers Induce Differential Gene Expression in Adult Human Brain Slices. *Journal of Biological Chemistry*, *287*(10), 7436–7445. https://doi.org/10.1074/jbc.M111.298471

Seger, R., & Krebs, E. G. (1995). The MAPK signaling cascade. *The FASEB Journal*, *9*(9), 726–735. https://doi.org/10.1096/fasebj.9.9.7601337

Serpa, J. A., & White, A. C. (2012). Neurocysticercosis in the United States. *Pathogens and Global Health*, *106*(5), 256. https://doi.org/10.1179/2047773212Y.0000000028

Shankaran, M., Marino, M. E., Busch, R., Keim, C., King, C., Lee, J., Killion, S., Awada, M., & Hellerstein, M. K. (2007). Measurement of brain microglial proliferation rates in vivo in response to neuroinflammatory stimuli: Application to drug discovery. *Journal of Neuroscience Research*, *85*(11), 2374–2384. https://doi.org/10.1002/JNR.21389

Sikasunge, C. S., Johansen, M. V., Phiri, I. K., Willingham, A. L., & Leifsson, P. S. (2009). The immune response in Taenia solium neurocysticercosis in pigs is associated with astrogliosis, axonal degeneration and altered blood-brain barrier

permeability. *Veterinary Parasitology*, *160*(3–4), 242–250. https://doi.org/10.1016/j.vetpar.2008.11.015

Sofroniew, M. V. (2005). Reactive Astrocytes in Neural Repair and Protection. *Http://Dx.Doi.Org/10.1177/1073858405278321*, *11*(5), 400–407. https://doi.org/10.1177/1073858405278321

Sofroniew, M. V. (2014). Multiple Roles for Astrocytes as Effectors of Cytokines and Inflammatory Mediators. *The Neuroscientist*, *20*(2), 160–172. https://doi.org/10.1177/1073858413504466

Sofroniew, M. V. (2015). Astrogliosis. *Cold Spring Harbor Perspectives in Biology*, *7*(2). https://doi.org/10.1101/CSHPERSPECT.A020420

Song, H., Mylvaganam, S. M., Wang, J., Mylvaganam, S. M. K., Wu, C., Carlen, P. L., Eubanks, J. H., Feng, J., & Zhang, L. (2018). Contributions of the hippocampal CA3 circuitry to acute seizures and hyperexcitability responses in mouse models of brain ischemia. *Frontiers in Cellular Neuroscience*, *12*. https://doi.org/10.3389/FNCEL.2018.00278/FULL

Steyn, T. J. S., Awala, A. N., de Lange, A., & Raimondo, J. V. (2023). What Causes Seizures in Neurocysticercosis?. Epilepsy Currents, 23(2), 105-112. https://doi.org/10.1177/15357597221137418

Stoppini, L., Buchs, P. A., & Muller, D. (1991). A simple method for organotypic cultures of nervous tissue. Journal of neuroscience methods, 37(2), 173-182. https://doi.org/10.1016/0165-0270(91)90128-M

Stringer, J. L., Marks, L. T. M., White, A. C., & Robinson, P. (2003). Epileptogenic activity of granulomas associated with murine cysticercosis. *Experimental Neurology*, *183*(2), 532–536. https://doi.org/10.1016/S0014-4886(03)00179-1

Sugama, S., Fujita, M., Hashimoto, M., & Conti, B. (2007). Stress induced morphological microglial activation in the rodent brain: Involvement of interleukin-18. *Neuroscience*, *146*(3), 1388–1399. https://doi.org/10.1016/j.neuroscience.2007.02.043

Szu, J. I., & Binder, D. K. (2016). The Role of Astrocytic Aquaporin-4 in Synaptic Plasticity and Learning and Memory. *Frontiers in Integrative Neuroscience*, *10*(FEB2016), 8. https://doi.org/10.3389/FNINT.2016.00008

Taeniasis/cysticercosis. (2016). Retrieved May 4, 2023, from https://www.who.int/news-room/fact-sheets/detail/taeniasis-cysticercosis

Tanaka, T., Akira, S., Yoshida, K., Umemoto, M., Yoneda, Y., Shirafuji, N., Fujiwara, H., Suematsu, S., Yoshida, N., & Kishimoto, T. (1995). Targeted disruption of the NF-IL6 gene discloses its essential role in bacteria killing and tumor cytotoxicity by macrophages. *Cell*, *80*(2), 353–361. https://doi.org/10.1016/0092-8674(95)90418-2

Tang, S. C., Arumugam, T. V., Xu, X., Cheng, A., Mughal, M. R., Dong, G. J., Lathia, J. D., Siler, D. A., Chigurupati, S., Ouyang, X., Magnus, T., Camandola, S., & Mattson, M. P. (2007). Pivotal role for neuronal Toll-like receptors in ischemic brain injury and functional deficits. *Proceedings of the National Academy of Sciences of the United States of America*, *104*(34), 13798–13803. https://doi.org/10.1073/PNAS.0702553104/SUPPL_FILE/02553FIG7B.JPG

Terrazas, C. A., Sánchez-Muñoz, F., Mejía-Domínguez, A. M., Amezcua-Guerra, L. M., Terrazas, L. I., Bojalil, R., & Gómez-García, L. (2011). Cestode Antigens Induce a Tolerogenic-Like Phenotype and Inhibit LPS Inflammatory Responses in Human Dendritic Cells. *International Journal of Biological Sciences*, *7*(9), 1391–1400. https://doi.org/10.7150/ijbs.7.1391

Thurman, D. J., Beghi, E., Begley, C. E., Berg, A. T., Buchhalter, J. R., Ding, D., Hesdorffer, D. C., Hauser, W. A., Kazis, L., Kobau, R., Kroner, B., Labiner, D., Liow, K., Logroscino, G., Medina, M. T., Newton, C. R., Parko, K., Paschal, A., Preux, P. M., … Wiebe, S. (2011). Standards for epidemiologic studies and surveillance of epilepsy. *Epilepsia*, *52*(SUPPL. 7), 2–26. https://doi.org/10.1111/J.1528-1167.2011.03121.X

Toledo, A., Osorio, R., Matus, C., Lopez, Y. M., Cruz, N. R., Sciutto, E., Fragoso, G., Arauz, A., Carrillo-Mezo, R., & Fleury, A. (2018). Human Extraparenchymal Neurocysticercosis: The Control of Inflammation Favors the Host…but Also the

Parasite. *Frontiers in Immunology*, *9*(NOV), 2652. https://doi.org/10.3389/FIMMU.2018.02652

Torii, K., Takagi, S., Yoshimura, R., & Miyata, S. (2022). Microglial proliferation attenuates sickness responses in adult mice during endotoxin-induced inflammation. *Journal of Neuroimmunology*, *365*, 577832. https://doi.org/10.1016/J.JNEUROIM.2022.577832

Tsai, I. J., Zarowiecki, M., Holroyd, N., Garciarrubio, A., Sanchez-Flores, A., Brooks, K. L., Tracey, A., Bobes, R. J., Fragoso, G., Sciutto, E., Aslett, M., Beasley, H., Bennett, H. M., Cai, J., Camicia, F., Clark, R., Cucher, M., De Silva, N., Day, T. A., … Valdes, V. (2013). The genomes of four tapeworm species reveal adaptations to parasitism. *Nature*, *496*(7443), 57–63. https://doi.org/10.1038/NATURE12031

Turrin, N. P., & Rivest, S. (2004). Innate immune reaction in response to seizures: implications for the neuropathology associated with epilepsy. Neurobiology of disease, 16(2), 321-334. https://doi.org/10.1016/j.nbd.2004.03.010

Uddin, J., Garcia, H. H., Gilman, R. H., Gonzalez, A. E., & Friedland, J. S. (2005). Monocyte-Astrocyte Networks and the Regulation of Chemokine Secretion in Neurocysticercosis. *The Journal of Immunology*, *175*(5), 3273–3281. https://doi.org/10.4049/JIMMUNOL.175.5.3273

Uddin, J., Gonzalez, A. E., Gilman, R. H., Thomas, L. H., Rodriguez, S., Evans, C. A. W., Remick, D. G., Garcia, H. H., & Friedland, J. S. (2010). Mechanisms Regulating Monocyte CXCL8 Secretion in Neurocysticercosis and the Effect of Antiparasitic Therapy. *The Journal of Immunology*, *185*(7), 4478–4484. https://doi.org/10.4049/JIMMUNOL.0904158

Uematsu, S., Matsumoto, M., Takeda, K., & Akira, S. (2002). Lipopolysaccharide-Dependent Prostaglandin E2 Production Is Regulated by the Glutathione-Dependent Prostaglandin E2 Synthase Gene Induced by the Toll-Like Receptor 4/MyD88/NF-IL6 Pathway. *The Journal of Immunology*, *168*(11), 5811–5816. https://doi.org/10.4049/JIMMUNOL.168.11.5811

Venneti, S., Wiley, C. A., & Kofler, J. (2009). Imaging microglial activation during neuroinflammation and Alzheimer's disease. In *Journal of Neuroimmune Pharmacology* (Vol. 4, Issue 2, pp. 227–243). Springer. https://doi.org/10.1007/s11481-008-9142-2

Verástegui, M., González, A., Gilman, R. H., Gavidia, C., Falcón, N., Bernal, T., & Garcia, H. H. (2000). Experimental infection model for Taenia solium cysticercosis in swine. *Veterinary Parasitology*, *94*(1–2), 33–44. https://doi.org/10.1016/S0304-4017(00)00369-1

Verastegui, M. R., Mejia, A., Clark, T., Gavidia, C. M., Mamani, J., Ccopa, F., Angulo, N., Chile, N., Carmen, R., Medina, R., García, H. H., Rodriguez, S., Ortega, Y., & Gilman, R. H. (2015). Novel Rat Model for Neurocysticercosis Using Taenia solium. *The American Journal of Pathology*, *185*(8), 2259. https://doi.org/10.1016/J.AJPATH.2015.04.015

Verhoog, M. B., Goriounova, N. A., Obermayer, J., Stroeder, J., Johannes Hjorth, J. J., Testa-Silva, G., Baayen, J. C., de Kock, C. P. J., Meredith, R. M., & Mansvelder, H. D. (2013). Mechanisms Underlying the Rules for Associative Plasticity at Adult Human Neocortical Synapses. *Journal of Neuroscience*, *33*(43), 17197–17208. https://doi.org/10.1523/JNEUROSCI.3158-13.2013

Verma, A., Prasad, K. N., Cheekatla, S. S., Nyati, K. K., Paliwal, V. K., & Gupta, R. K. (2011). Immune response in symptomatic and asymptomatic neurocysticercosis. *Medical Microbiology and Immunology*, *200*(4), 255–261. https://doi.org/10.1007/s00430-011-0198-x

Vezzani, A., French, J., Bartfai, T., & Baram, T. Z. (2011). The role of inflammation in epilepsy. *Nature Reviews. Neurology*, *7*(1), 31. https://doi.org/10.1038/NRNEUROL.2010.178

Vezzani, A., & Granata, T. (2005). Brain Inflammation in Epilepsy: Experimental and Clinical Evidence. *Epilepsia*, *46*(11), 1724–1743. https://doi.org/10.1111/J.1528-1167.2005.00298.X

Villa, O. F., & Kuhn, R. E. (1996). Mice infected with the larvae of *Taenia crassiceps* exhibit a Th2-like immune response with concomitant anergy and downregulation

of Th1-associated phenomena. *Parasitology*, *112*(6), 561–570. https://doi.org/10.1017/S0031182000066142

Wang, P.-F., Fang, H., Chen, J., Lin, S., Liu, Y., Xiong, X.-Y., Wang, Y.-C., Xiong, R.-P., lv, F.-L., Wang, J., & Yang, Q.-W. (2014). Polyinosinic-Polycytidylic Acid Has Therapeutic Effects against Cerebral Ischemia/Reperfusion Injury through the Downregulation of TLR4 Signaling via TLR3. *The Journal of Immunology*, *192*(10), 4783–4794. https://doi.org/10.4049/JIMMUNOL.1303108/-/DCSUPPLEMENTAL

Wang, W. Y., Tan, M. S., Yu, J. T., & Tan, L. (2015). Role of pro-inflammatory cytokines released from microglia in Alzheimer's disease. *Annals of Translational Medicine*, *3*(10), 136. https://doi.org/10.3978/J.ISSN.2305-5839.2015.03.49

Wheless, J. W., Clarke, D. F., Arzimanoglou, A., Carpenter, D., Barbosa, C., Pedro Hispano, H., Patrick Berquin, P., Campos-Castello, J., Clinico San Carlos, H., Catherine Chiron, S., Necker, H., Athanasios Covanis, F., Cross, H., Curatolo, P., Des Portes, V., Debrousse, H., Bernard Echenne, F., Fazzi, E., Fohlen, M., … Sameer Zuberi, I. (2007). Treatment of pediatric epilepsy: European expert opinion, 2007. *Icnapedia.Org*, *9*(4), 353–412. https://doi.org/10.1684/epd.2007.0144

White, A. C. (1997). Neurocysticercosis: A Major Cause of Neurological Disease Worldwide. *Clinical Infectious Diseases*, *24*(2), 101–105. https://doi.org/10.1093/CLINIDS/24.2.101

White, A. C. (2000). NEUROCYSTICERCOSIS: Updates on Epidemiology, Pathogenesis, Diagnosis, and Management. In *Annu. Rev. Med* (Vol. 51). www.annualreviews.org

White, A. C., Robinson, P., & Kuhn, R. (1997). Taenia solium cysticercosis: host-parasite interactions and the immune response. *Chemical Immunology*, *66*, 209–230.

White, A. C., Tato, P., & Molinari, J. L. (1992). Host-parasite interactions in Taenia solium cysticercosis. In *Infectious agents and disease* (Vol. 1, Issue 4, pp. 185–193). https://europepmc.org/article/med/1365544

Willms, K., & Zurabian, R. (2010). Taenia crassiceps: in vivo and in vitro models. *Parasitology*, *137*(3), 335–346. https://doi.org/10.1017/S0031182009991442

Wirrell, E., Farrell, K., neurological, S. W.-C. journal of, & 2005, undefined. (2005). The epileptic encephalopathies of infancy and childhood. *Cambridge.Org*, *32*, 409–418. https://doi.org/10.1017/S0317167100004388

Wolock, S. L., Lopez, R., & Klein, A. M. (2019). Scrublet: Computational Identification of Cell Doublets in Single-Cell Transcriptomic Data. *Cell Systems*, *8*(4), 281-291.e9. https://doi.org/10.1016/j.cels.2018.11.005

World Health Organisation. (2016). *Epilepsy*. Fact Sheet.

World Health Organization. (2016). *Preventable epilepsy: Taenia solium infection burdens economies, societies and individuals : a rationale for investment and action.* 29.

Yousif, N. M., de Oliveira, A. C. P., Brioschi, S., Huell, M., Biber, K., & Fiebich, B. L. (2018). Activation of EP2 receptor suppresses poly(I: C) and LPS-mediated inflammation in primary microglia and organotypic hippocampal slice cultures: Contributing role for MAPKs. *Glia*, *66*(4), 708–724. https://doi.org/10.1002/GLIA.23276

Zahnow, C. A. (2009). CCAAT/enhancer-binding protein β: its role in breast cancer and associations with receptor tyrosine kinases. *Expert Reviews in Molecular Medicine*, *11*, e12. https://doi.org/10.1017/S1462399409001033

Zeng, Z., Lan, T., Wei, Y., & Wei, X. (2022). CCL5/CCR5 axis in human diseases and related treatments. *Genes & Diseases*, *9*(1), 12. https://doi.org/10.1016/J.GENDIS.2021.08.004

Zhang, L., Fan, D., & Wang, Q. (2017). Transition dynamics of a dentate gyrus-CA3 neuronal network during temporal lobe epilepsy. *Frontiers in Computational Neuroscience*, *11*, 61. https://doi.org/10.3389/FNCOM.2017.00061/BIBTEX

Zimmermann, K., Van Phi, V. D., Brase, A., & Phi-Van, L. (2015). Inhibition of serotonin transporter expression by C/EBPβ in LPS-activated macrophage cells (HD11). *Journals.Sagepub.Com*, *21*(4), 406–415. https://doi.org/10.1177/1753425914547434